CRREL REPORT 96-12

Ice Action on Riprap

Small-Scale Tests

Devinder S. Sodhi, Sharon L. Borland and Jesse M. Stanley September 1996

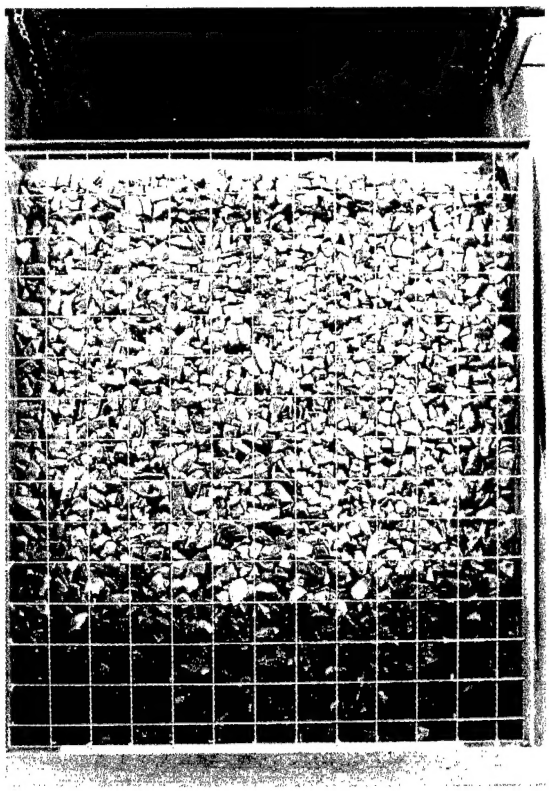

Abstract: We conducted 35 small-scale experiments to assess the damage on riprap-covered banks by ice shoving. A review of literature on this subject revealed very little experience or guidance available for the design of riprap in the cold regions, where presence of moving ice can cause substantial damage to a riprapped bank. During the experimental program, we changed the slope of the model riprap bank, the size and the mix of rocks, and the thickness of model ice sheets. Results of these tests are presented in terms of measured horizontal and vertical forces, outcome of interaction as pileup or ride-up events, and damage to the model riprap bank. From the observations made during the tests, the damage to the riprap appears to take place during pileup events, because the incoming ice sheet is forced to go between the riprap and the piled-up ice, bringing with it rocks from the bottom to the surface of an ice pile. To sustain no dam-age to the riprapped protective layer, maximum rock size (D_{100}) should be twice the ice thickness for shallow slopes (1V:3H) and about three times the ice thickness for steeper slopes (1V:1.5H).

Cover: Model rip-rap before (left) and after a test in which ice rode up the bank.

How to get copies of CRREL technical publications:

Department of Defense personnel and contractors may order reports through the Defense Technical Information Center:
DTIC-BR SUITE 0944
8725 JOHN J KINGMAN RD
FT BELVOIR VA 22060-6218
Telephone 1 800 225 3842
E-mail help@dtic.mil
msorders@dtic.mil
WWW http://www.dtic.dla.mil/

All others may order reports through the National Technical Information Service:
NTIS
5285 PORT ROYAL RD
SPRINGFIELD VA 22161
Telephone 1 703 487 4650
1 703 487 4639 (TDD for the hearing-impaired)
E-mail orders@ntis.fedworld.gov
WWW http://www.fedworld.gov/ntis/ntishome.html

A complete list of all CRREL technical publications is available from:
USACRREL (CECRL-TL)
72 LYME RD
HANOVER NH 03755-1290
Telephone 1 603 646 4338
E-mail techpubs@crrel.usace.army.mil

For information on all aspects of the Cold Regions Research and Engineering Laboratory, visit our World Wide Web site:
http://www.crrel.usace.army.mil

DISCLAIMER NOTICE

THIS DOCUMENT IS BEST QUALITY AVAILABLE. THE COPY FURNISHED TO DTIC CONTAINED A SIGNIFICANT NUMBER OF PAGES WHICH DO NOT REPRODUCE LEGIBLY.

CRREL Report 96-12

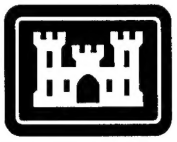

US Army Corps of Engineers
Cold Regions Research & Engineering Laboratory

Ice Action on Riprap
Small-Scale Tests

Devinder S. Sodhi, Sharon L. Borland and Jesse M. Stanley

September 1996

Prepared for
OFFICE OF THE CHIEF OF ENGINEERS

PREFACE

This report was prepared Dr. Devinder S. Sodhi, Research Hydraulic Engineer, Ice Engineering Research Division, Research and Engineering Directorate, Sharon L. Borland, Civil Engineer, Plans and Programs Office, and Jesse M. Stanley, Jr., Mechanical Engineering Technician, also of the Ice Engineering Research Division, U.S. Army Cold Regions Research and Engineering Laboratory, Hanover, New Hampshire. Funding was provided by U.S. Army Corps of Engineers Civil Works Project CWIS 32548, *Ice Effects on Riprap*.

The authors thank Kevin Carey and James Wuebben for technically reviewing the manuscript of this report.

The authors are grateful to J. L. Wuebben, J.-C. Tatinclaux, J. Wilkinson, C. Schelewa, M. Hopkins, R. Demars, R. Haehnel, P. Stark, and K. Chafe for their help in various ways in completing this project.

CONTENTS

Preface ii
Introduction 1
Review of slope protection in the cold regions 1
Experiments 6
  Setup 6
  Sizes and gradation of stones 8
  Placement of model riprap 9
  Ice growth procedure 9
  Measurement of model ice properties 10
  Carriage speed 10
  Data acquisition 10
  Procedure 11
Results 12
  Observations on ice ride-up and pileup 12
  Measured horizontal and vertical forces 15
  Observed failure of riprap 16
  Failure and nonfailure of riprap vs. ratio of ice thickness to rock size 19
Discussion 20
Summary and conclusions 20
Literature cited 20
Appendix A: Design of riprap protection against waves 23
Appendix B: Review of slope protection systems used in the Arctic 25
Appendix C: Plots of horizontal and vertical forces measured during the tests 27
Appendix D: Photographs and contour plots of the model riprap bank before and after each test 37
Abstract 65

ILLUSTRATIONS

Figure

1. Ice issues relating to Arctic slope protection and beach designs 2
2. Typical beach designs for Arctic structures 2
3. Typical winter ice action on sloping beaches 3
4. Typical ice action on caisson/berm structures 3
5. Forces acting during ice interaction with a sloping surface 5
6. Aluminum box used for model riprap bank 6
7. Box and the supporting platform prior to their installation under the carriage 6
8. Model supporting platform 7
9. Model support system 7
10. Partially installed layers of sand, filter fabric, and stones used to simulate a riprap-protected bank 8
11. Refrigerated test basin in the Ice Engineering Facility 9
12. Placement of grid over the model riprap bank 10

Figure

13. Measurement of the distance of the riprap surface from the strings at each grid point 11
14. Leveling rocks of model riprap in final preparation prior to each test 12
15. Cutting of slots in the model ice sheet prior to each test 12
16. Ride-up event 13
17. Model riprap before and after a test in which ice rode up the bank 13
18. Ice sheet after it is broken and pushed up the riprap bank 14
19. Stones brought up to the surface of an ice pile 14
20. Sequence of ride-up and pileup events for test 20 14
21. Typical plot of the horizontal component of the force acting on the riprap 15
22. Typical plot of the vertical component of the force acting on the riprap 15
23. Plot of maximum force recorded during each test vs. $b\rho_w g L^2$ 16
24. Ice pileup after test 4 16
25. Model riprap before and after test 4 17
26. Model riprap before and after test 5 17
27. Contour plots of the model riprap before and after test 5 18
28. Rocks found on top of the ice pile during melting of ice after test 20 18
29. Sand bed of model bank deformed by ice action after test 8 18
30. Damage to filter fabric by ice action after test 30 19
31. Plot of cumulative probability of damage vs. the ratio of ice thickness to D_{10} rock diameter 19

TABLE

Table

1. Values of various parameters used during the small-scale tests and some of the results obtained from the tests 11

Ice Action on Riprap
Small-Scale Tests

DEVINDER S. SODHI, SHARON L. BORLAND AND JESSE M. STANLEY

INTRODUCTION

According to the Coastal Engineering Research Center (1984), riprap is defined as a protective layer of quarry stones randomly placed to prevent erosion, scour or sloughing of an embankment of bluff. As listed in the publication by Construction Industry Research and Information Association (1991), the functions of a rock breakwater include attenuation of wave transmission and overtopping, dissipation of wave energy, and filtration. These two manuals contain extensive information on the design, construction and maintenance of the rock structures, so that the structures can perform their intended tasks with acceptable risk of failure and maximum possible benefit-to-cost ratios. In Appendix A, we have presented the formulas to compute the size of stones to be used for riprap protection against waves (Coastal Engineering Research Center 1984) and in a flood control channel (U.S. Army Corps of Engineers 1991). However, the guidance for the design of shore protection systems in the cold regions, where ice is present, is limited. This can largely be attributed to the small amount of coastal construction in the cold regions and particularly in the Arctic. Except for a few artificial islands built along the southern coast of Beaufort Sea for exploration of oil and gas resources in the 1970s and the 1980s, most of the construction of dams and coastal facilities in the cold regions has taken place outside the Arctic areas.

As in the case of open water, the processes taking place between an advancing ice sheet and individual rocks in a riprap structure are not simple to model theoretically. Small-scale physical model study is one of the means to assess the suitability of riprap as a slope protection system against ice action. In the following, we present a brief review of slope protection system employed for installations in the cold regions, state the objectives of this study, describe the procedure followed in conducting small-scale tests to assess the damage of riprap by direct ice action, and present the results obtained from this small-scale study.

REVIEW OF SLOPE PROTECTION IN THE COLD REGIONS

A few (≈ 10–20) man-made islands were built since the 1970s for exploration of oil and gas along the southern coast of the Beaufort Sea. Innovative means of slope protection for the Arctic coastal and offshore facilities were developed to minimize their construction costs. Other constraints associated with the construction in that area are the short construction season and high costs of labor, equipment and material.

The presence of ice is the major difference between the design of slope protection in the cold and warm regions (Croasdale et al. 1988). During the winter months, the presence of ice limits the wave climate and erosion, but the ice itself may damage the slope protection system. When the ice edge retreats during the summer months, zones of armor already damaged by ice may possibly further be damaged because of storm-generated waves in the open water. Three issues that may affect the design of slope protection in the Arctic: 1) an ice sheet may ride up the sloping surface and damage the surface facilities, 2) grounded rubble ice around an island or adjacent to a beach may form a protective barrier between the moving ice and a structure, and 3) the interaction between a discrete, thick ice feature and an underwater berm of beach or island slope may absorb the energy of the moving ice feature (Croasdale et al. 1988). These are illustrated in Figure 1.

As shown in Figure 2, three types of slope protection designs have been used for the Arctic: 1) sacrificial beaches, 2) sandbag-retained islands, and 3) caisson-retained islands (Croasdale et al.

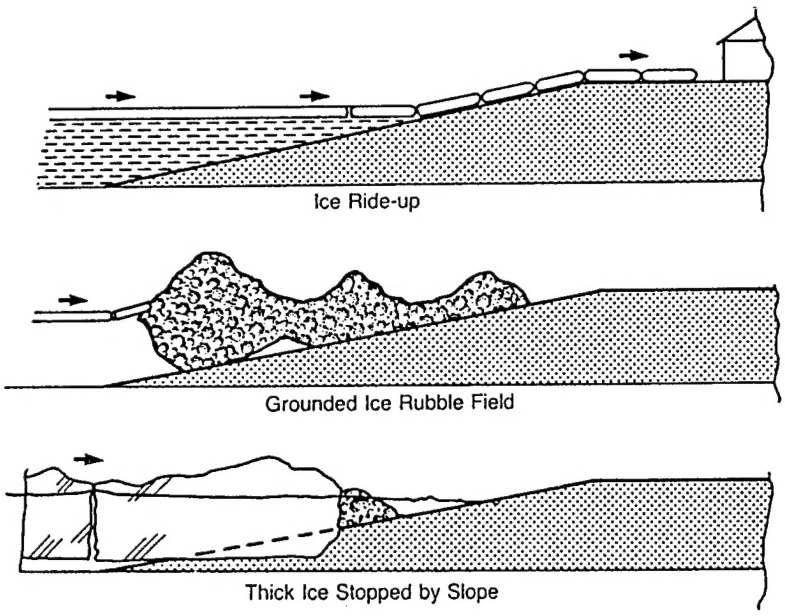

Figure 1. Ice issues relating to Arctic slope protection and beach designs (after Croasdale et al. 1988).

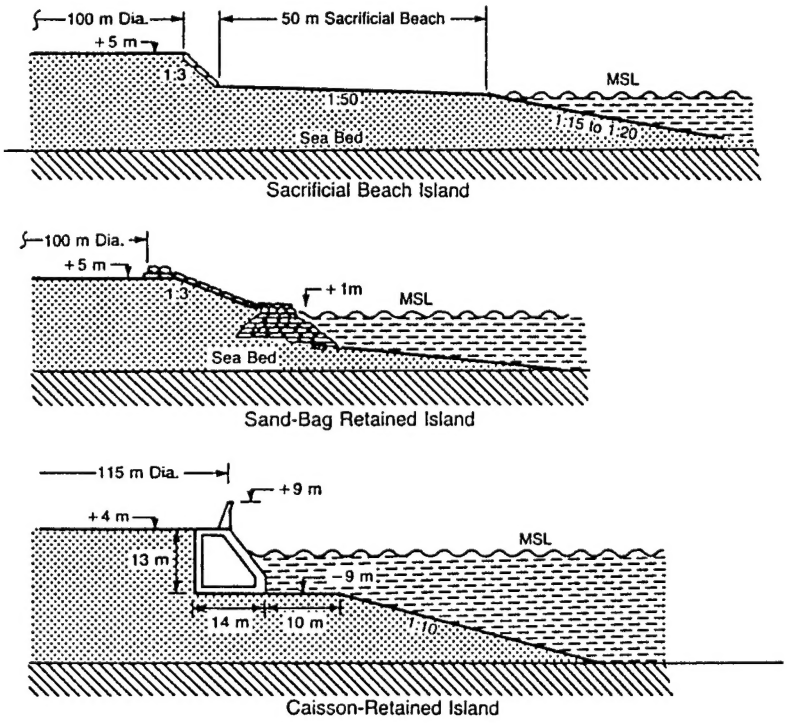

Figure 2. Typical beach designs for Arctic structures (after Croasdale et al. 1988).

1988). These designs evolved with the construction of islands in increasing depth of water from the early 1970s to the late 1980s.

Figure 3 shows a typical sequence of ice action on sloping beaches in the Arctic. At the start of a winter season, thin ice moves against an island and forms a grounded rubble ice zone. Part of this rubble ice close to the water surface freezes and forms a stable, protective rubble zone around an island. Any further ice action takes place at the outside edge of the consolidated rubble ice. In deeper water, caisson-retained islands (Fig. 4) have suc-

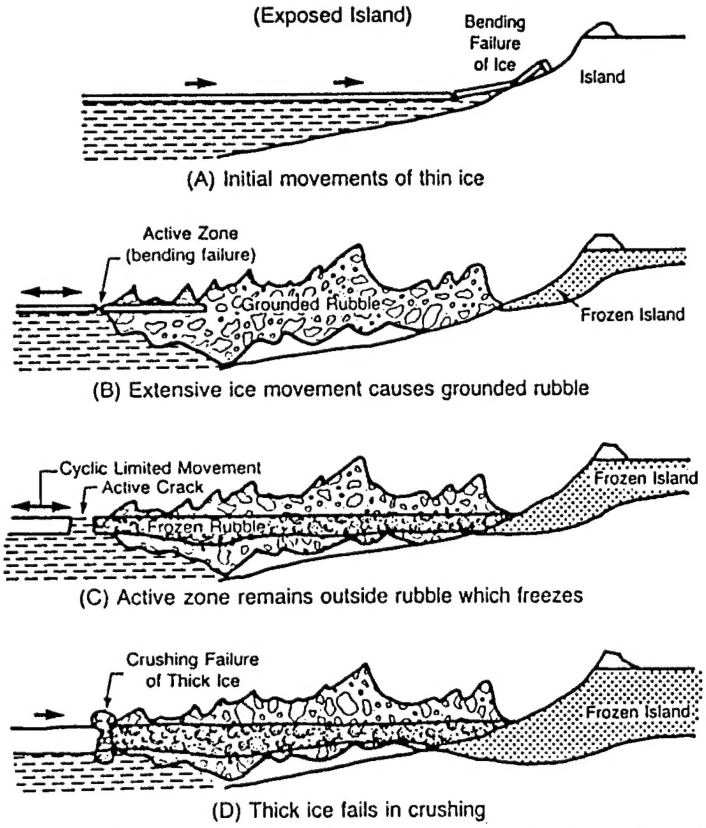

Figure 3. Typical winter ice action on sloping beaches (after Croasdale and Marcellus 1978).

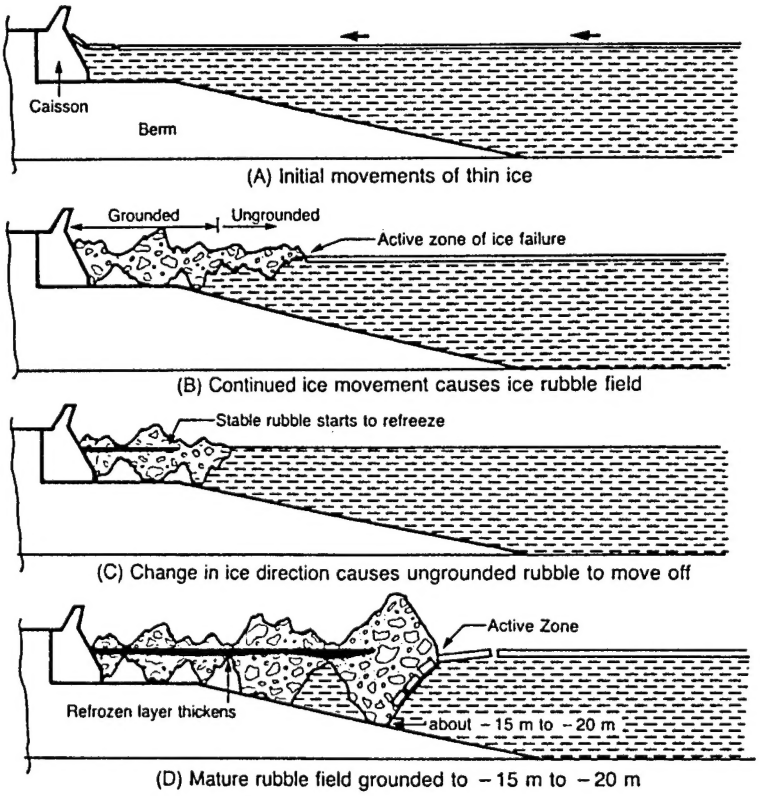

Figure 4. Typical ice action on caisson/berm structures (after Croasdale et al. 1988).

cessfully been used along the Canadian and the Alaskan offshore regions. The rubble ice may not remain stable in water depths greater than 10 m (33 ft), and an underwater berm may be needed for the caisson-retained islands to stabilize the protective rubble ice zone.

Some of the types of slope protection armor that have been used are sandbags (Gadd 1988), concrete mats (Leidersdorf 1988), riprap and armor stones (McDonald 1988), and large precast concrete armor units (Collins 1988). In Appendix B, we discuss the experiences with each of these types of slope protection armor.

Matheson (1988) surveyed the performance of riprap slope protection of Canadian and other dams. He found that the dominant mechanism of riprap deterioration was freeze-thaw action on riprap consisting of bedded sedimentary rocks, resulting in delamination and breakdown. While the sedimentary limestone and sandstone were prone to breakdown, such degradation was found to be negligible in the case of igneous and metamorphic rocks, e.g., granite. He described the following ice-related mechanisms that cause riprap damage: 1) "plucking" of riprap by rising and falling water levels, and 2) ice shoving. He found that the plucking action can affect riprap with rock size up to approximately the ice thickness, and that the riprap damage due to winter drawdown was significant for steeper slopes (1 vertical:1.75 hortizontal) and minimal for shallow slopes (1V:3H).

Doyle (1988) described the damage to public and private property, including the destruction of a bridge and several riprapped banks, from a sudden river ice breakup in January 1984 on the Nicola River and its two main tributaries in British Columbia, Canada. He attributed all damage either to the severe ice run within the channel or to flow forced out over the floodplain by ice jams. The ice run, caused by runoff generated by warm weather moving into the watershed after extremely cold weather, damaged seven riprapped bends in the Coldwater and Nicola Rivers. The riprap protection on 1V:2H slope banks consisted of a single layer of well-graded angular rocks having a maximum (D_{100}) and median (D_{50}) diameter of 750–900 mm and 500–600 mm, respectively. His field evidence suggests that the running ice took out individual rocks from riprap-protected banks, causing total destruction of the protective works. The damage sustained by trees in the path of running ice on the floodplains also would tend to corroborate the conclusion that running ice was able to remove moderately heavy rocks. Because such an event is believed to occur rarely, the repair to ice-damaged riprap was done in a conventional manner, rather than adopting a different, perhaps more costly, design.

Wuebben (1995) reviewed the literature on ice effects on riprap, river hydraulics and scouring of river beds. He pointed out that nonuniform or unsteady flows during ice jams can cause serious scour and degrade riprap performance. Ice jams can cause stages comparable to rare open water events, and it is necessary to consider protection of upper limits of banks.

Ice can damage a slope protection system by direct impact and shoving action. Even when the damage caused by direct ice action on an offshore artificial island may not be extensive, it can be exacerbated by the wave action during storms in the summer months (Gadd 1988). In a similar way, river ice can damage slope protection armor at a few places, and this damage can be extended over a large area by high water levels and currents following the breakup of ice.

When an ice sheet moves against a sloping bank protected with a riprap armor, the ice may ride up or pile up. Sodhi et al. (1983) conducted small-scale experimental studies to understand the factors that lead ice to pileup and found that ice pileup occurs more often on a rough sloping surface than on a smooth surface. At present, the set of conditions or parameters that can predict a ride-up or a pile-up of an ice sheet is not exactly known. Extensive ride-up of an ice sheet is not preferred because it may damage onshore facilities. A rough sloping surface may promote an ice pileup because the forces required for continued ride-up of an ice sheet become large. Croasdale et al. (1988) discussed the strategies to be employed in the design of a sloping surface to promote an ice pileup.

McDonald (1988) discussed the ice forces on a coastal structure caused by a moving ice floe or by thermal expansion of a restrained ice sheet. The global force exerted by an ice sheet against a large structure is not uniformly distributed across the width of the structure. The force (or pressure) that may develop on an individual armor unit may be very high at one place and almost negligible at another place. This is attributed to nonsimultaneous local ice failure, resulting in variation of ice pressure with respect to time and location. The normal component of this force may cause a pressure buildup to the ice crushing pressure, which is less than that sufficient to damage most stones. The shear component of ice force may act on an individual stone protruding into the ice mass, and

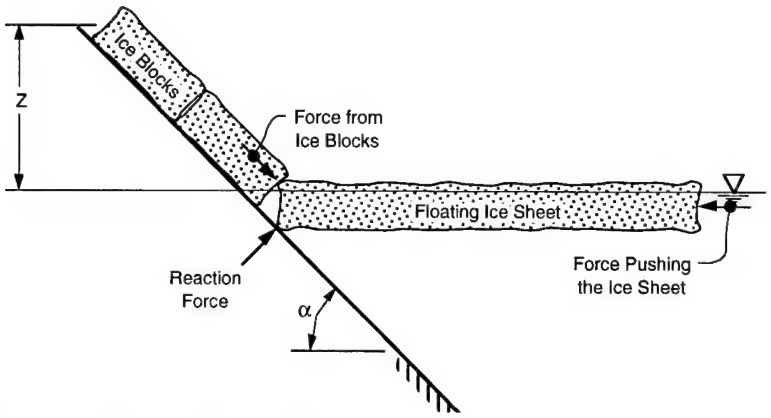

Figure 5. Sketch of forces acting during ice interaction with a sloping surface, where α is slope angle from the horizontal and z is the height of pushed-up ice blocks.

the pressure on an individual rock can be as high as that to crush ice. The shear component can introduce a rotation and dislodging of an individual stone if opposing moment cannot be developed from neighboring stones. To prevent such damage from ice, the individual rocks that make up the armor stone or riprap layers should be placed on the slope in such a way that the surface of the protective layer is relatively smooth. This is contradictory to the design practice of riprap to resist wave action, where a rough surface is intended to dissipate the wave energy.

Croasdale (1980) presented a two-dimensional formulation of the forces that result from an interaction between a floating ice sheet and a sloping structure, as shown in Figure 5. The horizontal force against a sloping surface results in a vertical force at the point of contact, which deflects the ice sheet up. When the maximum stress in the ice sheet exceeds the flexural strength, the ice sheet fails in bending. The broken pieces of ice are pushed up the slope and cause additional resistance to the advancing ice sheet. Nevel (1983) has given a similar, but more rigorous, formulation of ice failure by bending.

In general, the ice sheet deflected up by the sloping surface fails in bending into large ice blocks, which may further break into smaller blocks as they move upward and over irregular surface of the stones. Because of the nonsmooth surface of a riprap protection system, a detailed analysis of interactions between the ice blocks and the rocks is very complex. The damage in a riprap armor takes place by removal and transport of stones by ice, and keeping track of progressive damage is impossible in a simple theoretical analysis (e.g., Croasdale 1980, Kovacs and Sodhi 1980).

Using a two-dimensional, discrete-particle analysis, Hopkins (1995) simulated onshore pileup and ride-up of an ice sheet moving against an inclined surface. He compared the results of his simulation with measured values of forces and energy during a small-scale experiment. As part of this study, he also attempted a two-dimensional, discrete-particle simulation of ice action on a sloping surface protected by two layers of stones. The simulation showed movement of a few rocks until they were embedded in an ice pile. Though this simulation looks to be promising, the two-dimensional aspect of this analysis is a limiting factor in establishing a relationship between the riprap damage and the extent of ice action. Small-scale experimentation is one of the means with which we can study the ice effects on riprap armor in terms of stone size, ice thickness, slope angle, and ice flexural strength and elastic modulus.

The purpose of this study is to assess the damage to riprap protection by the shoving action of an ice sheet. The focus of this study is for seasonally occurring ice on rivers and lakes in the cold regions, such as the northern tier of the United States. In those areas, it is possible for riprap to have varying degrees of fixity to the bank during a given ice impact event. The degree of attachment can range between two extremes: 1) when a riprap is strongly attached to the bank by being frozen in place, and 2) when a riprap is not frozen to the bank. Generally, a riprap frozen to the underlying bank will be less prone to damage by ice action. Because ascertaining and simulating varying degree of fixity of a riprap to the bank is difficult, we chose to conduct the physical model test program using the riprap in an unfrozen condition.

The objectives of this small-scale experimental study are 1) to conduct small-scale tests of ice shoving against a sloped surface protected with a

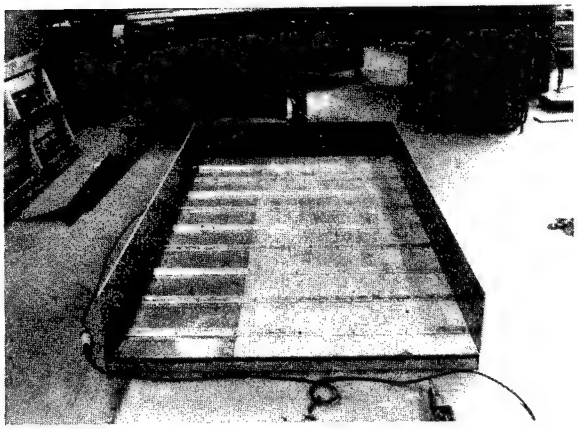

Figure 6. Aluminum box used for model riprap bank.

model riprap, 2) to measure the forces generated during the ice–riprap interaction during the tests, and 3) to determine the conditions when ice shoving damages a riprap armor. In this report, we describe the experimental apparatus and procedure used to simulate a riprap-protected sloping bank being impacted by model ice, present the data obtained during the 35 tests, and discuss the results and their implications on design criteria for riprap protection in ice-affected areas. The focus of this study is for situations in rivers and lakes in the cold regions. Generally, a riprap frozen to the underlying material will be less prone to ice damage. We decided to keep the model riprap armor in an unfrozen condition so that the results of this study will be conservative for the riprap armor frozen to the material underneath.

EXPERIMENTS

We constructed a physical model of an inclined riprap-covered embankment at a scale of one-eighth the actual size, based on typical ice flexural strength. To simulate ice shoving on a riprap bank, we mounted the model under the carriage spanning the refrigerated test basin of CRREL's Ice Engineering Facility, and pushed it against ice sheets grown in the test basin. We could vary the slope of the model riprap surface to three particular values and change the size and the mix of rocks for different tests. We installed load cells at appropriate places in the supporting structure of the model to measure the horizontal and the vertical forces generated as a result of interaction between the ice and the riprap. Thirty-five tests were conducted to model various combinations of the variables.

Setup

Figure 6 is a photograph of the aluminum box in which we built each model riprap bank. It was 1.32 m (52 in.) wide and 2.44 m (96 in.) long. We attached sides to the box to confine the sand bed, filter, model riprap and ice in the model area during a test. We left the top side of the model bank open so that the ice reaching the top end during a test could fall into the basin. We made the bottom of this box with plywood reinforced with angle iron, and we attached 25-mm- (1-in.-)×25-mm-(1-in.-) aluminum angles to the plywood surface, extending from side to side.

We installed the box containing the model riprap in a supporting platform (Fig. 7), which enabled us to measure the horizontal and the vertical forces on the bank during the tests. Figure 8 shows a schematic drawing of a two-tiered frame, which supported the model riprap bank. We installed the whole assembly under the main carriage beams so

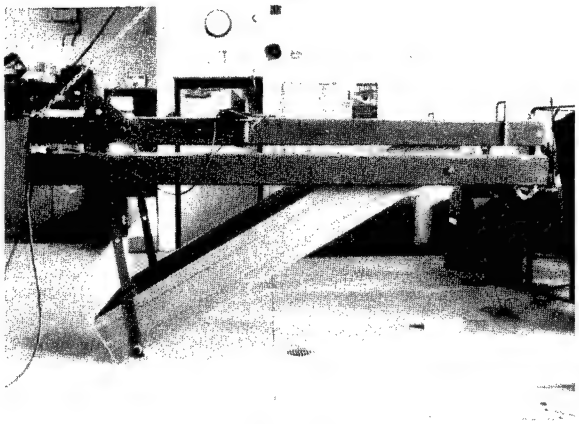

a. Side view.

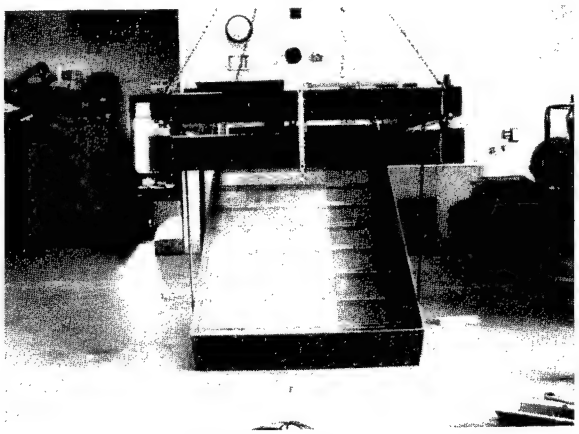

b. Front view.

Figure 7. Box and the supporting platform prior to their installation under the carriage.

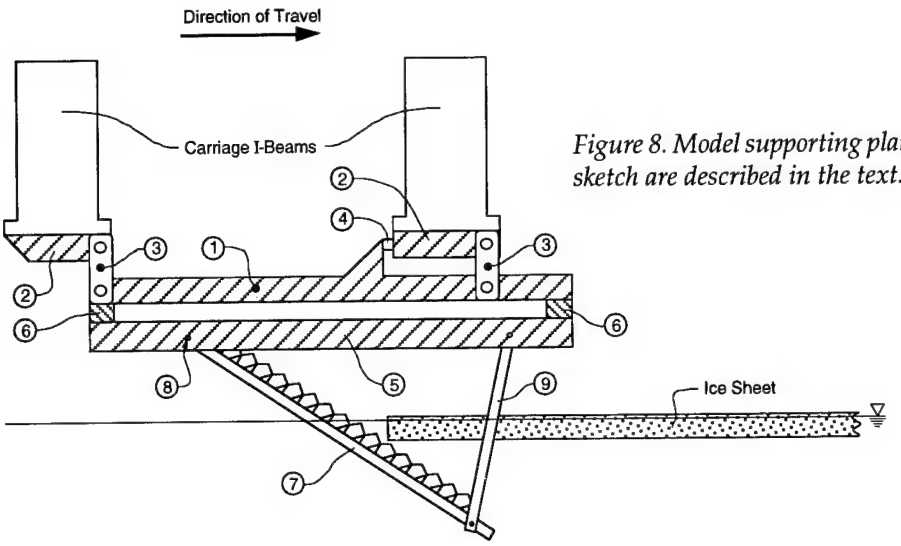

Figure 8. Model supporting platform. Items numbered in this sketch are described in the text.

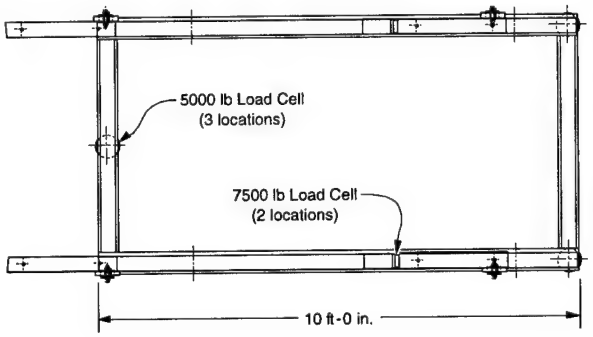

Figure 9. Model support system, in which the locations of five load cells are shown.

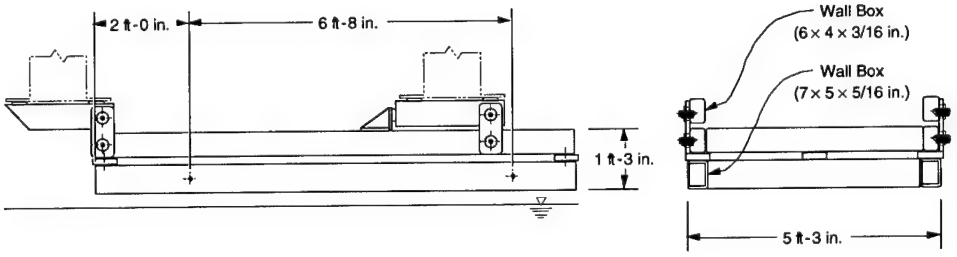

that the model was partially submerged in the basin (Fig. 8). Figure 9 shows the engineering drawings of the frame. We suspended the upper frame (1) from steel box sections (2), which were bolted to the carriage, with the help of four bar linkages (3) so that it could freely swing back and forth and allow transmission of horizontal forces on the model bank through two load cells (4) installed on the carriage. We supported a lower frame (5) under the upper frame (1) through three vertical load cells (6). Figure 9 also shows the location all load cells. We installed the model bank (7) on the lower frame (5), as shown in Figure 8. We supported one end of the model riprap frame (7) at a pivot point (8) on the lower frame (5) and the other end on two steel bars (9). By adjusting the length of the two steel bars, we could change the slope of the model riprap surface. We could set three slope angles, 18°, 27°, and 34° from the horizontal, corresponding to vertical to horizontal distance ratios of 1V:3H, 1V:2H, 1V:1.5H , respectively.

All load cells were calibrated to maximum capacity using standard calibration load cells prior to the test program. After installing the test fixture under the carriage, we calibrated the load measuring system, by applying a known load through another calibrated load cell, and compared the known load to the sum of horizontal and vertical forces measured by the load cells in the model.

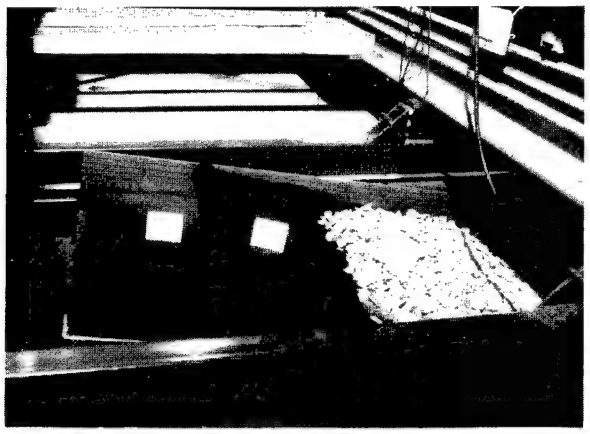

Figure 10. Partially installed layers of sand, filter fabric, and stones used to simulate a riprap-protected bank. In this view, the model and supporting platform are attached to the main carriage in the test basin.

The model bank riprap installation simulated a typical field installation as much as possible. We placed a 38-mm- (1.5-in.-) deep layer of sand on the bank (held in place by the transverse aluminum angle strips), covered the sand with a filter fabric, and placed manufactured stones to model the riprap material (Fig. 10). The practice in many field applications is to apply the riprap over a filter material, which prevents fine materials of an underlayer from being washed through the voids of a coarse upper layer. Where geotechnical conditions permit, a filter cloth (or geotextile) is often specified for the filter to lower construction costs. This type of filter material offers less frictional resistance to the riprap compared to a filter made of gravel. In previous laboratory studies on the angle of repose of riprap, the riprap was found to be less stable when placed on filter cloth than when placed on a simulated gravel filter. We used the filter cloth for the underlying filter material in our model, because the use of a filter fabric in our tests will better simulate the conditions for the growing number of bank protection projects using geotextile filters, and it will be conservative for those riprap installations using a gravel filter.

Sizes and gradation of stones

We used scaled-down stones in approximate gradations as suggested by the U.S. Army Corps of Engineers (1991) to model the riprap. In general, we followed the guidance given by the Corps on the stone characteristics and installation techniques for the purpose of making model ripraps. The guidelines and the convention used in specifying stone size are summarized here for reference.

Stone shape should be blocky, not elongated, to enable the stones to "nest" together more effectively to increase their resistance to movement. We used rocks within a certain range of shape factor, which is defined roughly as the ratio of the longest dimension to the shortest dimension of the rock, to limit the number of rocks that were too elongated to be effective as riprap. The guidance provide by U.S. Army Corps of Engineers (1991) is that no more than 30% of the material should have shape factors greater than 2.5, and no more than 15% should exceed 3.0.

The stone size is defined as the equivalent spherical diameter D of a stone of a given weight W, and it can be calculated using the standard equation for computing the volume of a sphere:

$$D = \{6W/(\pi\gamma_s)\}^{1/3}$$

where γ_s is the specific weight of a stone. Conventionally, stone size is expressed as D_n, where D denotes the equivalent spherical diameter of the stone and the subscript n denotes the percentage of the total weight of the graded material that contains stones of smaller weight. Similarly, the stones can be graded according to the weight expressed as W_n, where W denotes the weight for which a percentage n is lighter on the cumulative distribution curve. In the U.S. Army Corps of Engineers (1991), standardized gradations having a narrow range in sizes ($1.4 < D_{85}/D_{15} < 2.2$) are given in tabular form. The manual recommends that the gradation limits should not be too restrictive to make the production cost high. In general, the guidance simply suggests that gap-graded or widely graded stone distributions may not be suitable as effective riprap. According to the manual, most graded riprap have ratios D_{85}/D_{15} less than 3; for our tests, we followed this guidance for the model riprap to have the ratio D_{85}/D_{15} less than 3.

We obtained manufactured stone from a local quarry (West Lebanon, N.H.) for the model riprap. The rock from this source is a metamorphic and has a density of 2600 kg/m^3 (160 lb/ft^3). The shape of an individual rock was typically blocky to slightly elongated with angular edges. We manually sifted the rocks to reject rocks with shape factor greater than 2.5. The large-size stones were sieved into the desired size fractions because of the unavailability of standard sieves and the difficulty in handling.

Although stone size is often represented in terms of the D_{50} or D_{30} size for open-water riprap installations, we have found that, for the case of ice shov-

ing, D_{100} is a better indicator of performance. We used four different sizes of stone in this study: a relatively large stone size of D_{100} = 127 mm (5 in.), a medium stone size of D_{100} = 76 mm (3 in.), and a small stone size of D_{100} = 38 mm (1.5 in.). The thickness of the riprap blanket was approximately 1.5 to 2 times the D_{100} stone. We determined the bulk rock porosity by weighing a known volume of rocks, and found it to be approximately 0.30 for all size distributions of rock used.

We scaled down the distribution of stone sizes for D_{100} = 127 mm (5 in.) from a recommended distribution of riprap in the U.S. Army Corps of Engineers (1991). Approximately, the distribution of stone by weight was given in the following: 127-mm- (5-in.-) diam. stone 15%, 102-mm- (4-in.-) diam. stone 45%, 76-mm- (3-in.-) diam. stone 24%, and 38 mm- (1.5-in.-) diam. stone and smaller 16%. This distribution is equivalent to D_{85} = 102 mm (4 in.), and D_{15} = 38 mm (1.5 in.). The ratio D_{85}/D_{15} = 2.7.

The distribution of stone sizes for D_{100} = 76 mm (3 in.) was more uniformly graded with basically two stone sizes in the mix. Approximately 50% by weight of the total stone distribution was 76-mm- (3-in.-) diam. stone and the diameter of the other 50% of the stone was 38 mm (1.5 in.) and less. The resulting D_{85} = 76 mm (3 in.), and D_{15} = 38 mm (1.5 in.) gave a D_{85}/D_{15} ratio equal to 2.

The distribution of stone size for D_{100} = 38 mm (1.5 in.) was a well-graded standard mix direct from the plant designed to be used for grading septic systems. The shape of this rock was slightly blocky with angular edges. We estimated the ratio D_{85}/D_{15} for this mix was about 2.

Placement of model riprap

Because we did not want any rock breakage (which was observed to occur as a result of rough handling during previous small-scale tests), we distributed the larger stones evenly over the model bank by hand as widely and evenly as possible. Although placing the riprap by hand was a laborious and time-consuming process, we made every attempt to place the stone in a consistent fashion for each test run. We did not dump the stones from a great height, nor were they keyed in by hand. Because the stone placement took considerable time, we did not replace all the rock after every test, although that would have been ideal. Instead of removing and then replacing all the stone to ensure that the riprap was not being "wedged-in" to the bank by repeated ice shoving events, we carefully rearranged the rocks on the bank after every test. When relatively large quantities of rocks were shoved by the ice over the top of the bank into the basin during a test, we replaced the lost rocks with a mix of rocks that had the same gradation as that of the original mix.

Ice growth procedure

The test basin at CRREL is 36.6 m (120 ft) long, 9.1 m (30 ft) wide, and 2.4 m (8 ft) deep (Fig. 11). It holds a solution of urea in water, 1% by weight, at a temperature of approximately 0°C (32°F). To grow an ice sheet, the temperature in the room is lowered to –10°C (14° F). The water is kept mixed with a bubbler system to prevent ice growth during this pull-down time. When the ambient temperature in the room reaches –10°C (14° F), we spray fresh water into the air above the water surface to seed an ice sheet. During the seeding process, ice crystals form in the air and fall onto the surface of the water. This seeding technique results in growth of small-size columnar ice crystals. The room is then cooled further to a temperature of –20°C (–4°F) to proceed with the ice growth.

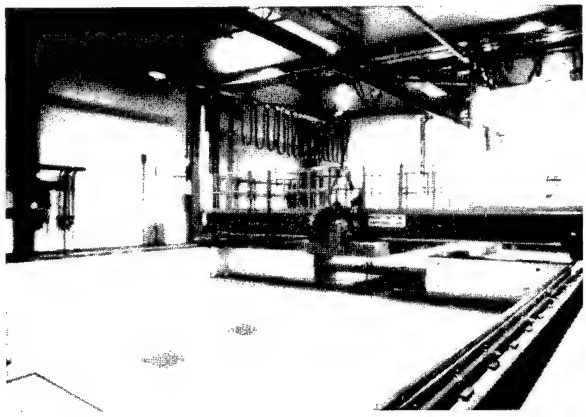

Figure 11 Refrigerated test basin in the Ice Engineering Facility.

Total growth time of our model ice sheets depends on the required ice thickness. Once the thickness is achieved, the desired strength was obtained by "tempering" the ice sheet at a higher room temperature of 0°C (32° F). The ice impurities (trapped between crystal platelets) weaken the ice when the ice warms slowly. The flexural strength of the ice is measured during the tempering process until the desired strength is reached. The desired flexural strength of a model ice sheet is about 87.5 kPa (12.5 psi), which is one-eighth of the full-scale value of 700 kPa (100 psi). While test-

ing with thin ice sheets, we did not temper the ice, because the maximum flexural strength of thin ice sheets is usually less than 87.5 kPa (12.5 psi).

Measurement of model ice properties

The ice sheet was characterized by measuring the characteristic length and the flexural strength. These properties were measured in situ using standard testing procedures, as described below.

The characteristic length was measured by placing a known dead weight P on a floating ice sheet and measuring the resulting elastic deflection δ (Sodhi et al. 1982). The characteristic length L was then calculated as

$$L = [P/(8\rho_w g\delta)]^{1/2}$$

where $\rho_w g$ is the specific weight of water.

We measured the flexural strength by cutting cantilever beams and breaking them in the upward or downward direction. The dimensions of the beam were proportional to the ice thickness. The length of beams was about five to six times the ice thickness, and the width was about two times the ice thickness. We measured the maximum force F (applied at their tips) required to break the beams, and also the dimensions of broken beams. The flexural strength σ_f was then calculated as

$$\sigma_f = 6F\lambda/(wh^2)$$

where λ = the beam length
w = the width
h = the ice thickness.

Carriage speed

On rivers, water velocities during spring breakup can exceed 5 m/s (16.40 ft/s) in extreme events (Wuebben 1995). The ice action would most likely be a combination of ice shoving and shearing along a river bank at high velocity (≈ 1 m/s or 3.28 ft/s). In a reservoir situation where there could be purely normal ice shoving action on a bank, the ice would be driven by wind or thermal expansion at speeds of less than 1 m/s (3.28 ft/s).

We used the main carriage to push the model through an ice sheet at a constant speed of 40 cm/s (1.31 ft/s) for all tests but the first two. We conducted the first two tests at speeds of 80 cm/s (2.62 ft/s) and 20 cm/s (0.66 ft/s) for shakedown purposes. We found little effect of speed on the measured forces if the ice failure took place in bending. A speed of 40 cm/s (1.34 ft/s) in model tests scales to full-scale speed of 1.13 m/s (3.71 ft/s), which is a reasonable speed of ice shoving during a typical ice breakup.

Data acquisition

We measured or noted the following variables during each test: ice thickness, flexural strength of ice, carriage speed, horizontal force, vertical force, topography of riprap before and after each test, and an assessment of damage. In some tests, we measured the topography of the ice pile and its maximum height. In Table 1, we have given the values of parameters or variables that were either set or measured during each test. We measured and recorded the horizontal and the vertical forces along with the carriage speed using a data-acquisition system, which we programmed to scan at 150 samples/second per channel. We used antialiasing, 45-Hz low-pass filters to remove high-frequency noise at the analog input stage. We programmed the data acquisition system to acquire the data when the carriage was in motion, i.e., start and stop triggers were set on the carriage movement. We also saved pre- and post-trigger data for a period of 10 seconds.

To profile the rock surface, we placed a frame containing a 102- × 102-mm (4-in. ×4-in.) grid made of strings (Fig. 12) on top of the fixed aluminum sides of the model bank, which provided a fixed reference for each set of measurements. With a ruler, we measured the perpendicular distances from the rock surface to the strings at each grid point (Fig. 13). The width of the grid frame was the same as that of the box (1.32 m or 52 in.) and its length was 1.52 m (60 in.). With this grid, we measured the riprap surface profiles at 168 grid points, which enabled us to get a reasonably good profile. We profiled the rocks before and after each

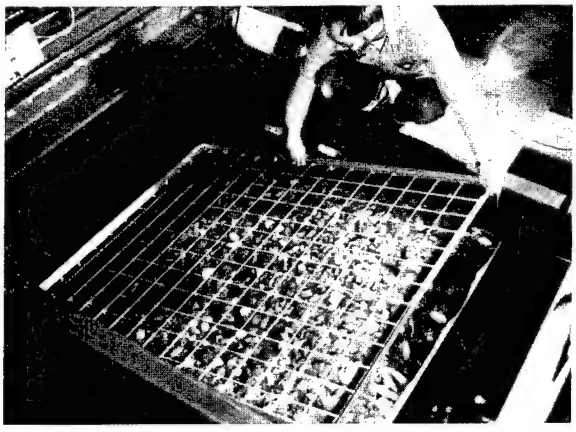

Figure 12. Placement of grid over the model riprap bank.

Table 1. Values of various parameters used during the small-scale tests and some of the results obtained from the tests.

Test	Date	Carriage speed (cm/s)	Stone size (D100) (mm)	Ramp slope (deg)	Ice thickness (mm)	Flexural strength Down (kPa)	Flexural strength Up (kPa)	Characteristic length (m)	Level of damage 0 = none; 3 = H	Maximum horizontal force (N)
1	29 Nov 93	80	38	18	50	118	70	0.90	0	8007
2	3 Dec 93	20	38	18	45	93	44	0.64	3	5338
3	8 Dec 93	40	38	18	40	106	45	0.58	1	1779
4	10 Dec 93	40	38	18	43	104	45	0.66	3	6895
5	15 Dec 93	40	38	18	35	90	37	0.40	3	4226
6	7 Jan 94	40	38	18	34	90		0.42	2	3114
7	12 Jan 94	40	38	18	24	102	40	0.37	2	2224
8	21 Jan 94	40	38	18	35	57		0.38	3	2447
9	26 Jan 94	20	38	18	35	75	31	0.40	2	2669
10	28 Jan 94	40	38	27	40	103	50	0.54	2	4671
11	2 Feb 94	40	38	34	31	80	31	0.36	1	2669
12	4 Feb 94	40	38	34	36	98	37	0.47	1	4893
13	9 Feb 94	40	38	27	37	107	34	0.50	1	3781
14	11 Feb 94	40	38	27	41	90	51	0.54	2	6228
15	16 Feb 94	40	38	34	38	108	59	0.54	3	5560
16	18 Feb 94	40	127	18	37	95	31	0.47	0	4448
17	23 Feb 94	40	127	18	33	79	32	0.38	0	2224
18	25 Feb 94	40	127	18	54	116	79	0.84	0	3559
19	1 Mar 94	40	127	34	53	100	52	0.84	1	11121
20	8 Mar 94	40	127	27	53	108	56	0.79	0	8674
21	11 Mar 94	40	127	27	55	85	42	0.75	1	11009
22	15 Mar 94	40	127	34	56	118	68	0.80	0	8585
23	18 Mar 94	40	127	34	41	128	72	0.58	0	7340
24	22 Mar 94	40	127	34	34	108	41	0.42	0	3225
25	25 Mar 94	40	127	18	43	90	45	0.69	0	6450
26	5 Apr 94	40	76	18	42	124	56	0.58	0	6005
27	7 Apr 94	40	76	18	40	94		0.53	0	6005
28	12 Apr 94	40	76	18	65	117	53	0.84	3	7562
29	15 Apr 94	40	76	27	55	101		0.90	1	13345
30	19 Apr 94	40	76	34	55	95		0.97	3	17793
31	22 Apr 94	40	76	18	42	122	49	0.56	2	3559
32	26 Apr 94	40	76	27	46	102		0.63	0	6895
33	29 Apr 94	40	76	34	46	114	56	0.63	1	4448
34	4 May 94	40	76	18	25	122	49	0.31	0	6228
35	6 May 94	40	76	27	33	93	31	0.40	0	3114

Figure 13. Measurement of the distance of the riprap surface from the strings at each grid point.

ice-free test. This technique provided a repeatable means of quantifying the amount of rock moved during a test by ice shoving.

Procedure

Before each test, we carefully leveled the rocks on the model riprap bank and filled in gaps in the riprap layer where necessary, as shown in Figure 14. The angle of the model bank was adjusted by changing the effective length of the support rods at the front (submerged) end of the model. Prior to freezing an ice sheet, we adjusted the water level in the test basin so that the model was submerged about halfway. We measured the water level relative to the model bank for each test and profiled the rocks using a grid technique explained above. We took photographs of the rocks directly above the model from a fixed vantage point before, dur-

Figure 14. Leveling rocks of model riprap in final preparation prior to each test.

Figure 15. Cutting of slots in the model ice sheet prior to each test.

ing and after each test.

After measuring and documenting the ice properties, we cut slots in the ice sheet along the length of the tank using chain saws mounted on a slow-moving carriage (Fig. 15). These slots were located such that the ice would not hit the side walls of the model riprap bank. This left a long strip of ice sheet no wider than the model bank, approximately 1.22 m (48 in.) wide, and as long as the test basin, approximately 30 m (100 ft) long. On each side, we cut two more slots 15 cm (6 in.) apart, and removed the ice between these slots.

Immediately prior to each test run, we recorded the initial values measured by the load cells. When we moved the carriage, the model riprap moved against the model ice sheet. We continued the test as long as there was sufficient ice to shove onto the model bank. After completion of each test, we recorded final force values.

We made video recordings of the ice interaction with the model bank during each test. We recorded the first eight tests from the front, and the remaining tests from the side. Some of the video recordings show the initial ice ride-up, followed by a gradual transition to ice pileup.

After the ice pile was removed from the model, we photographed the rocks again from the same position above the model to serve as a record of rock displacement. We profiled the rocks again using the grid technique explained above.

RESULTS

As mentioned earlier, Table 1 lists the values of parameters or variables that were either set or measured during each test. It also lists the maximum horizontal force measured during each test as well as the severity of damage to the model riprap bank. Some of the observations made during the tests are given below.

Observations on ice ride-up and pileup

We observed ice ride-up only during two tests: 3 and 18. The slope angle α of the bank in both these tests was 18.4° (1V:3H). During an ice ride-up event, we observed that the ice sheet was being pushed up the riprap slope and continually slid up and over the top edge of the model and back into the tank. During the ice ride-up events, the ice sheet dislodged some rocks upon initial impact, but generally did not displace enough rocks to expose the bank. Figure 16a shows an ice sheet riding up the model riprap bank for test 3. The action of the ice sheet sliding on top of the riprap shaved the underside of the ice sheet and filled in the interstitial spaces between the rocks, causing the riprap surface to become smooth. Figure 16b shows the riprap surface filled with ice shavings after we removed the ice sheet. Figure 17a and 17b show the riprap bank before and after test 3, respectively. As can be seen, there was very little displacement of the riprap.

During the initial stages of a test with a pileup, an ice sheet would contact the riprap, break into pieces, and ride up on top of the riprap, as shown in Figure 18. Although the ride-up continued for a long time in a few tests, the ice would usually pile up above the waterline and offer resistance to the incoming ice pieces. As the ice pile grew larger, there were instances when we observed an ice sheet pushing under the ice pile, gouging the model riprap, and bringing up small stones (Fig. 19). Figure 20 shows a sequence of photographs of an ice pileup during its formation. These photographs were taken during test 20, in which the bank angle was 27° (1V:2H) and the ice thickness was 53

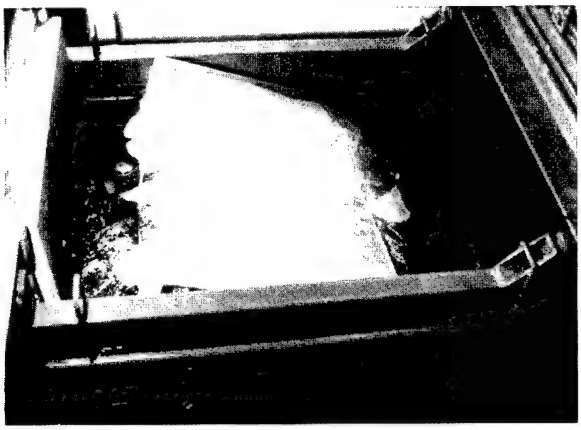

a. Ice riding up during a test run.

b. Riprap with shaved ice packed in the interstitial spaces between the rocks after the ice sheet was removed at the completion of a test.

Figure 16. Ride-up event.

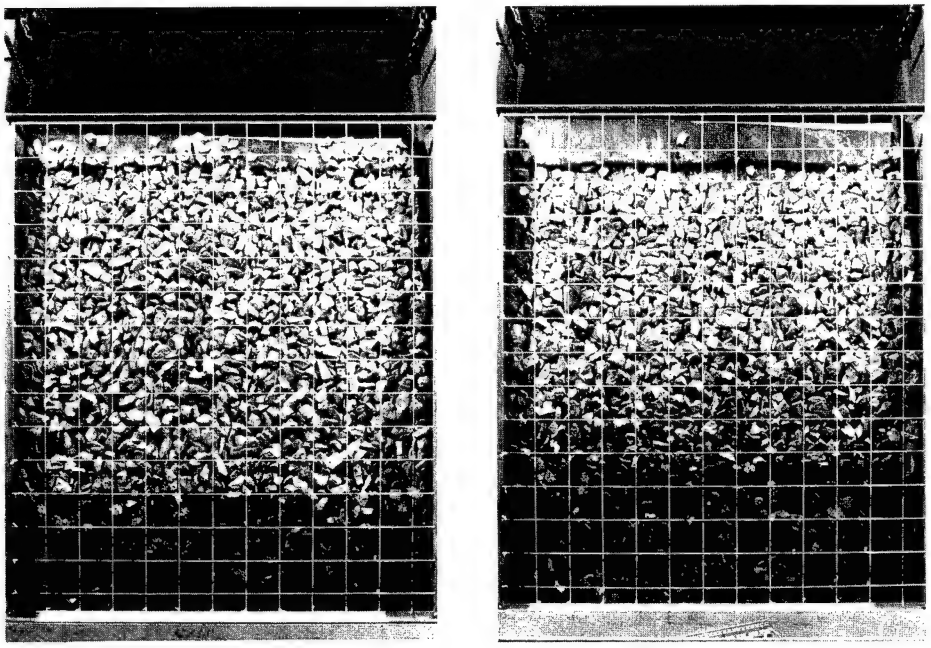

a. Before. *b. After.*

Figure 17. Model riprap before and after a test in which ice rode up the bank.

mm (2.1 in.). As shown in Figure 20a, the ice sheet broke into roughly rectangular-shaped pieces approximately 25 cm (10 in.) square as soon as the ice sheet contacted the bank above the waterline. Figure 20b shows the broken-up ice sheet going over the top edge of the bank and starting to pile up on one side of the riprap bank. Figure 20c shows the ice sheet riding up and over the top edge of the bank on one side of the model, and beginning to pile up on the other side. As more of the ice sheet continued to shove onto the bank, the ice pieces stacked up on the previously deposited ice pieces (Fig. 20d). At this stage, no ice was being pushed off at the top edge of the bank because all the ice pieces piled up high, creating a steep incline for the incoming ice sheet. Figure 20e and f show that the ice sheet piled up and crushed into the ice pile. In these last two views, it is possible to see rocks being brought to the surface of the ice pile by the ice sheet. We observed the rocks being transported from the bed to the surface of the ice pile during most of the tests in which the ice piled up on the bank.

At times, the ice sheet would buckle one or more

Figure 18. Ice sheet after it is broken and pushed up the riprap bank.

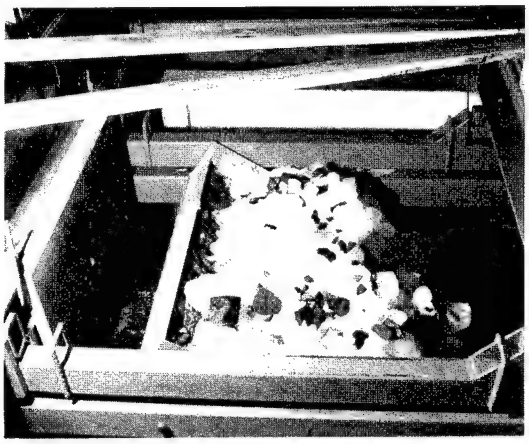

Figure 19. Stones brought up to the surface of an ice pile.

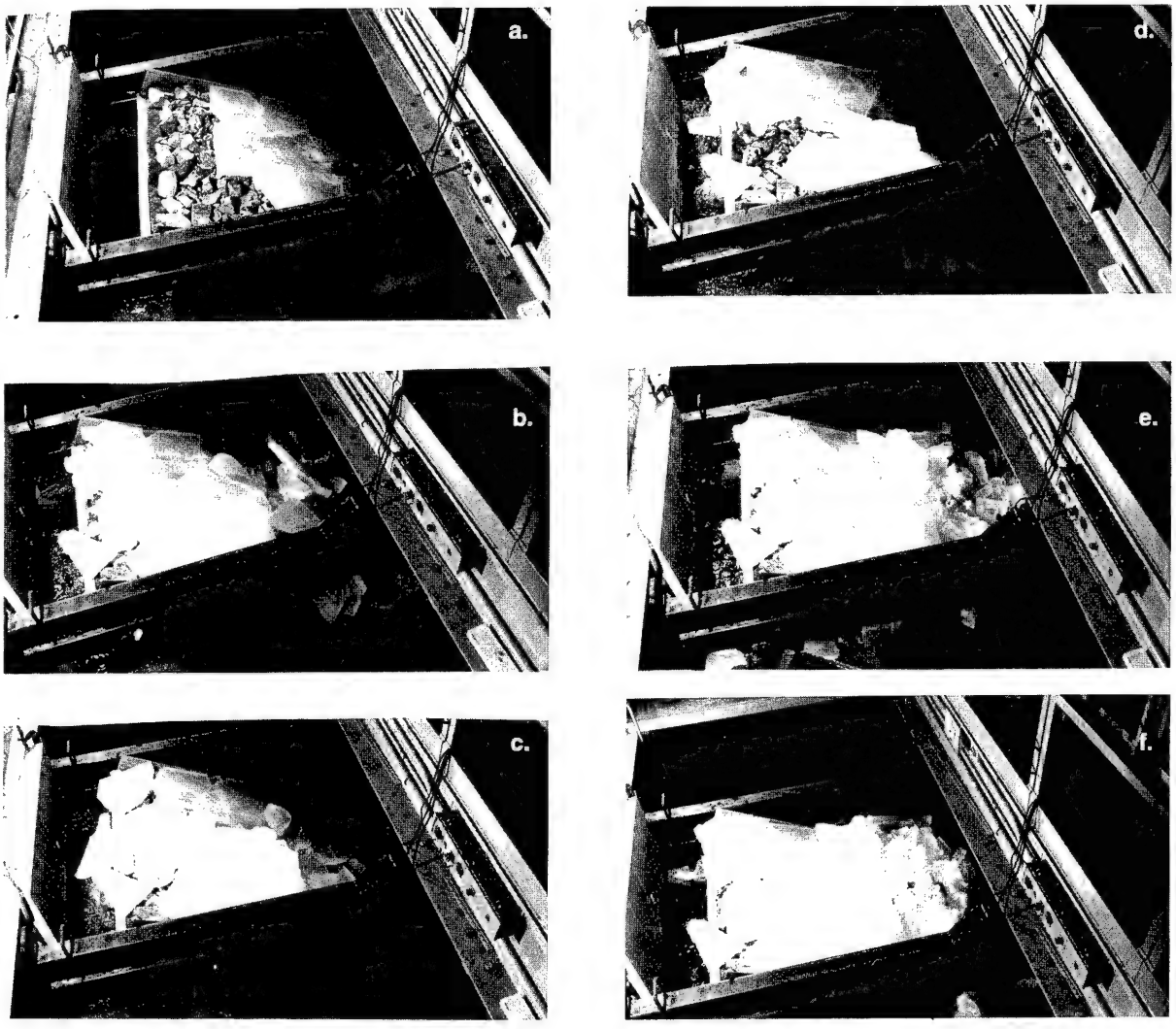

Figure 20. Sequence of ride-up and pileup events for test 20, in which the ice thickness was 53 mm (2.1 in.), and the bank slope was 27° (1V:2H).

times during a test. As discussed later, the forces associated with buckling represent the maximum force that a model ice sheet could impart on the model riprap. Buckling events represent large-scale failure of the model ice sheet, and this did not cause large-scale failure of riprap in our tests. However, the model ice sheet caused small-scale damage by removing individual stones one at a time.

Measured horizontal and vertical forces

The forces on the model during open water test runs (without any ice) were much smaller than those measured during tests with model ice. Figure 21 shows typical time-history plots of the horizontal force, which were obtained by summing the load measured by two load cells (Fig. 8). This

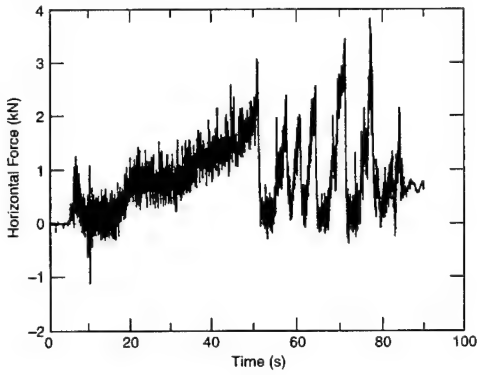

Figure 21. Typical plot of the horizontal component of the force acting on the riprap.

plot shows a slight increase in the force, caused by the edge of the ice sheet first coming in contact with the model, at about 7 seconds after the start. For the next 10 seconds, the ice rode up and over the model bank, as indicated by the relatively constant horizontal force. This force was the result of the friction force between the ice sheet and the riprap. For the next 30 seconds, the horizontal force gradually increased until it reached a peak value at about the 50-second mark. Figure 21 has several cycles of increasing force followed by sudden reductions in force during the remaining duration of the test. Each reduction in force was due to buckling failure of the ice sheet during the interaction. In this study, buckling failure limits the force that could be imparted to the model riprap by the model ice sheet.

To obtain the total vertical load acting on the model riprap, we summed the output of three load cells placed between the two frames (Fig. 8). Figure 22 shows a typical time-history plot of verti-

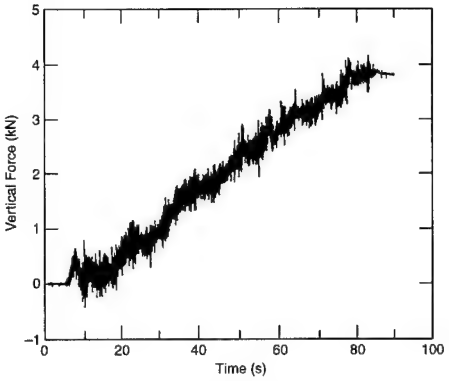

Figure 22. Typical plot of the vertical component of the force acting on the riprap.

cal force, which generally increased with time because the force was largely a measure of the weight of accumulated ice on the model. During a few tests, one of the forward two load cells for measurement of the vertical force stopped functioning. Because of symmetry in the longitudinal direction, the measured force from the other forward load cell was multiplied by two and added to the measured value from the third load cell to get the total vertical load. After the defective load cell was replaced with a new load cell, the outputs of three load cells were added to obtain the total vertical load.

Plot of maximum horizontal force

In Appendix C, we have given the plots of horizontal and vertical forces from all ice tests. In Table 1, we have also tabulated the maximum horizontal force in each test. These maximum force values were in the range of 1.8 and 17.8 kN (405–4000 lb).

During the model tests, we observed crushing, bending and buckling failures of the ice sheet during its interaction with a model riprap bank. Crushing of ice occurred in localized areas where the ice came in contact with the stones during ice ride-up. An intact sheet predominantly broke up into pieces by bending failure that took place in longitudinal as well as transverse directions. These ice pieces either rode over or piled on top of the riprap surface. Ride-up occurred for low values of the bank slope, whereas a pileup formed for high values of the bank slope. At times, the ice sheet plowed through the piled up material, gouged the riprap at the bottom, and brought out stones with it. This took place as long as the ice sheet was capable of exerting sufficient force, which was limited by the buckling failure of ice. Therefore, the maximum

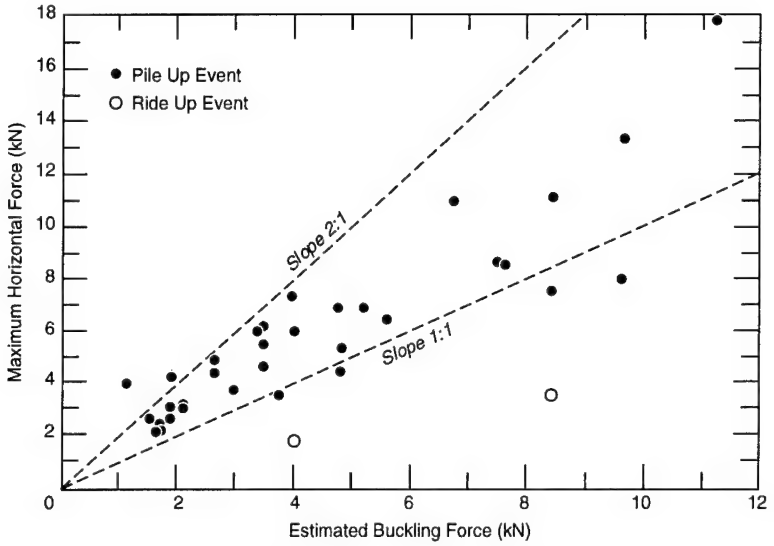

Figure 23. Plot of maximum force recorded during each test vs. $b\rho_w g L^2$, *where* b *is the width of ice sheet,* $\rho_w g$ *is the specific weight of water, and* L *is the characteristic length of floating ice sheet.*

force that we could expect to measure during a test is the force required to buckle an ice sheet. The buckling force of a semi-infinite beam of floating ice is between $b\rho_w g L^2$ and $2b\rho_w g L^2$, corresponding to the frictionless and hinged boundary conditions (Hetenyi 1946), respectively, where b is the width of the beam, $\rho_w g$ is the specific weight of water, and L is the characteristic length of floating ice sheet. Figure 23 shows the plot of maximum measured force vs. $b\rho_w g L^2$ for all tests. Most of the data fall between the lines having a slope of 1 and 2, indicating that the boundary condition on the edge of the ice sheet was something between that of frictionless and hinged.

Though buckling failure limits the horizontal force in model tests, the forces in full-scale situations will be limited by the amount of environmental forces (wind and water stresses or thermal expansion) acting on an ice sheet, by the momentum of moving ice floes, or by the forces required to fail an ice sheet in bending, crushing, or buckling. During initial stages of ice shoving, the bending failure of ice will limit the force that an ice sheet can exert on the riprap, because this failure mode requires the least force per unit width of the ice sheet. If the ice sheet forms an ice pileup, the ice sheet may be possibly confined to fail in crushing or buckling. It is also possible for the zone of failure to progress offshore, creating a rubble field.

Observed failure of riprap

An ice pileup consisted of the ice sheet breaking into small pieces and piling one on top another. An ice pileup most often caused failure of the riprap when the advancing ice sheet was forced to go between the riprap and the piled up ice. In general, we defined the riprap to have failed if enough rock material was displaced to expose underlying areas of the riprap-protected bank. For example, the ice piled up significantly in test 4, as shown in Figure 24. During that test, the ice gouged away enough riprap to expose large areas of the bank, as shown in Figure 25. In test 5, an ice pileup formed below the water line, as can be seen by the damage to riprap shown in Figure 26. Figures 27a and b show the contour plots of the rock surface, which were generated from the rock profile data taken before and after test 5. Such contour plots help to visualize the total displacement of the riprap during a test. The contour plots

Figure 24. Ice pileup after test 4.

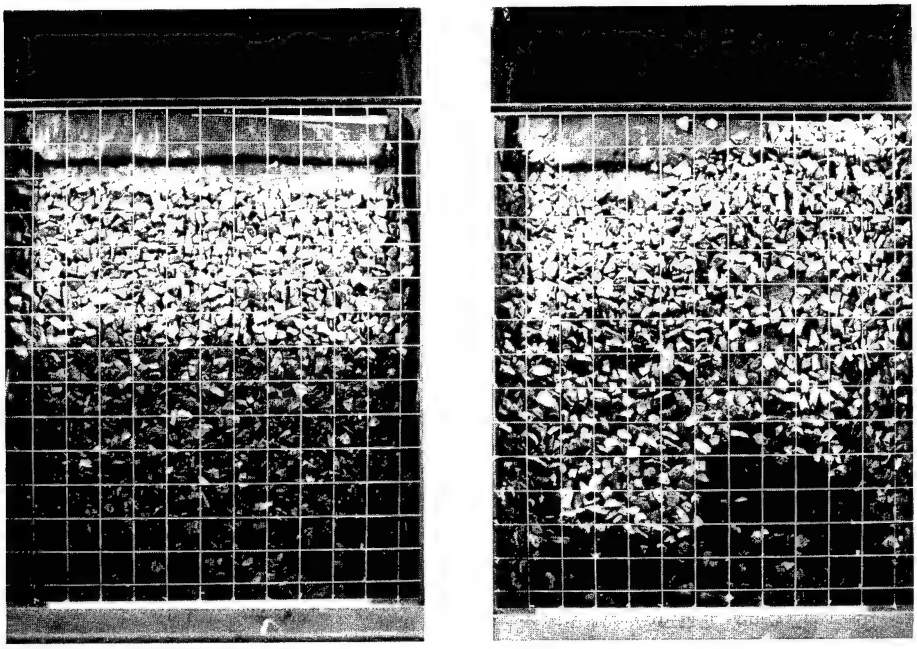

a. Before test. *b. After test.*

Figure 25. Model riprap before and after test 4. The difference between these photographs indicates the extent of rock movement.

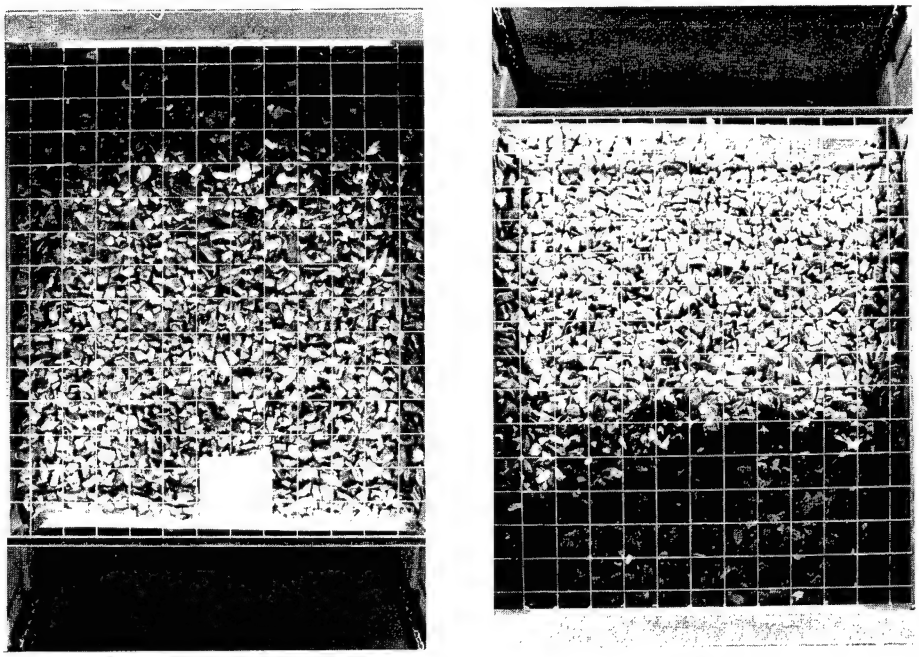

a. Before. *b. After.*

Figure 26. Model riprap before and after test 5. The difference between these photographs indicates the extent of rock movement.

shown in Figure 27 show a typical pattern of ice action on riprap, in that the rock was gouged out just below or at the waterline and was deposited in a hump above the waterline.

During a test in which ice piled up, we observed that some of the rock material was removed from the bed and deposited on top of the ice pile. In some tests, the rocks were tossed from the bed and over the top edge of the bank. Figure 19 shows the rocks in the ice pile towards the end of the test 20. After

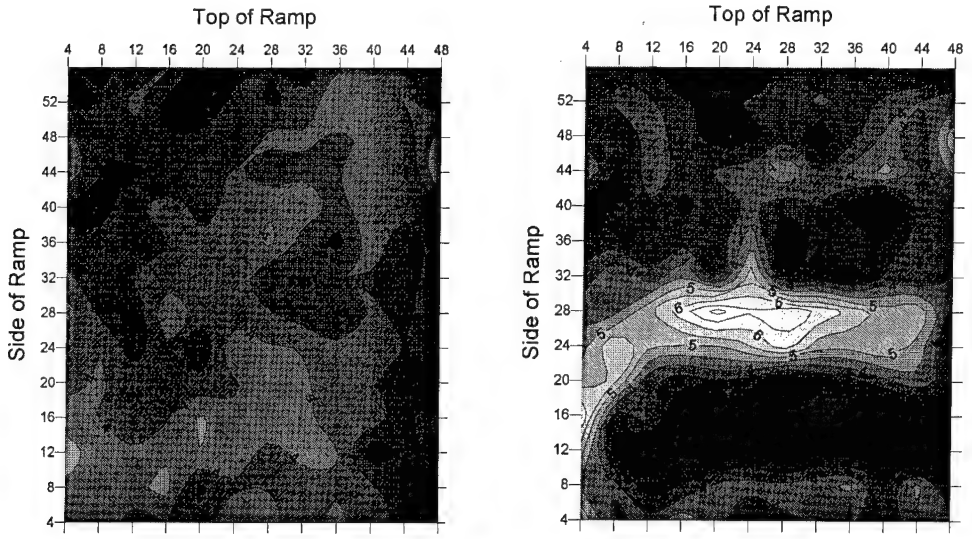

a. Before. *b. After.*

Figure 27. Contour plots of the model riprap before and after test 5. These contour plots show both extent and amount of rock movement during test 5. The numbers along contour lines denote measured distance from the string in the grid frame.

Figure 28. Rocks found on top of the ice pile during melting of ice after test 20.

this particular test, we allowed the ice to melt on top of the damaged riprap and observed that the model bank was barren of rock under the last bit of ice, as shown in Figure 28. Later, when the ice melted away completely, the rocks on top of the ice were deposited onto the barren patch, though not quite covering it. We observed this "self healing" behavior in many tests after an ice pileup. In the open-water bank protection by riprap, this self healing of riprap also takes place, which makes riprap a popular choice for projects that require low maintenance.

After an ice run on the smallest stone size (test 8), we observed that the ice sheet had deformed the sand bed as well as the riprap, as shown in Figure 29. After test 30, we observed a far greater amount of ice damage than usually encountered; the ice tore the filter fabric (Fig. 30). These observations indi-

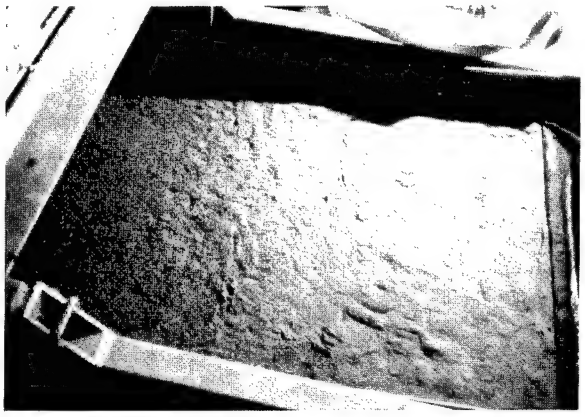

Figure 29. Sand bed of model bank deformed by ice action after test 8.

Figure 30. Damage to filter fabric by ice action after test 30.

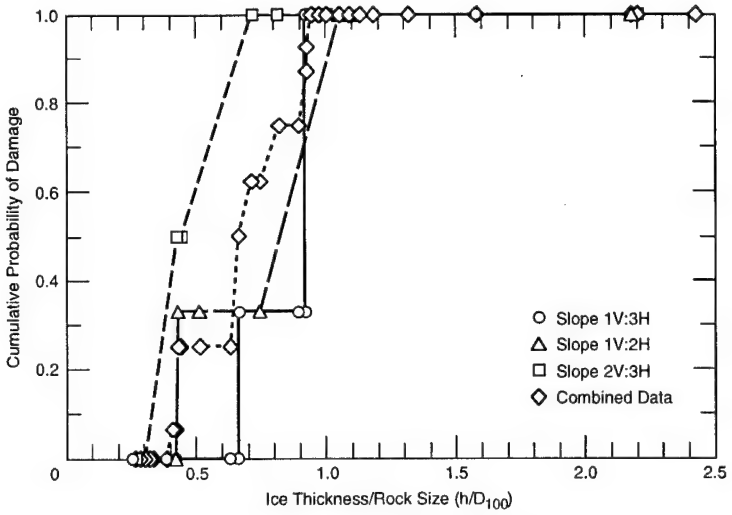

Figure 31. Plot of cumulative probability of damage vs. the ratio of ice thickness to D_{100} rock diameter.

cate that the small-stone riprap was not only inadequate to resist these ice actions, but also made the underlying bank material highly vulnerable to damage by ice.

In Table 1, we have given numerical values to the level of riprap failure, as visually apparent to us in terms of exposure of filter fabric underneath the stones. A failure level designated by 0 was assigned to tests when we did not observed significant displacement of rocks. A failure level designated by 1 was assigned to slight damage during tests in which we observed small areas, on the order of 20 cm^2 (3 $in.^2$), of filter fabric. A failure levels designated by 2 was assigned to damages in those tests where we observed moderate area of riprap damage (20–65 cm^2 or 3–10 $in.^2$). Lastly, a failure level of 3 was assigned to damages in those tests in which we observed large areas of riprap gouged from the bank, resulting in exposed bank areas of 65 cm^2 (10 $in.^2$) or more. In Appendix D, we have also presented the photographs of the riprap taken before and after each test.

Failure and nonfailure of riprap vs. ratio of ice thickness to rock size

The damage to the riprap takes place as a result of interaction between an ice sheet and an individual rock. However, we do not know the exact nature and magnitude of the ice pressure on an individual rock. It is for this reason that we have done model tests, as in the case of waves and currents, to determine the ice damage to the riprap.

We conducted model tests with three bank slopes, and the damage the riprap was noted in each test. For each bank slope angle, we calculated to the ratio of ice thickness to the maximum rock diameter and ranked this ratio from smallest value to the largest value. When the outcome of a test was associated in terms of riprap failure or nonfailure, we found that there was no damage to the riprap when the ice thickness was small compared to the maximum rock size. On the other hand, we found that the ice sheet always damaged the riprap when it was large compared to maximum rock diameter. In Figure 31, we have plotted these results for each bank slope in terms of cumulative probability of riprap failure vs. ratio of ice thickness to D_{100} rock diameter. There was a range of ice-thickness/rock-size ratios in which the damage to the riprap was random.

The plots in Figure 31 show that the values of ice-thickness/rock-diameter (h/D_{100}) ratio at which transition from nonfailure to failure takes place decrease with the increase in the bank slope angle. By combining the data from all tests for the three bank slope angles, we have plotted the cumulative probability of riprap failure with respect to the ratio of ice thickness to nominal rock diameter. These plots indicate that there is no damage to the riprap when h/D_{100} is less than 0.35 and that the riprap is always damaged when h/D_{100} is greater than 1. From the results shown in Figure 31, the riprapped banks with shallow slope (1V:3H) are less prone to damage by ice shoving than those with steeper slopes (1V:1.5H). For shallow slope (1V:3H) banks, the rock size should be about twice the ice thickness to sustain no damage by ice shoving. For steeper slopes (1V:1.5H), the rock size (D_{100}) should be about three times the ice thickness to prevent damage by ice shoving.

DISCUSSION

The functions of a riprap armor are to protect a sloping embankment against waves or currents in a channel at a minimum-cost balance between initial construction cost and future maintenance. In cold regions, the design procedures against wave action or erosive forces of currents remain the same as those in warm regions. In addition, Matheson (1988) discussed that one should consider the breakdown of rocks due to freeze-thaw action, plucking of rocks by rising and falling ice sheets due to water level changes, and shoving action by moving ice sheets.

The observations made in relation to dams and rivers (Matheson 1988, Doyle 1988, Wuebben 1995) have been discussed earlier. To avoid plucking of rocks by rising ice sheets, Matheson (1988) suggested that riprap should have a D_{50} in excess of the maximum winter ice thickness. Though based on a limited number of tests, the results of this study show that the maximum rock size (D_{100}) in a riprap should be two to three times the ice thickness to avoid any damage to riprap by ice shoving. Costs of construction and maintenance for a given site should also be considered. It may be cost-effective to protect those areas of an embankment that are more prone to damage by ice shoving, according to the results of this study. Frequency of damage by ice shoving is another factor that needs to be considered in the design of a riprap protection of a bank, because it may be cost-effective to repair riprap damage that occurs rarely (Doyle 1988).

SUMMARY AND CONCLUSIONS

A review of literature on ice effects on riprap revealed practically no guidance available for design of riprap in the cold regions, where the presence of moving ice can cause considerable damage to a riprapped bank. To generate data on riprap damage by ice shoving, we conducted a series of small-scale tests in which we pushed a model riprap-covered embankment against 1.22-m-wide model ice sheets grown in the test basin of our laboratory. During the 35 tests, we changed the slope of the model riprap bank, the size and the mix of rocks, and the thickness of model ice sheets. Except during the first two tests, we moved the carriage at a constant speed of 40 cm/s. The interaction between the model riprap bank and the ice mostly resulted in ice pileup, except during two tests when ice rode up the bank. We measured the horizontal and the vertical components of the interaction force during the tests. We observed that the ice sheet buckled many times during a test, and that the buckling failure limited the maximum force an advancing ice sheet could exert during the small-scale tests.

There was very little or no damage to the riprap during ice ride-up events, which occurred on shallow-slope (1V:3H) banks. Most of the riprap damage occurred when the ice piled up on the riprap, and the incoming ice sheet was forced to go between the riprap and the piled-up ice. We observed that some of the rock material was removed from the bed and brought up to the surface of the ice pile. The most severe damage occurred at or below the water level. We considered the riprap to have failed if the rock material was displaced by ice to expose a certain amount of area on the bank. From the results of these tests, we conclude that the maximum size (D_{100}) of rocks should be twice the ice thickness for shallow slopes (1V:3H) to sustain no damage by ice shoving, and that the maximum rock size (D_{100}) should be about three times the ice thickness for steeper slopes (1V:1.5H).

LITERATURE CITED

Construction Industry Research and Information Association (1991) *Manual on the Use of Rock in Coastal and Shoreline Engineering*. Construction Industry Research and Information Association, CIRIA Special Publication 83, CUR Report 154. Rotterdam: A.A. Balkema Publishers.

Collins, J.I. (1988) Large precast concrete armor units in the Arctic. In *Arctic Coastal Processes and Slope Protection Design* (A.T. Chen and C.B. Leidersdorf, Ed.). Technical Council on Cold Regions Engineering Monograph, American Society of Civil Engineers, New York, p. 208–215.

Coastal Engineering Research Center (1984) Shore Protection Manual. U.S. Army Corps of Engineers Waterways Experiment Station, Vicksburg, Mississippi, Vol. I and II.

Croasdale, K.R. (1980) Ice forces on fixed, rigid structures. In *Working Group on Ice Forces on Structures* (T. Carstens, Ed.). USA Cold Regions Research and Engineering Laboratory, Special Report 80-26, p. 34–106.

Croasdale, K.R., R.W. Marcellus (1978) Ice and wave action on artificial islands in the Beaufort Sea. *Canadian Journal of Civil Engineering*, **5**(1): 98–113.

Croasdale, K.R., N. Allyn and W. Roggensack (1988) Arctic slope protection: Considerations for ice. In *Arctic Coastal Processes and Slope Protection Design* (A.T. Chen and C.B. Leidersdorf, Ed.). Technical

Council on Cold Regions Engineering Monograph, American Society of Civil Engineers, New York, p. 216–243.

Doyle, P.F. (1988) Damage resulting from a sudden river ice breakup. *Canadian Journal of Civil Engineering*, **15**(4): 609–615.

Gadd, P.E. (1988) Sand bag slope protection: Design, construction and performance. In *Arctic Coastal Processes and Slope Protection Design* (A.T. Chen and C.B. Leidersdorf, Ed.). Technical Council on Cold Regions Engineering Monograph, American Society of Civil Engineers, New York, p. 145–165.

Hopkins, M.A. (1995) The ice pile-up problem: A comparison between experiments and simulations. In *Ice Mechanics—1995* (J.P. Dempsey and Y.D.S. Rajapakse, Ed.). American Society of Mechanical Engineers, New York, AMD, vol. 207, p. 211–218.

Hetenyi, M. (1946) *Beams on Elastic Foundations*. Ann Arbor, Michigan: University of Michigan Press.

Kovacs, A. and D.S. Sodhi (1980) Shore pile-up and ride-up. Field observations, models, theoretical analyses. *Cold Regions Science and Technology*, **2**: 209-288.

Leidersdorf, C.B. (1988) Concrete mat slope protection for Arctic applications. In *Arctic Coastal Processes and Slope Protection Design* (A.T. Chen and C.B. Leidersdorf, Ed.). Technical Council on Cold Regions Engineering Monograph, American Society of Civil Engineers, New York, p. 166–189.

Matheson, D.S. (1988) Performance of riprap in northern climates. Contract report to the Canadian Electrical Association, CEA No. 625 G 571, Acres International Limited, Winnipeg, Manitoba, Canada.

McDonald, G.N. (1988) Riprap and armor stone. In *Arctic Coastal Processes and Slope Protection Design* A.T. Chen and C.B. Leidersdorf, Ed.). Technical Council on Cold Regions Engineering Monograph, American Society of Civil Engineers, New York, p. 190-207.

Nevel, D.E. (1983) Pressure ridge forces. In *Proceedings, 7th International Conference on Port and Ocean Engineering Under Arctic Conditions (POAC '83), 5–9 April, Technical Research Centre of Finland, Helsinki, Finland.* Espoo, Finland: Valtion Teknillinen Tutkimuskeskus, vol. 1, p. 212–220.

Sodhi, D.S., K. Kato, F.D. Haynes and K. Hirayama (1982) Determining the characteristic length of model ice sheets. *Cold Regions Science and Technology*, **6**(6): 99–104.

Sodhi, D.S., K. Hirayama, F.D. Haynes and K. Kato (1983) Experiments on ice ride-up and pile-up. *Annals of Glaciology*, **4**: 266–270.

U.S. Army Corps of Engineers (1991) Hydraulic design of flood control channels. Engineer Manual EM 1110-2-1601, Washington, D.C.

Van der Meer, J.W. (1988) Rock slopes and gravel beaches under wave attack. Doctoral thesis, Delft University of Technology; also Delft Hydraulics Communication 396.

Wuebben, J.L. (1995) Ice effects on riprap. In *River, Coastal and Shoreline Protection: Erosion Control Using Riprap and Armourstone* (C.R. Thorne, S.R. Abt, F.B.J. Barends, S.T. Maynord and K.W. Pilarczyk, Ed.). New York: Wiley, p. 513–530.

APPENDIX A: DESIGN OF RIPRAP PROTECTION AGAINST WAVES

Wind-generated waves induce one of the most powerful forces on coastal structures. A given structure may be subjected to nonbreaking, breaking, and broken waves during different stages of a tidal cycle. The significant wave height is obtained from historical data to represent the wave condition at a site. The riprap stability formula (Coastal Engineering Research Center 1984), based on small-scale and large-scale model testing, is given by:

$$W_{50} = \frac{\rho_r g H^3}{K_D (S_r - 1)^3 \cot\theta} \qquad \text{(A1)}$$

where W_{50} = median weight of individual armor unit in primary cover layer,
ρ_r = density of armor unit
g = acceleration due to gravity
H = design wave height at the structure ($\approx H_{1/10}$ average of the highest 10% of all waves)
S_r = ρ_r/ρ_w ratio of the armor density to the water density
θ = angle of structure slope measured from the horizontal
K_D = stability coefficient that varies primarily with the shape of the armor units, roughness of the armor unit surface, sharpness of edges, and the degree of interlocking obtained in placement
= 3.5 for breaking waves
= 4.0 for nonbreaking waves.

Because of its simplicity, the above formula is easy to work with. The values of K_D have been derived for a wide range of armor units and configurations. However, the above formula has many limitations. This formula is based on small-scale model tests, and does not account for the level of damage, storm duration and wave period.

As reported in CIRIA Special Publication 83 (1991), Van der Meer (1988) proposed a number of formulas for deep and shallow water conditions and for plunging and surging waves. These formulas, which incorporate the effect of wave period, the storm duration, the permeability of the structure, and clearly defined damage level, are given in CIRIA Special Publication 83 (1991).

Design of riprap protection of flood control channels

The guidance for the riprap slope protection of flood control channels (U.S. Army Corps of Engineers 1991) applies to open channels having a slope of less than 2%. The ability of the riprap material to resist the erosive forces of channel flow depends on the following parameters: shape, size, weight and durability of stone; gradation and layer thickness of riprap; and alignment, cross section, gradient and velocity distribution in a channel. The basic equation for the representative stone size in straight or curved channels is given by

$$D_{30} = S_f C_s C_v C_T d \left[\left(\frac{\gamma_w}{\gamma_s - \gamma_w} \right)^{1/2} \frac{v}{\sqrt{K_1 g d}} \right]^{2.5} \qquad \text{(A2)}$$

where D_{30} = riprap size of which 30% is finer by weight
S_f = safety factor (≈ 1.1)
C_s = stability coefficient for incipient failure
C_v = coefficient related to vertical velocity distribution
C_T = thickness coefficient
d = local depth of flow
γ_w = specific weight of water
γ_s = specific weight of stone
v = local average velocity
K_1 = side slope correction factor = $\sqrt{1 - (\sin^2\theta / \sin^2\phi)}$
θ = angle of side slope
ϕ = angle of repose
g = acceleration due to gravity.

Recommended values of various coefficients and factors are given in EM 1110-2-1601 (U.S. Army Corps of Engineers 1991). Special attention needs to be given for the design of toe protection and filter material between the riprap and the underlying material. Construction quality needs to be maintained for the size, the shape and the gradation of stones.

APPENDIX B: REVIEW OF SLOPE PROTECTION SYSTEMS USED IN THE ARCTIC

Sand bag slope protection

Since 1972, sand bag slope protection has been used effectively in the offshore islands built along the Canadian and the Alaskan coasts of the southern Beaufort Sea. Gadd (1988) described the design and the development of slope protection by the use of sand bags. He discussed the placement of sand bag armor on two artificial islands: Resolution Island in 2.4-m water depth, and Seal Island in 12-m water depth. Both these islands had a design life of three years. Because of the limited design life and also unavailability of large stone at the sites, sand bag slope protection was considered to be the only viable option.

Resolution Island required about 100,000 m^3 (3.5×10^6 ft^3) of gravel that was delivered to the site by barges from a gravel pit onshore. The 1.5-m^3 (53-ft^3) bags were filled from a barge-based bagging plant and were placed end-to-end fashion (no overlapping) with a 60-ton crane at a maximum rate of 30 bags per hour. After completion of construction in 1980, annual inspection of slopes above and below water were conducted. Damaged bags were replaced in 1981 and 1984. Because of shallow water and resulting mild environment, damage due to wave action alone was not observed. The principal cause of bag loss was due to ice abrasion and puncture, followed by fill loss due to wave action on torn bags.

Seal Island was constructed in 1982 about 17 km (10.5 miles) northwest of Prudhoe Bay. The environmental forces of moving ice and summer wave action were larger at this sites than those at any previous site in Alaska. To construct the island core, about 535,000 m^3 (18.9×10^6 ft^3) of gravel was transported to the site from an onshore quarry in winter over an artificially thickened floating ice road. About 17,100 gravel bags, each 3 m^3 (106 ft^3) capacity, were used to protect the slope. Based on the results of model testing, the bags were arranged in a 50% overlap configuration above –6 m (–20 ft) level to enhance their stability. Bags were produced on-site at an average rate of 400 bags per day. Floating ice damaged the sand bags located between elevations +1.5 m (+5 ft) and –6 m (–20 ft). The ice would tear the bag fabric, allowing the gravel fill to escape. During two late summer storms, many bags were removed by the 2-m-high wave action, yielding armor gaps near the waterline. Due to the 50% overlap bag placement configuration, there were abundant bags that could slide down slope to cover the voids and provide slope protection for the life (ca. 5–10 years) of the island.

Sand bag slope armor has proven to be effective protection for short-lived offshore structures in the Arctic. However, it can be damaged by ice during both summer and winter, and also by ultraviolet radiation affecting the strength of bag fabric. Periodic repairs should be conducted to prevent progressive deterioration and to prolong the functional life of a sand-bag slope armor system.

Concrete mat slope protection

As mentioned above, the sand bag armor is susceptible to damage from ice impacts and loss of fabric strength from exposure to ultraviolet radiation. Moreover, the filling and placement of sand bags are time-consuming and labor-intensive operations. Because suitable quarry sites are scarce along the Beaufort Sea coast, articulated concrete mats have been selected as an effective and economical slope protection in the Arctic since 1980. Leidersdorf (1988) has given a summary of Arctic experience with concrete mat armor installed at six sites along the Alaskan Beaufort Sea coast. Potential advantages of concrete mat armor are 1) low weight per unit area because of interblock linkages, 2) resistance to damage from ice impacts and low temperatures, 3) ability to accommodate changes in the subgrade without major fill loss, and 4) modular placement and removal. Leidersdorf (1988) discussed hydraulic, ice, and material design considerations; fabrication and installation procedures; and additional research needed to understand their failure modes, hydraulic stability, and long-term durability. The capital costs of installing a concrete mat armor are higher than those for sand bag armor, but the maintenance costs are comparatively lower. Hybrid slope protection systems, consisting of sand bag armor and concrete mat armor, have been used to cut down the construction cost. On Northstar Island, the concrete mat extended from +1.5 m (+5 ft) to –6 m (–20 ft) levels, and sand bag armor was used above and below the concrete mat armor (Leidersdorf 1988).

Riprap and armor stone

McDonald (1988) discussed the use of quarry stone for slope protection in the northern environment. He cites two examples where stone was used for slope protection, both in Nome, Alaska. The first example is the 1067-m- (3500-ft-) long seawall, constructed in 1950. It has been overtopped by wind-driven, first-year ice many times without sustaining any damage. The seawall contains 125,000 tons of granite stone, ranging in size up to 6 tons. The second example is that of jetties built for the Nome Harbor in 1920. These jetties were protected with stone, which suffered damage from storms and ice. These were replaced with steel sheet pile and concrete jetties in 1939.

Experience with the action of multiyear ice on riprap stone does not exist in the Arctic(McDonald 1988). This may be attributed to lack of quarries and transportation systems along the Beaufort Sea coast. McDonald (1988) discussed the damage caused by the buoyant uplift of submerged ice frozen to stones. He mentioned that loss of stone due to buoyancy of ice is not common and is usually restricted to small-size stones.

Collins (1988) reviewed the behavior and performance of large concrete units for arctic slope protection, and found that there is little knowledge of their expected performance in thick ice. He commented that the experience of slope protection in the Great Lakes, Gulf of Labrador, and Gulf of Finland cannot be extrapolated to high Arctic conditions.

APPENDIX C: PLOTS OF HORIZONTAL AND VERTICAL FORCES MEASURED DURING THE TESTS

TEST 1

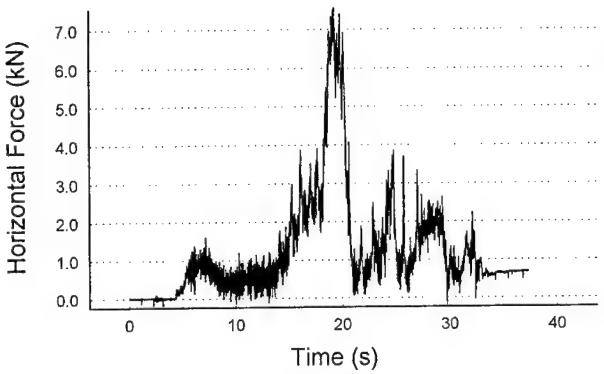

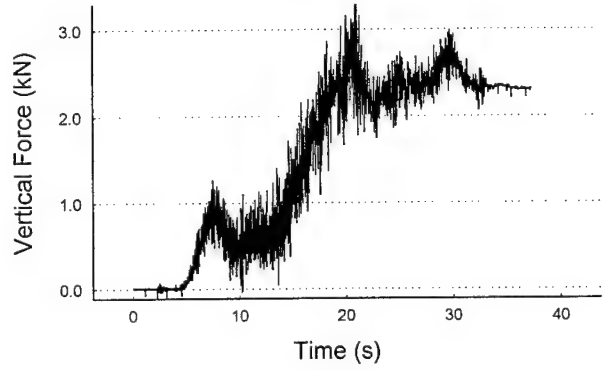

TEST 2

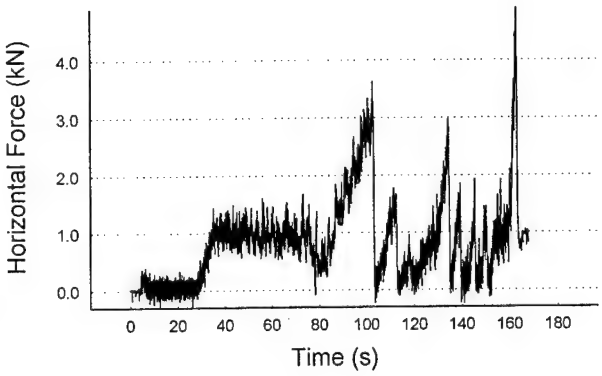

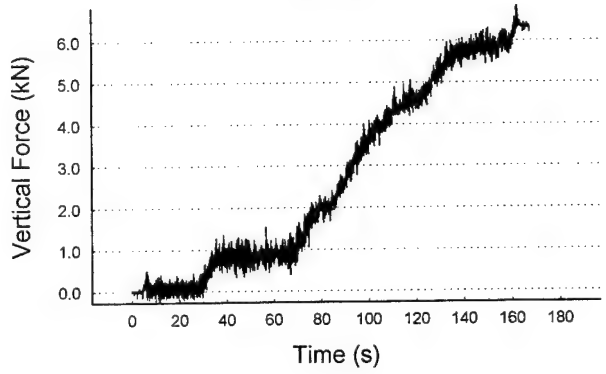

TEST 3

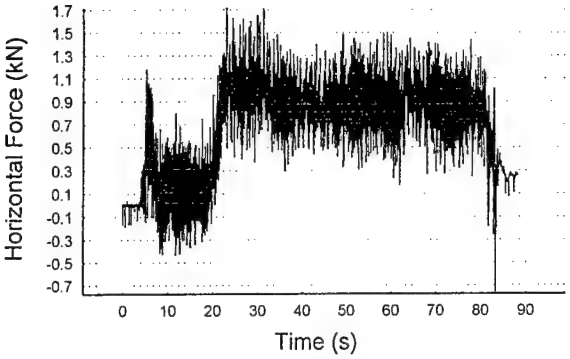

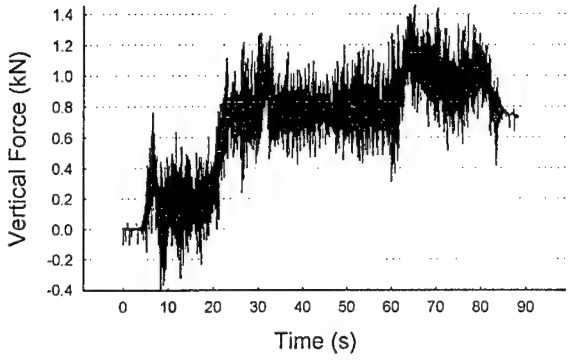

TEST 4

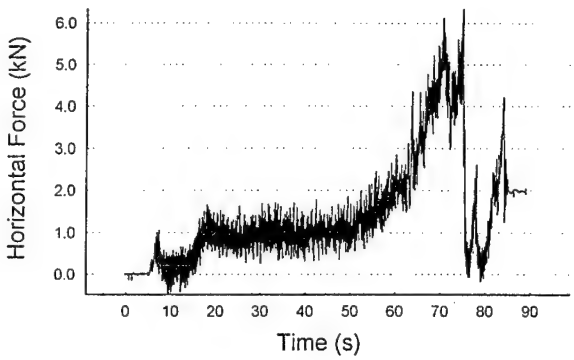

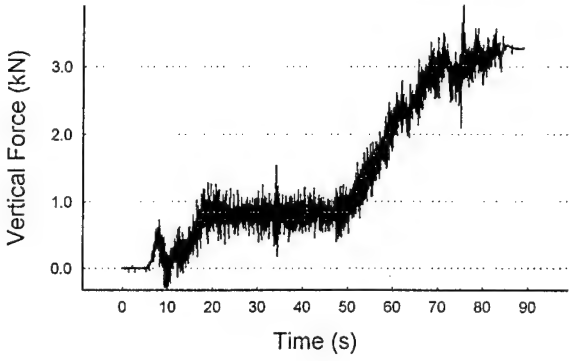

TEST 5

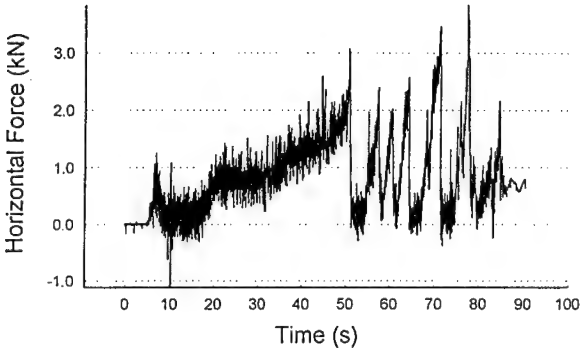

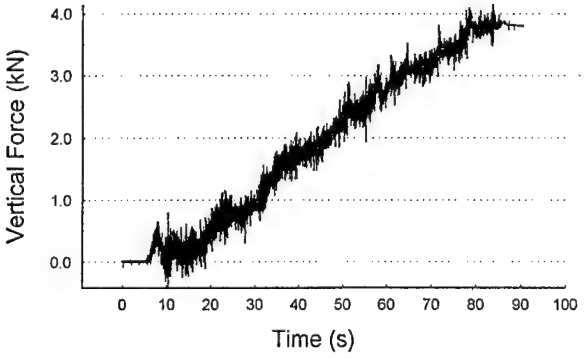

TEST 6

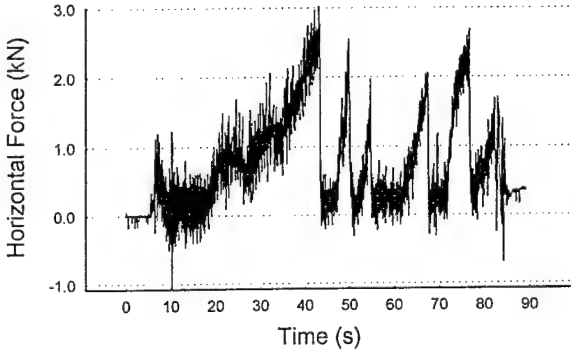

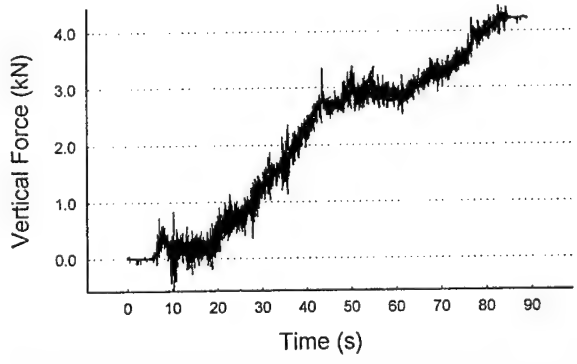

TEST 7

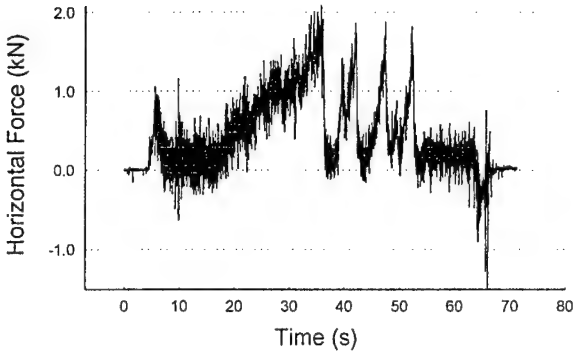

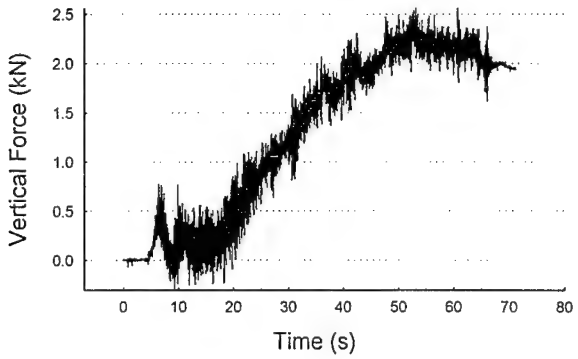

TEST 8

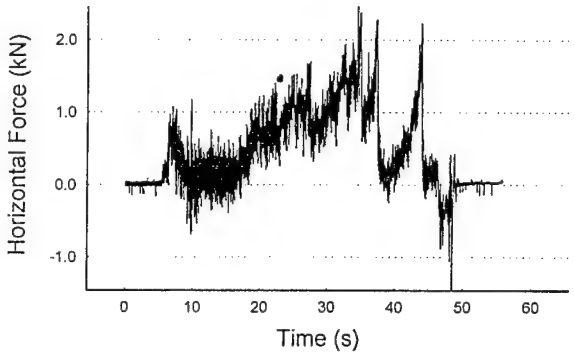

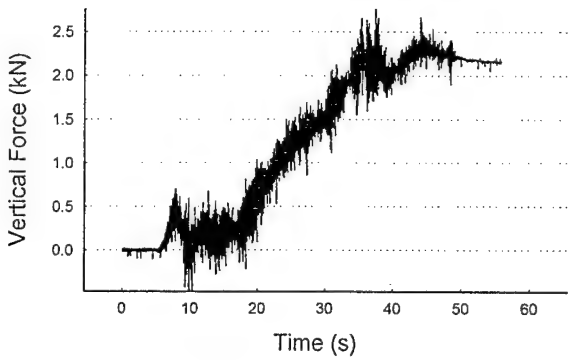

TEST 9

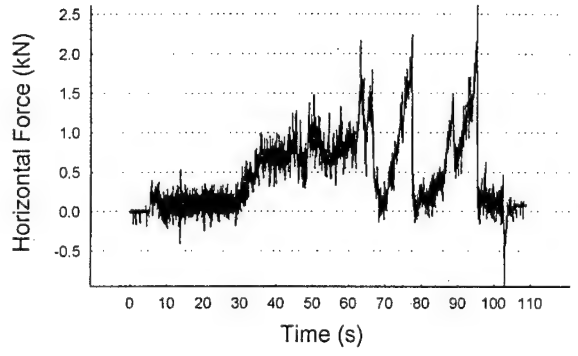

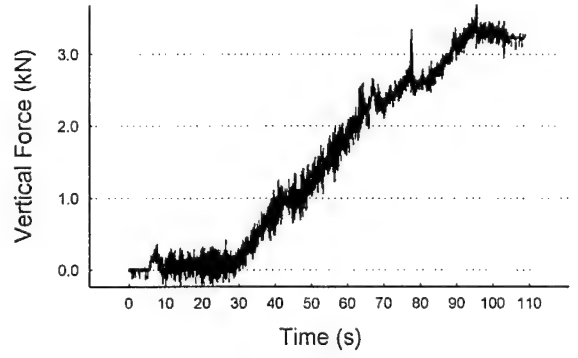

TEST 10

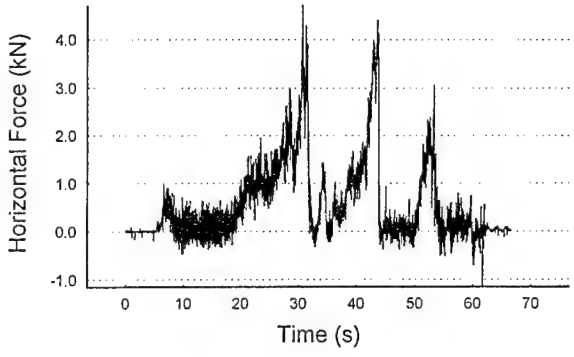

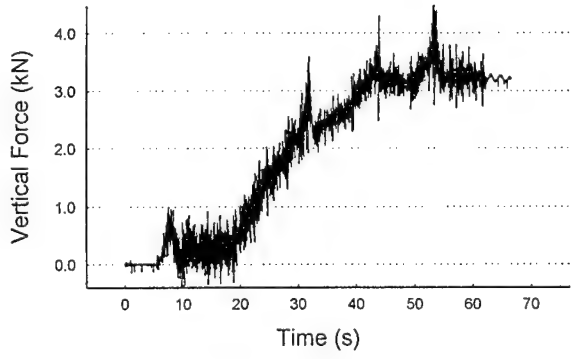

TEST 11

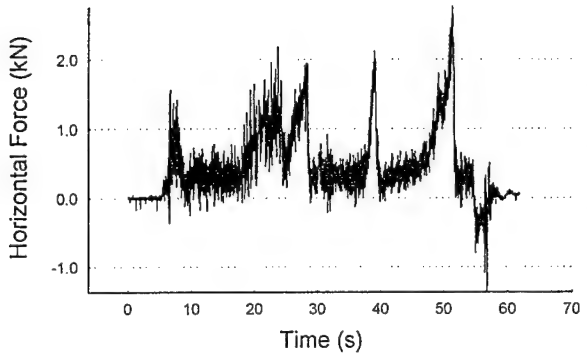

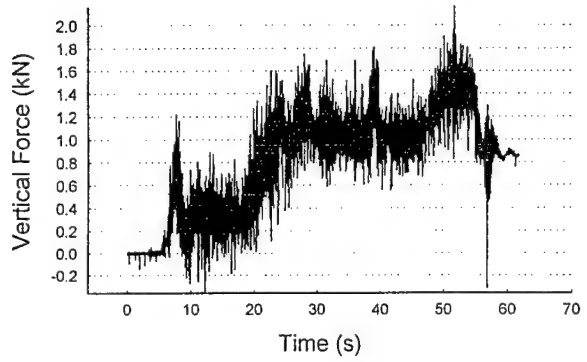

TEST 12

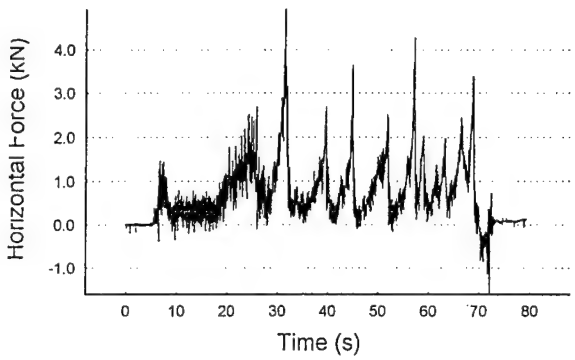

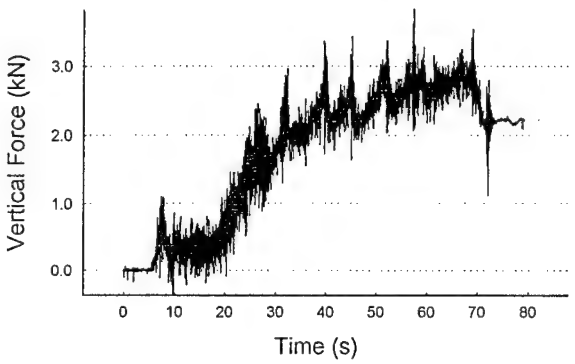

TEST 13

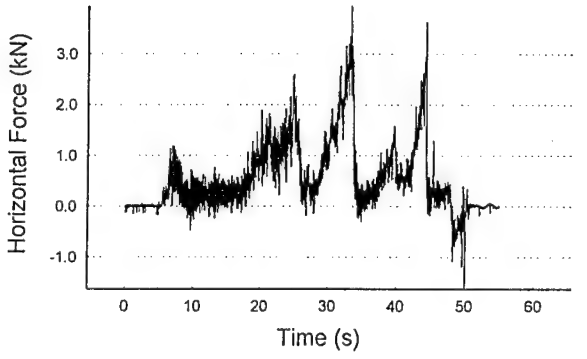

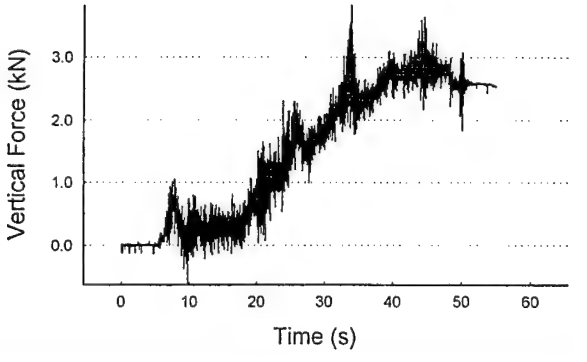

TEST 14

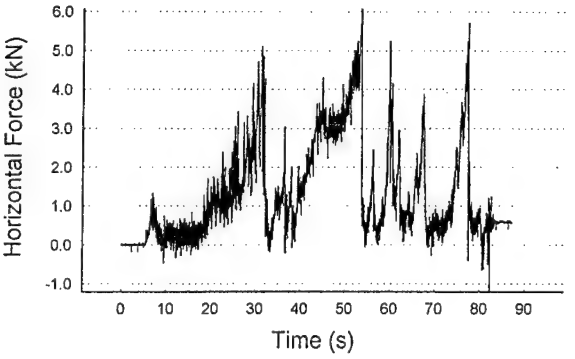

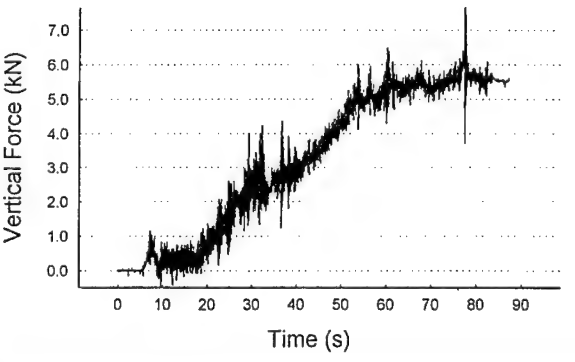

TEST 15

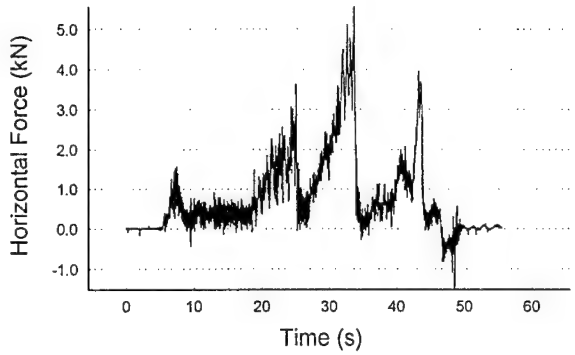

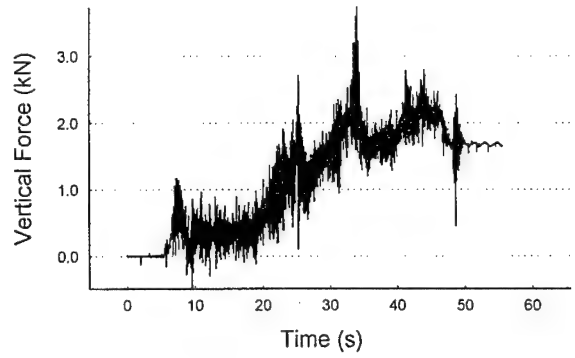

TEST 16

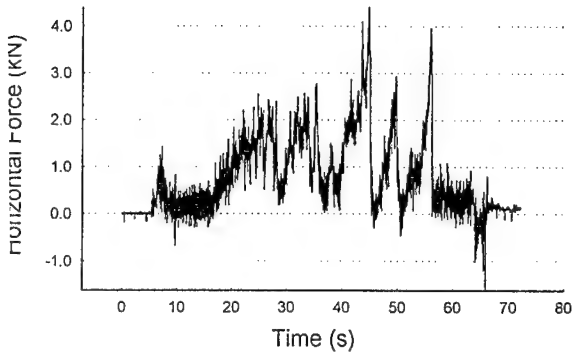

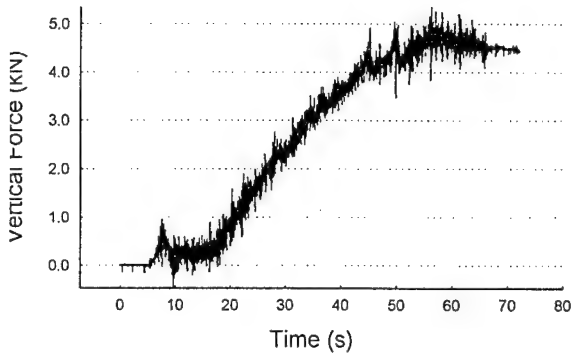

TEST 17

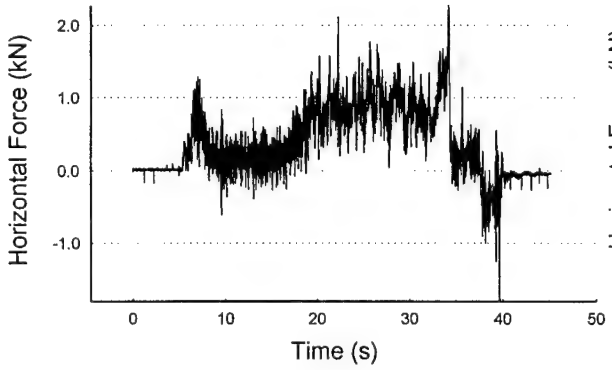

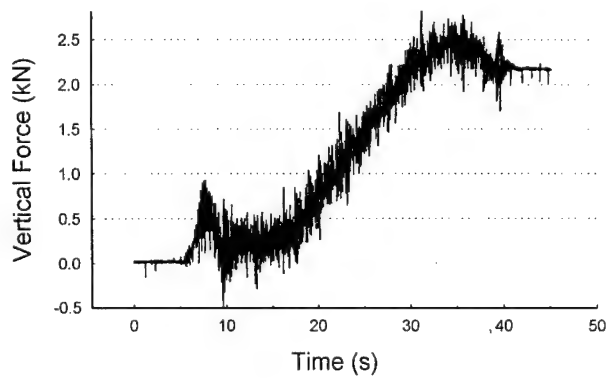

TEST 18

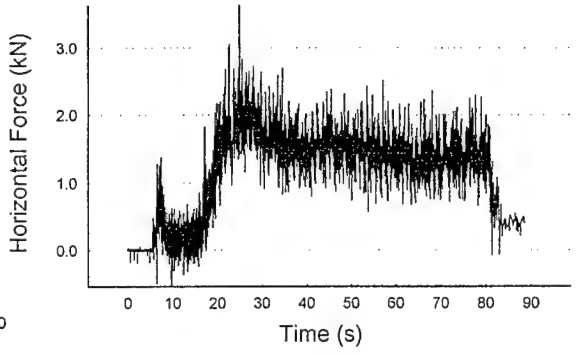

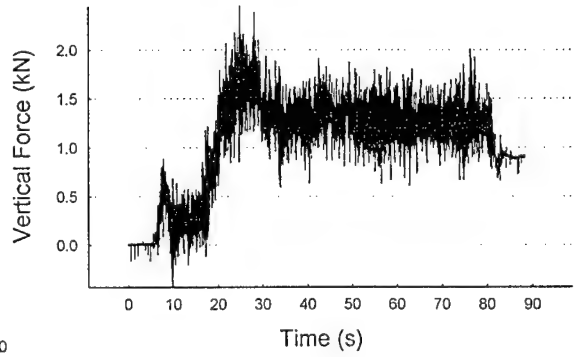

TEST 19

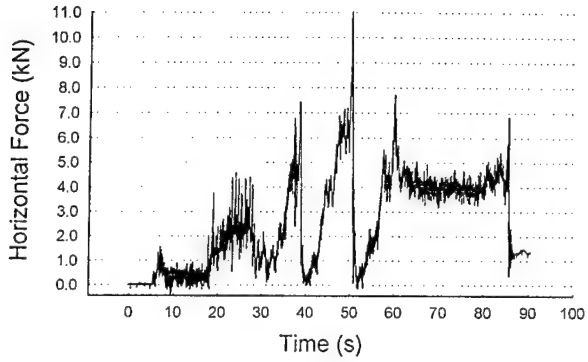

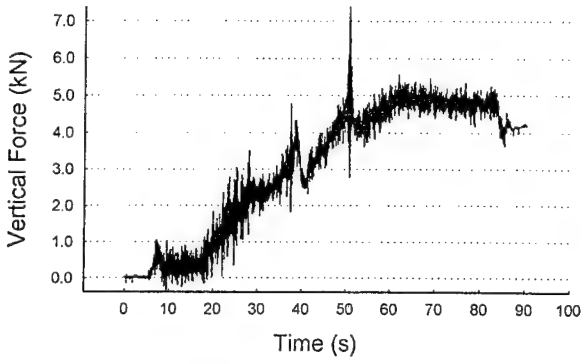

TEST 20

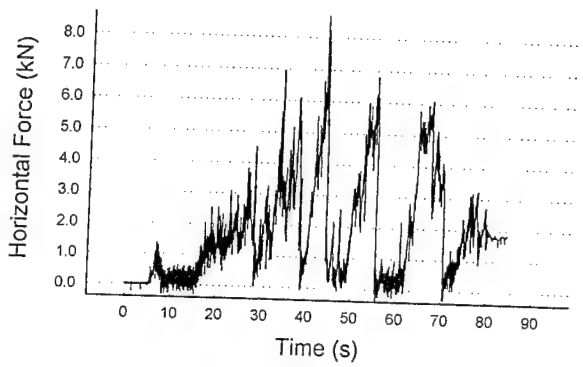

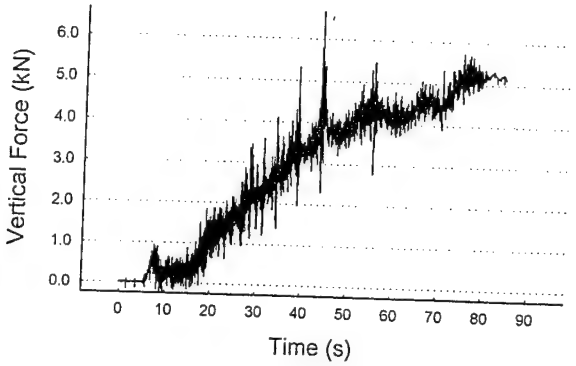

TEST 21

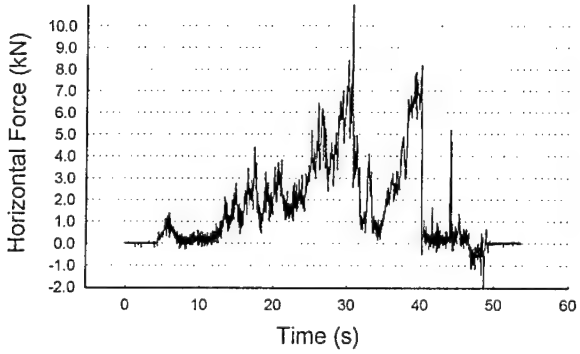

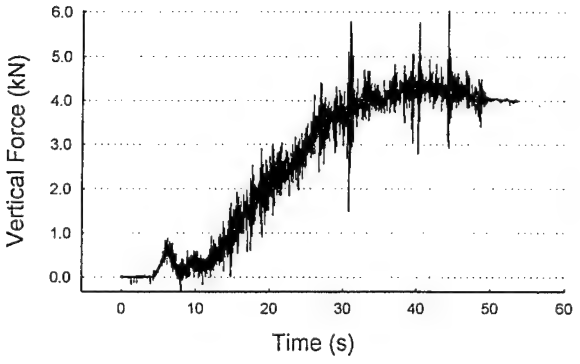

TEST 22

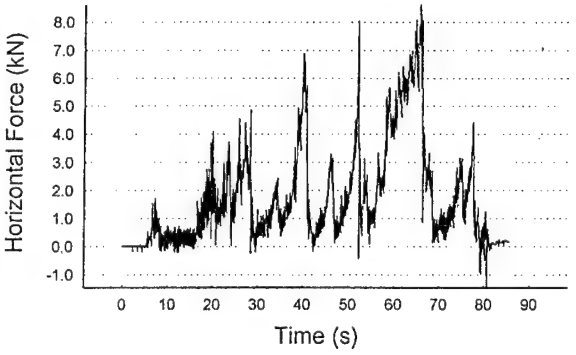

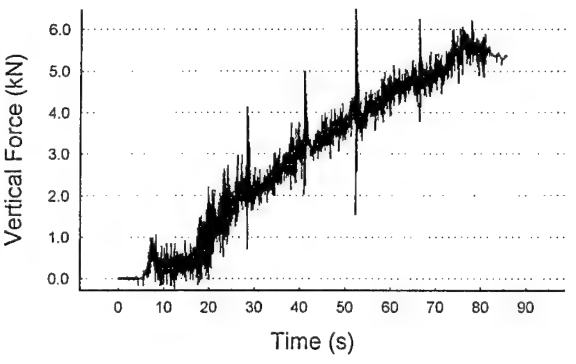

TEST 23

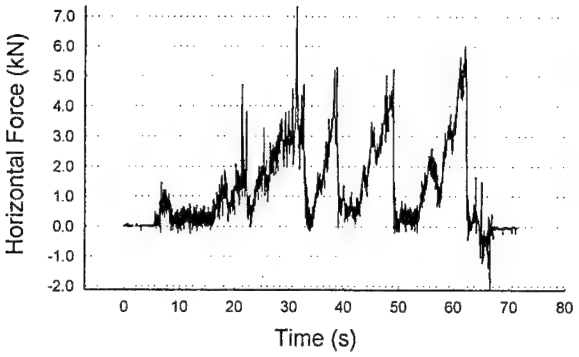

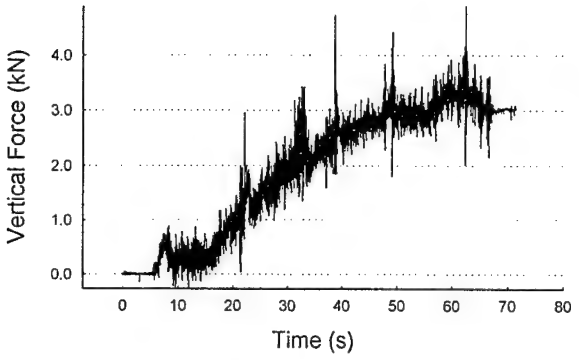

TEST 24

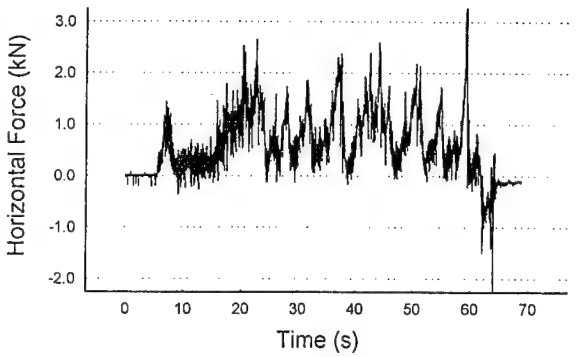

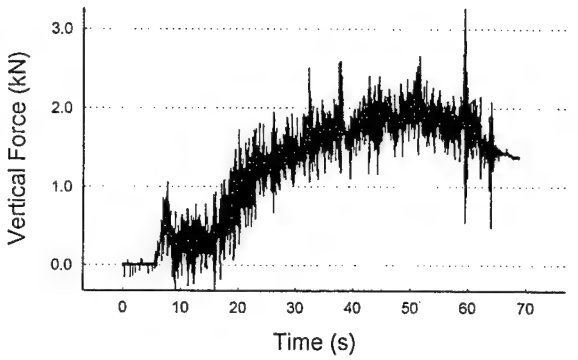

TEST 25

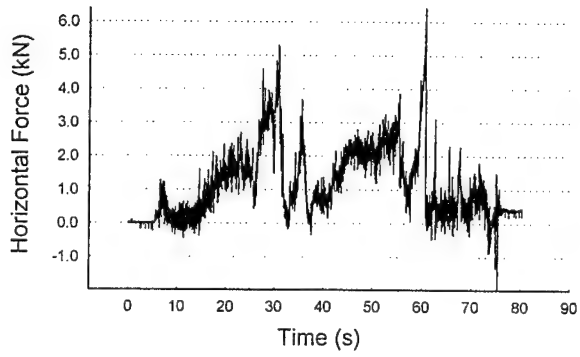

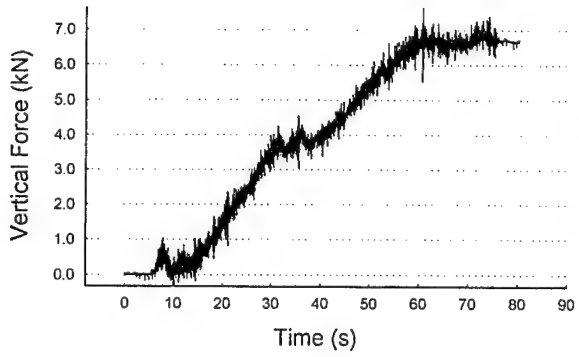

TEST 26

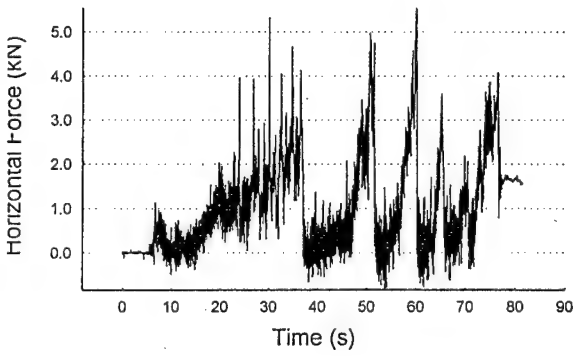

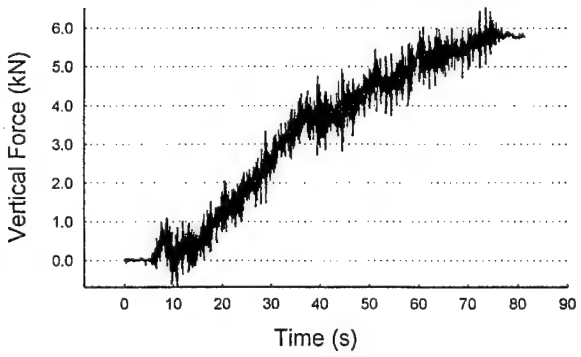

TEST 27

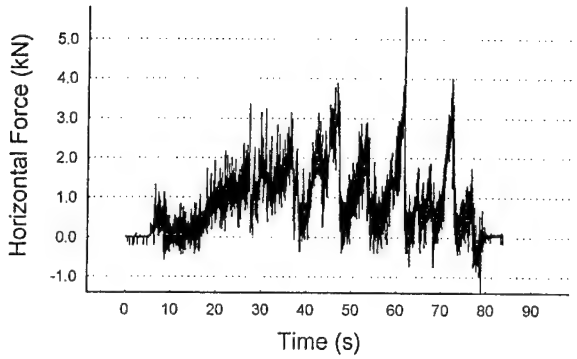

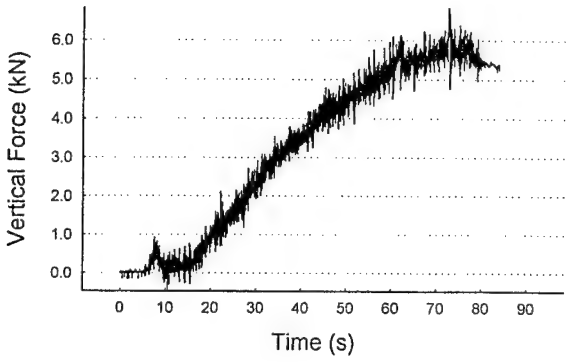

TEST 28

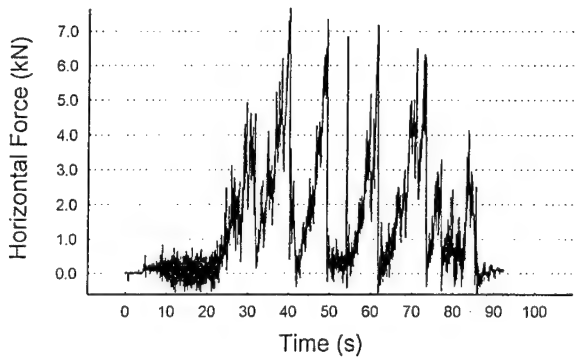

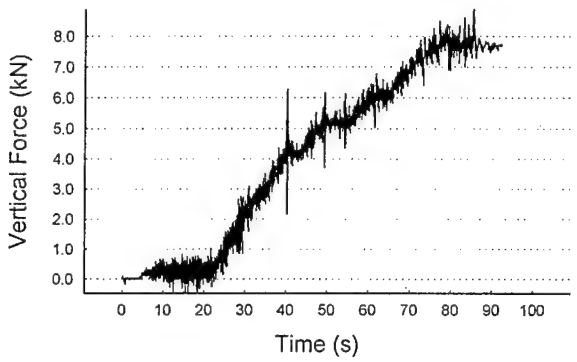

TEST 29

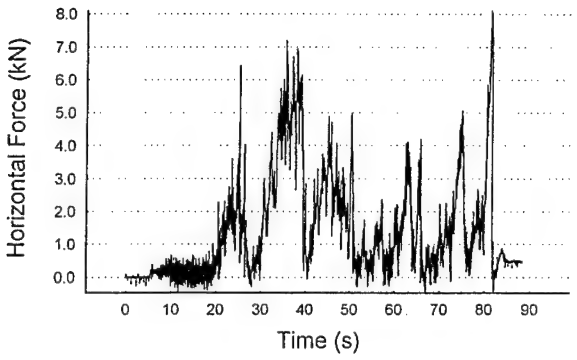

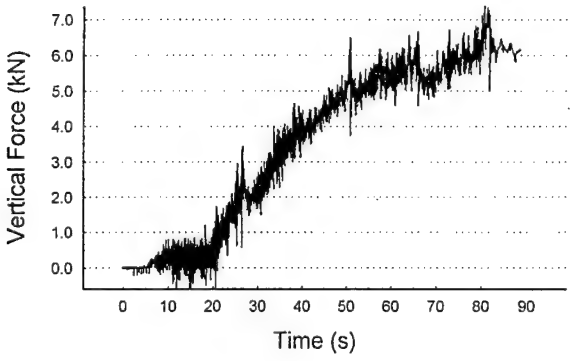

TEST 30

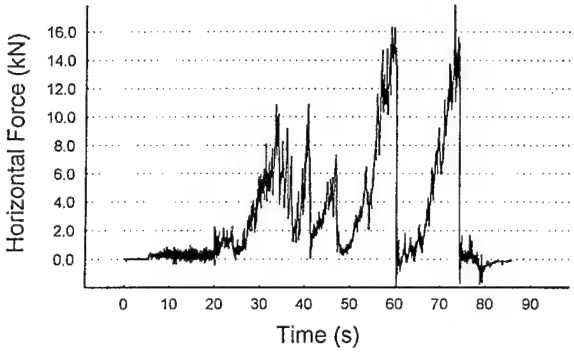

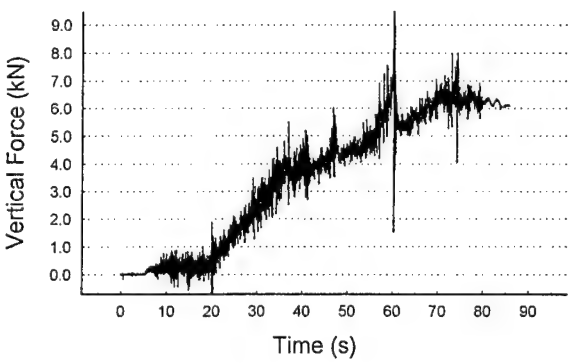

TEST 31

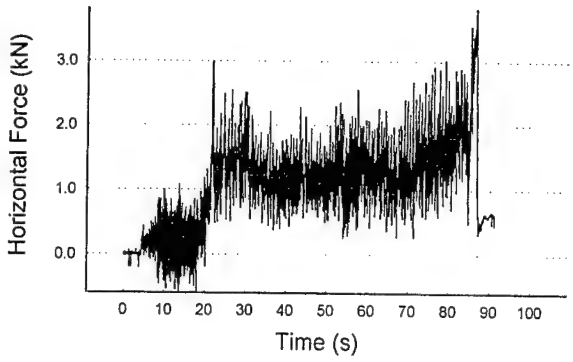

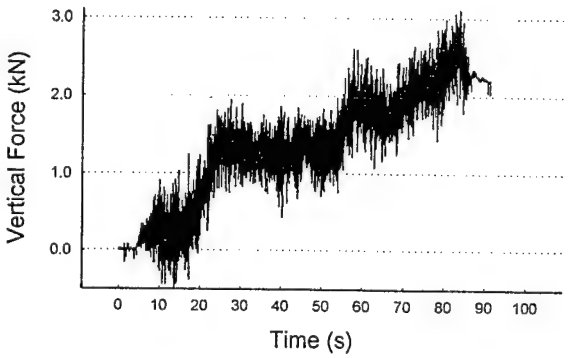

TEST 32

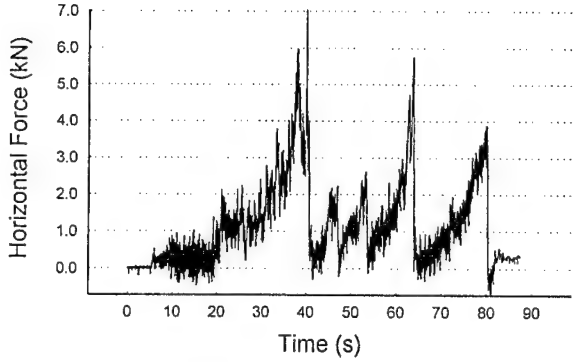

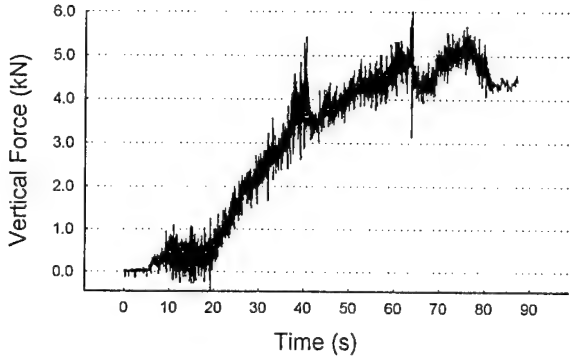

TEST 33

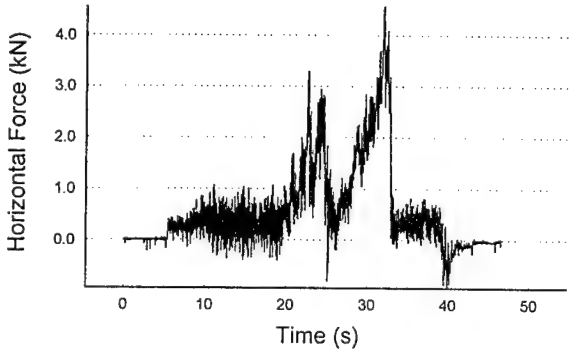

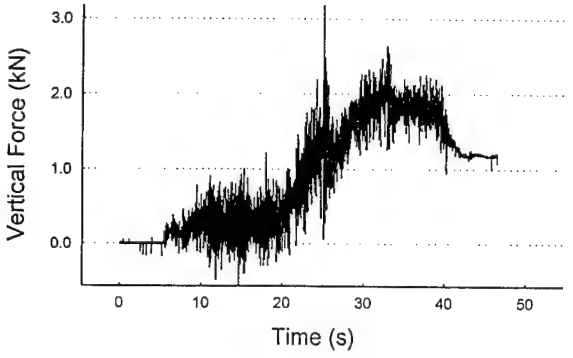

TEST 34

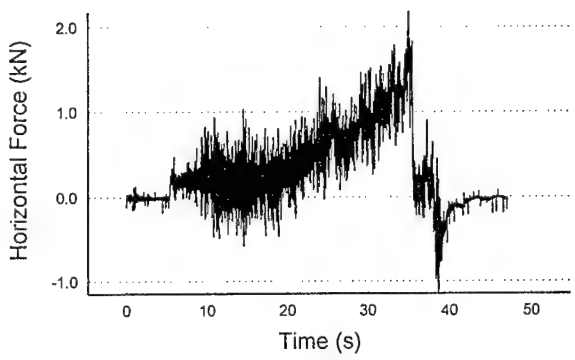

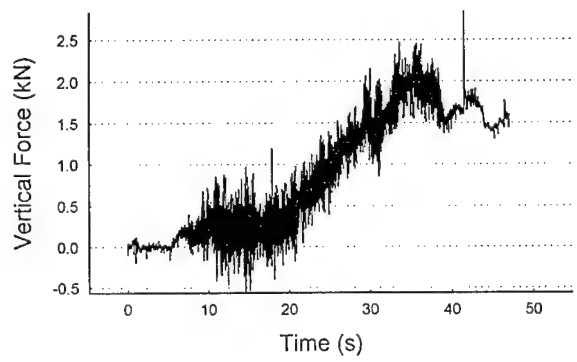

TEST 35

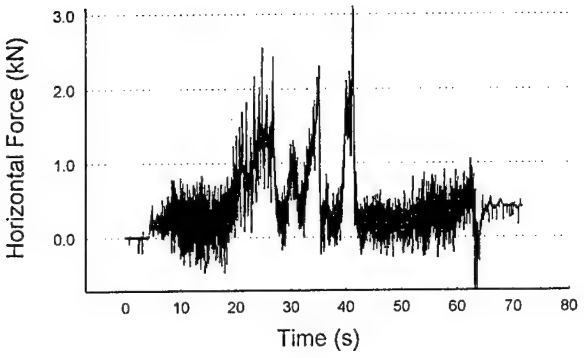
Horizontal Force (kN)
3.0
2.0
1.0
0.0
0
10
20
30
40
50
60
70
80
Time (s)

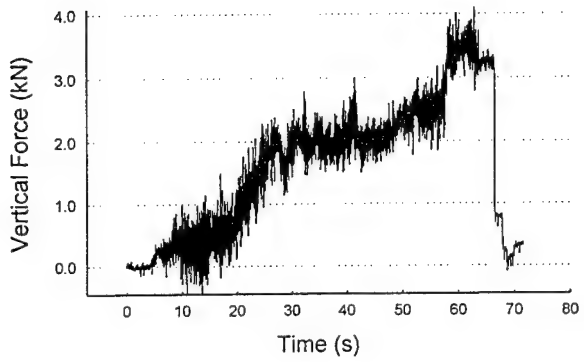
Vertical Force (kN)
4.0
3.0
2.0
1.0
0.0
0
10
20
30
40
50
60
70
80
Time (s)

APPENDIX D: PHOTOGRAPHS AND CONTOUR PLOTS OF THE MODEL RIPRAP BANK BEFORE AND AFTER EACH TEST

This appendix contains photographs and contour plots of the model riprap bank before and after each test. The numbers along contour lines denote the distance measured from the strings in the grid frame.

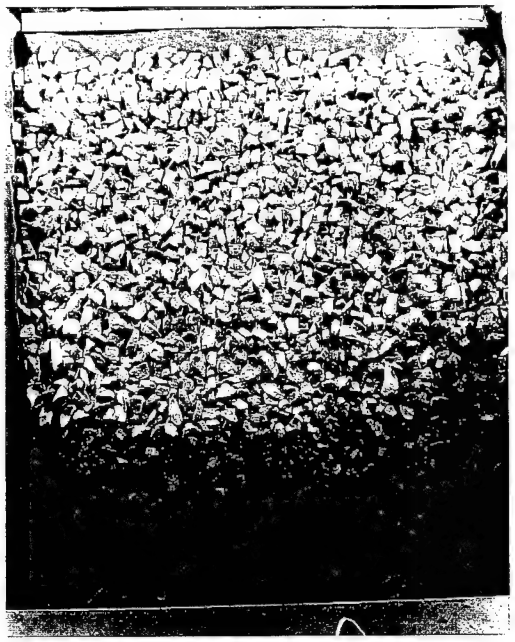

Top of Ramp

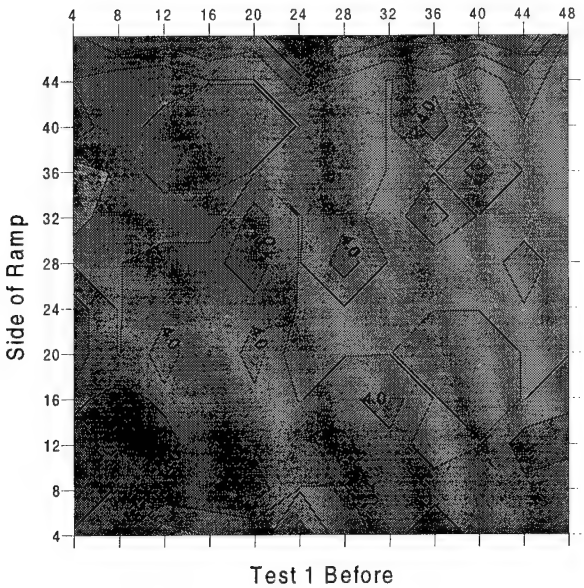

Test 1 Before

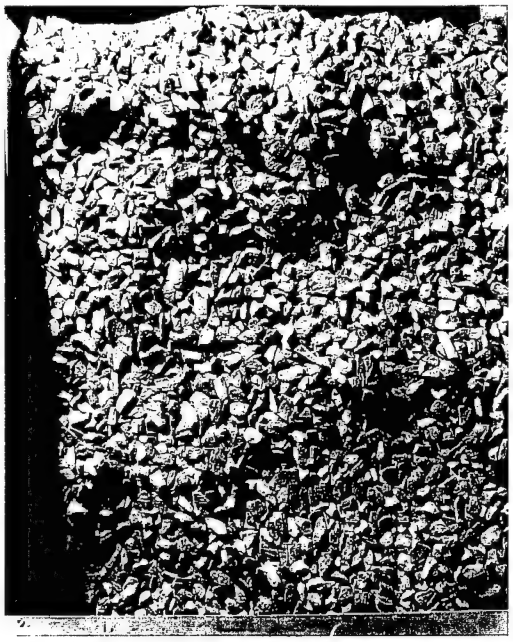

Top of Ramp

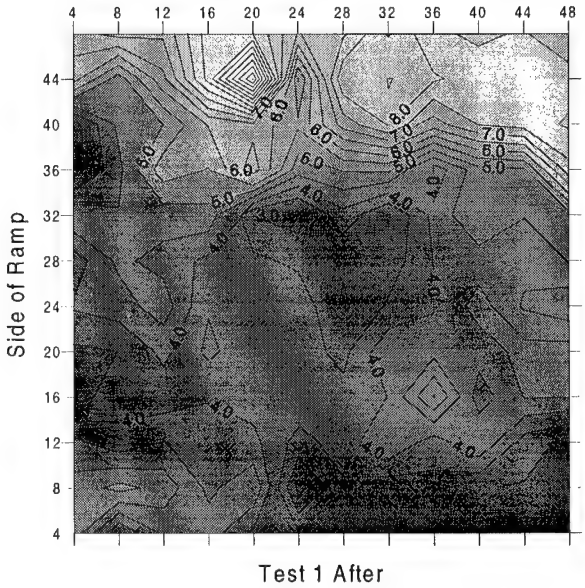

Test 1 After

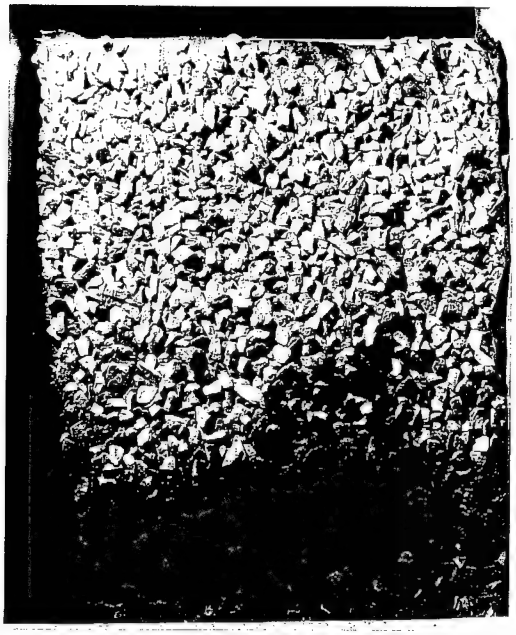

Top of Ramp

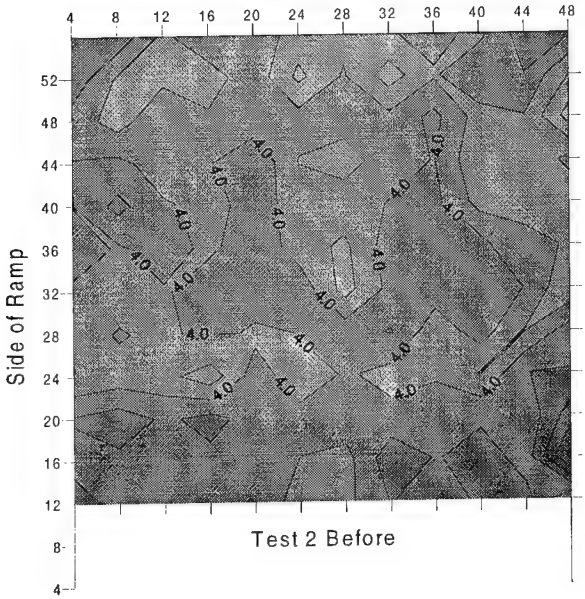

Test 2 Before

Top of Ramp

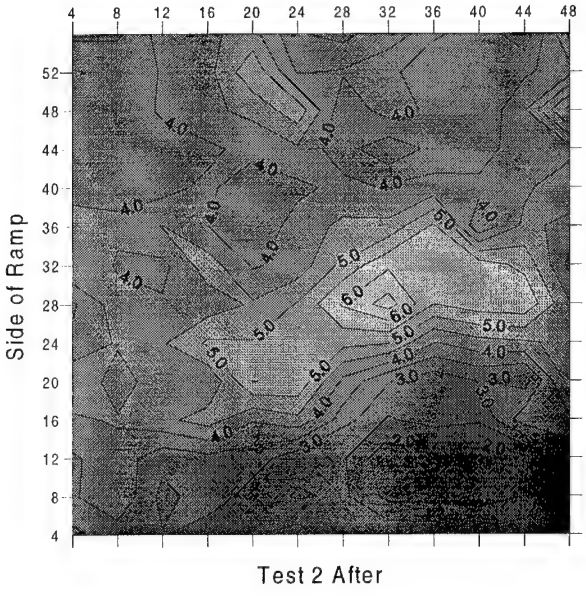

Test 2 After

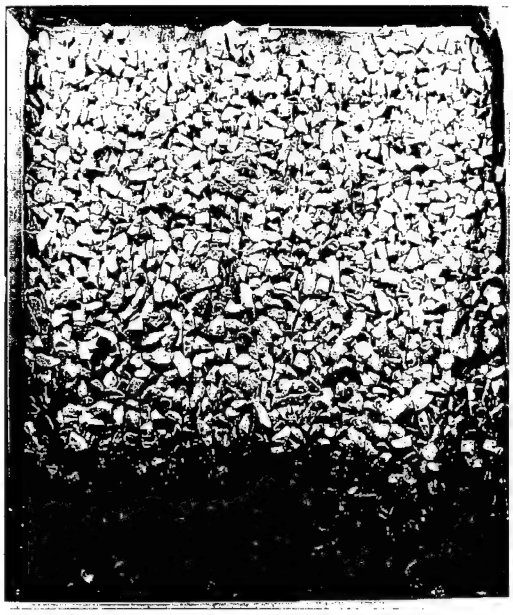

Top of Ramp

Top of Ramp

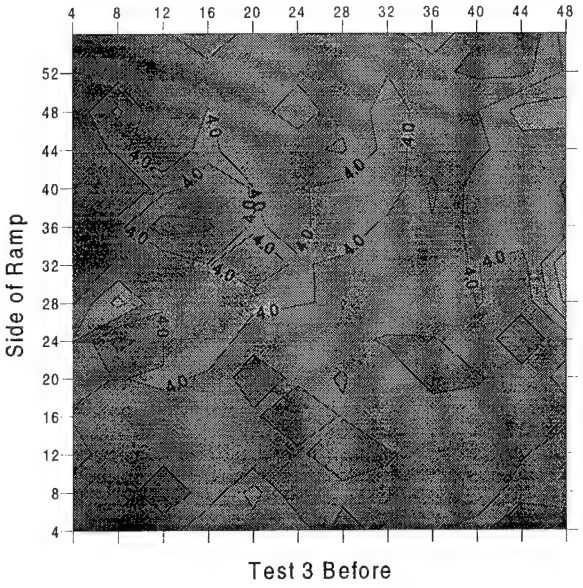

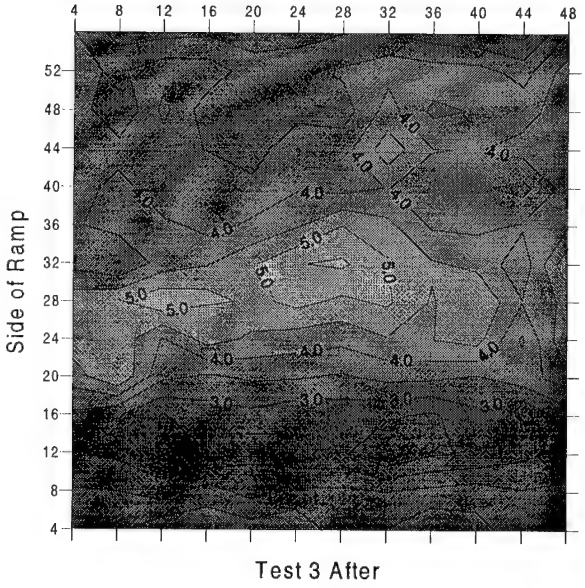

Top of Ramp

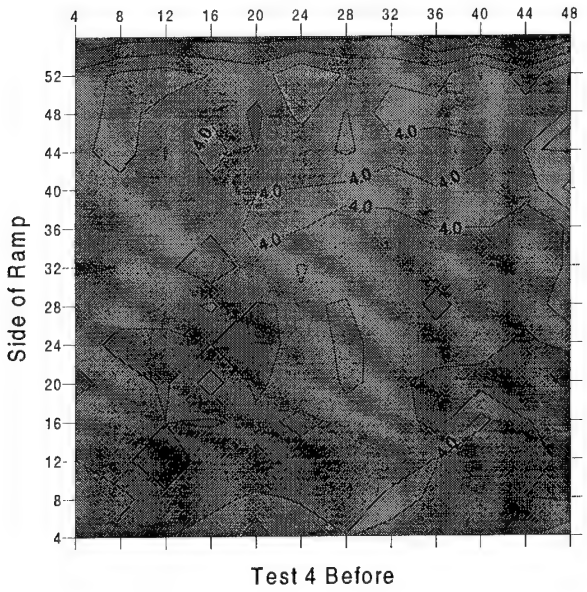

Test 4 Before

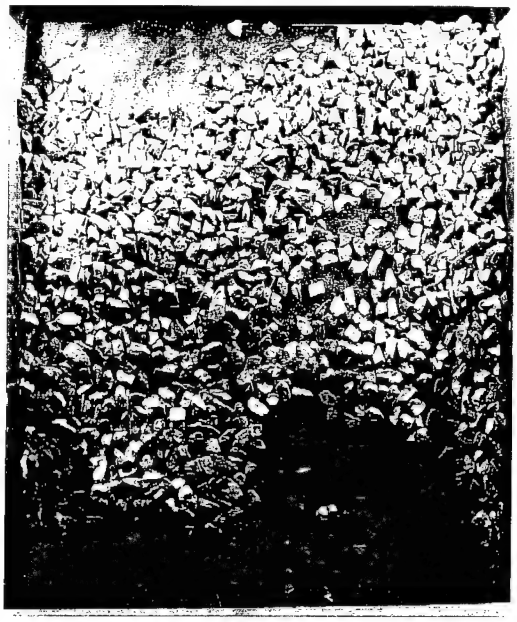

Top of Ramp

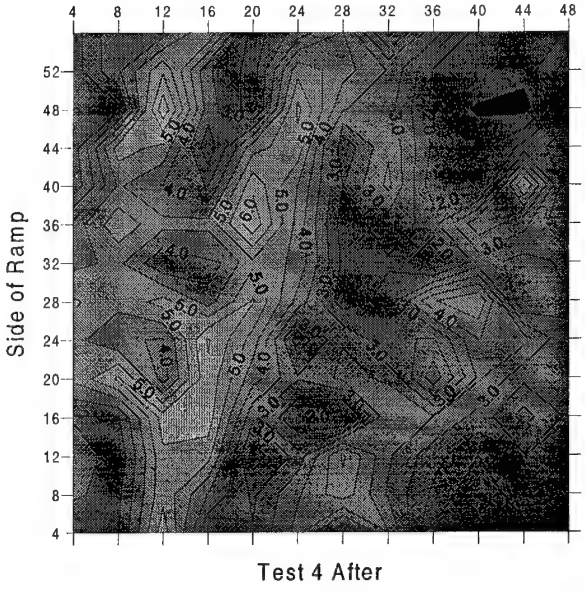

Test 4 After

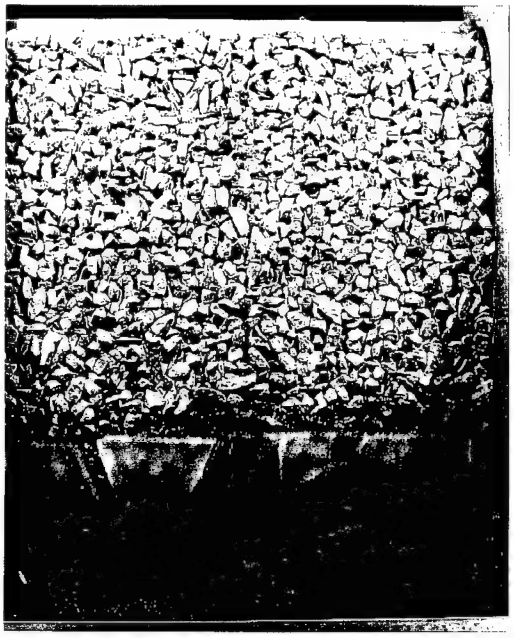

Top of Ramp

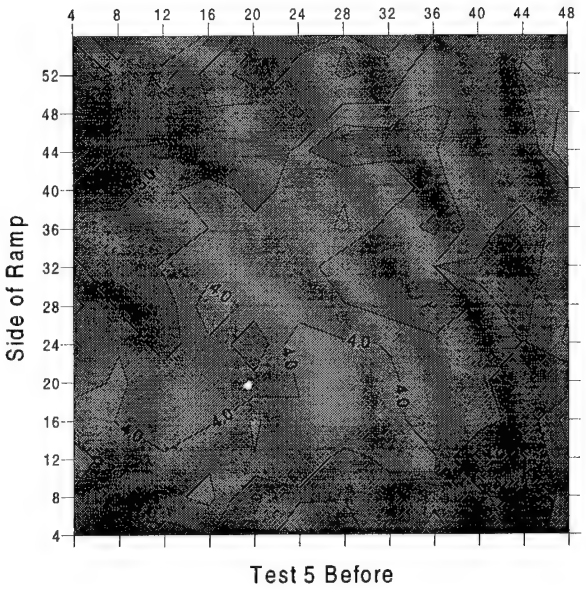

Test 5 Before

Top of Ramp

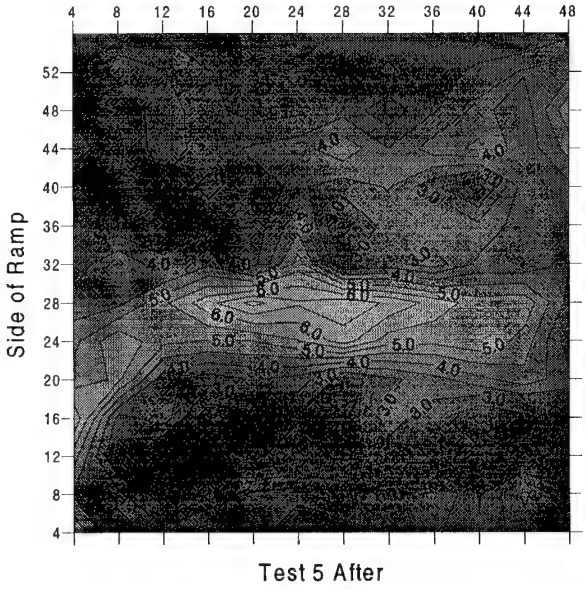

Test 5 After

Top of Ramp

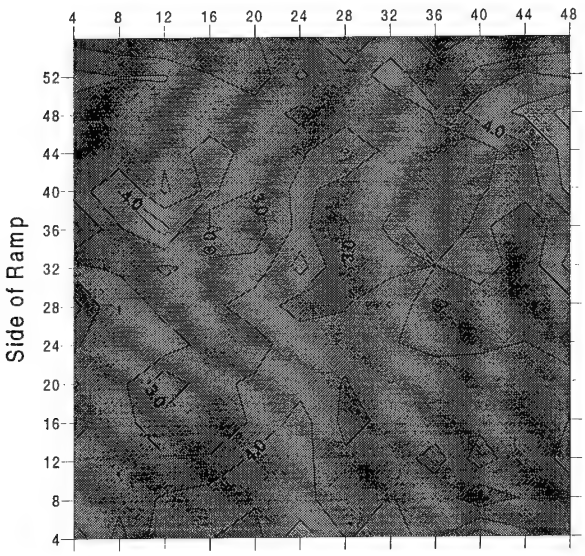

Test 6 Before

Top of Ramp

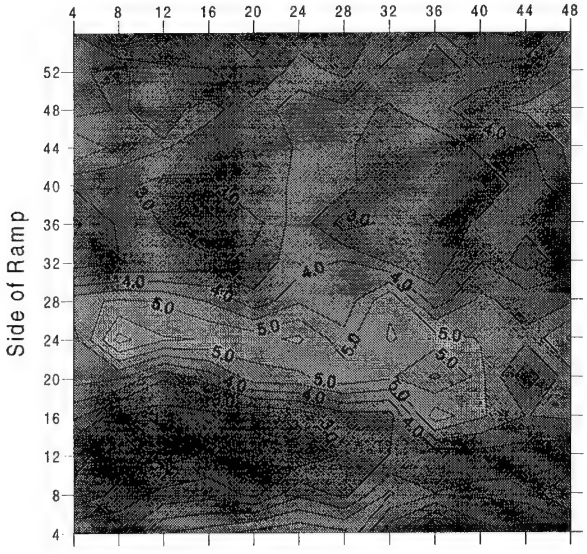

Test 6 After

Top of Ramp

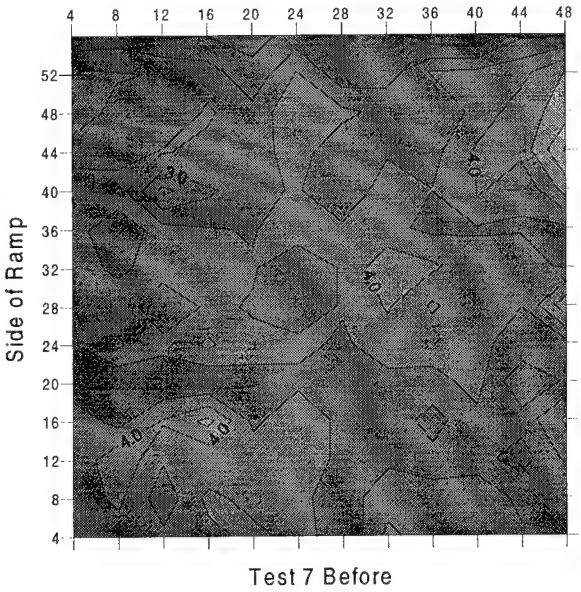

Test 7 Before

Top of Ramp

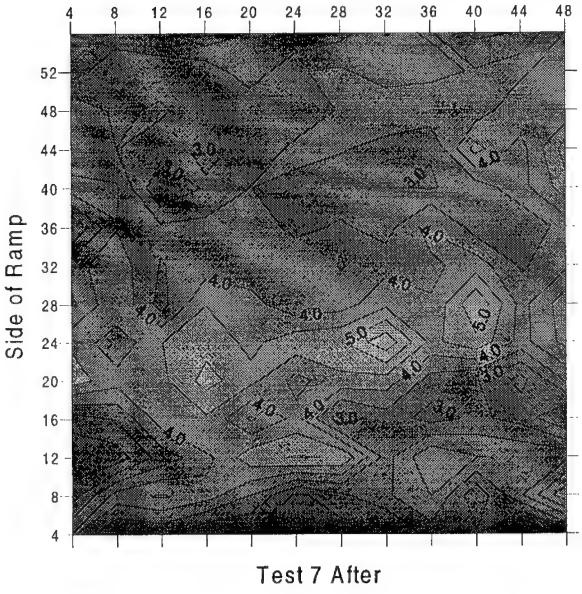

Test 7 After

Top of Ramp

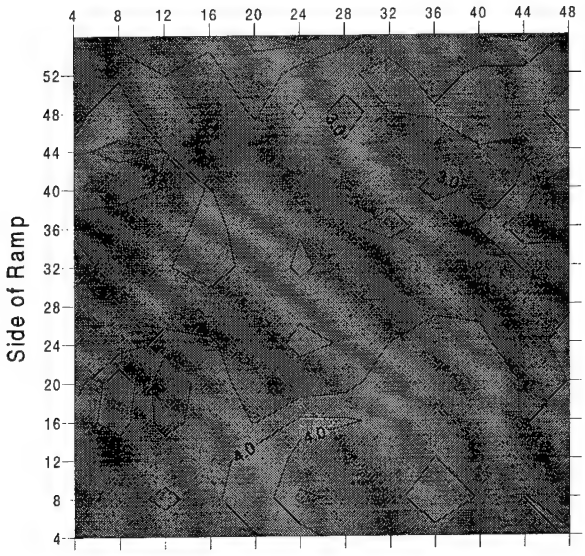

Test 8 Before

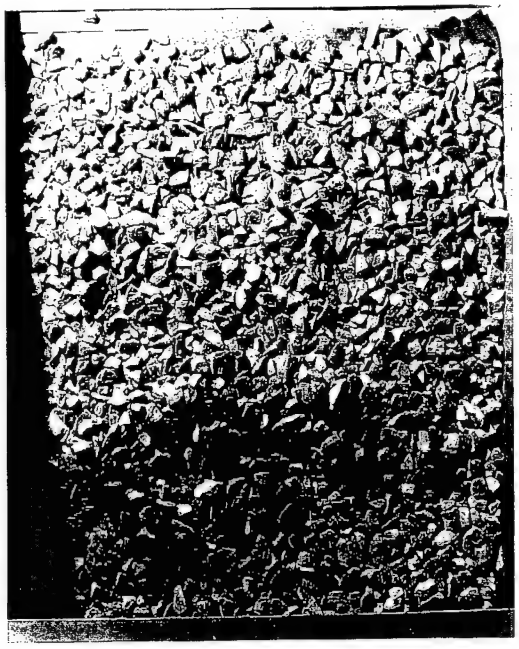

Top of Ramp

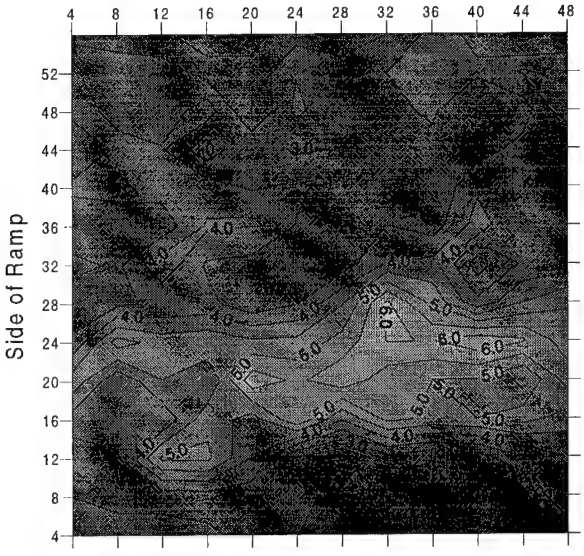

Test 8 After

Top of Ramp

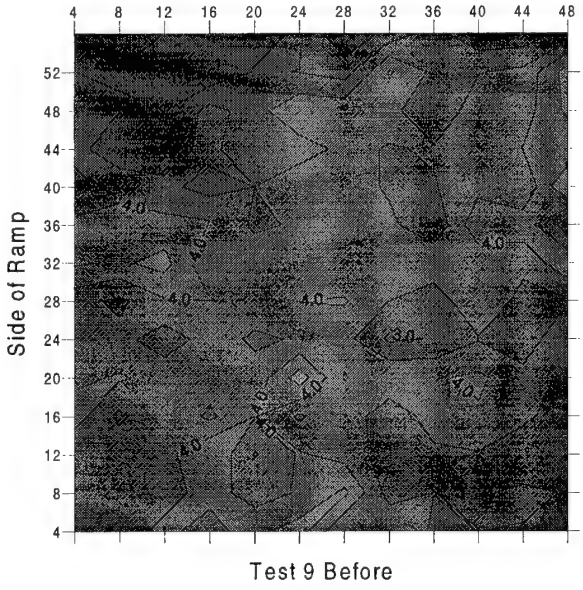

Test 9 Before

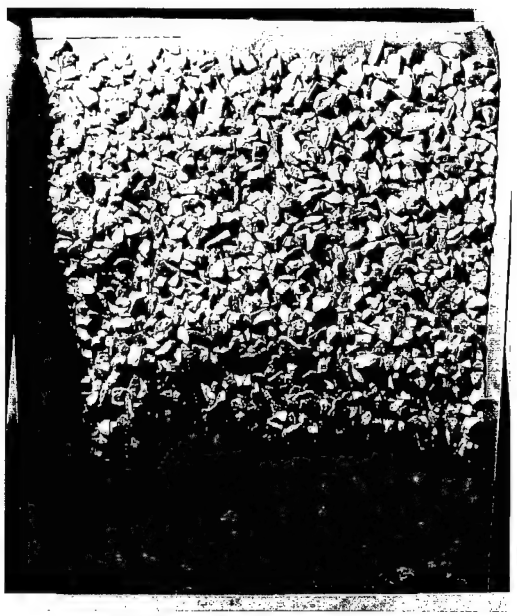

Top of Ramp

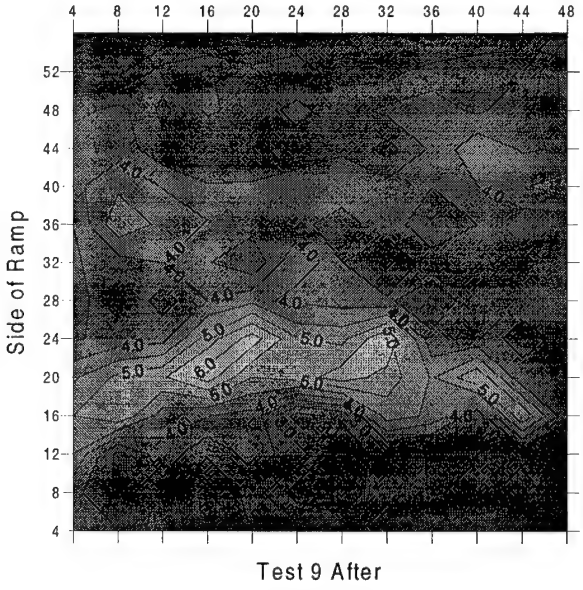

Test 9 After

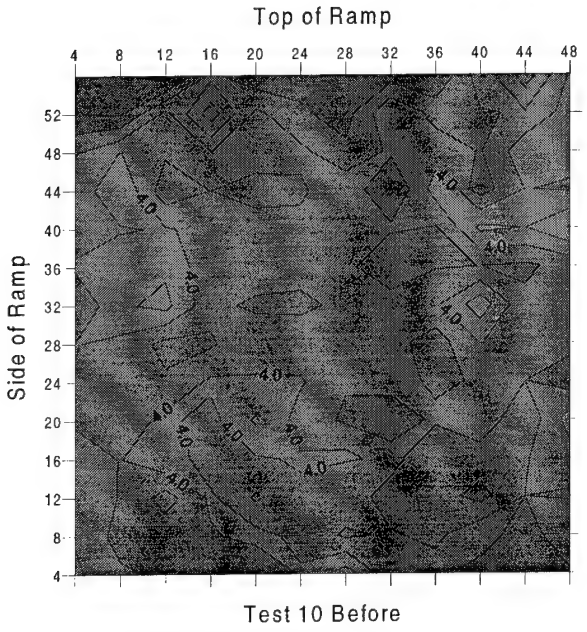
Top of Ramp
Side of Ramp
4 8 12 16 20 24 28 32 36 40 44 48
52 48 44 40 36 32 28 24 20 16 12 8 4
4.0
Test 10 Before

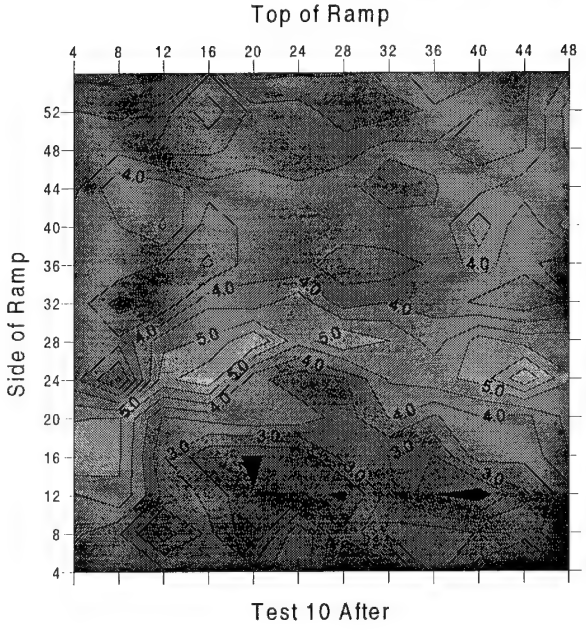
Top of Ramp
Side of Ramp
4 8 12 16 20 24 28 32 36 40 44 48
52 48 44 40 36 32 28 24 20 16 12 8 4
4.0
5.0
3.0
Test 10 After

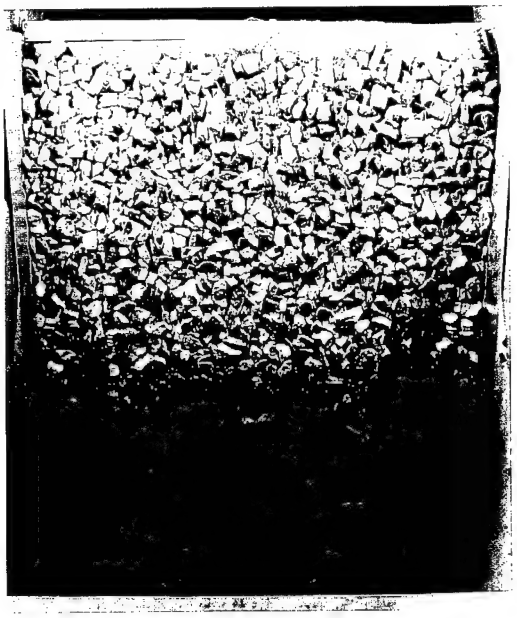

Top of Ramp

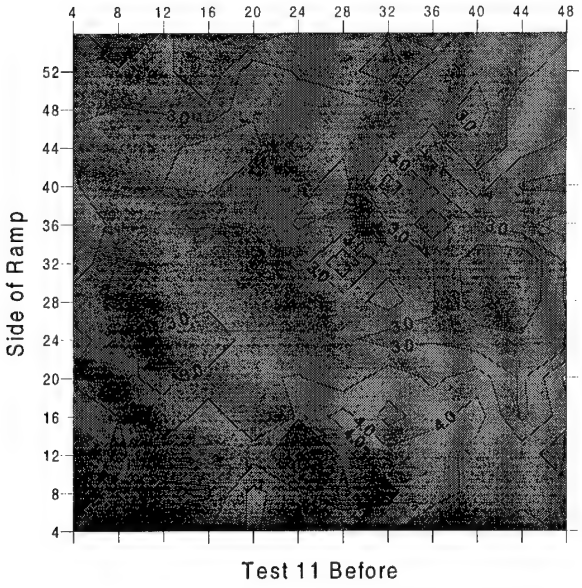

Test 11 Before

Top of Ramp

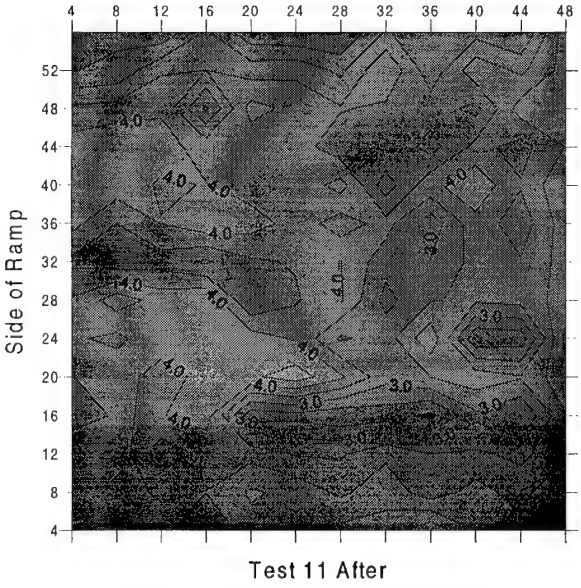

Test 11 After

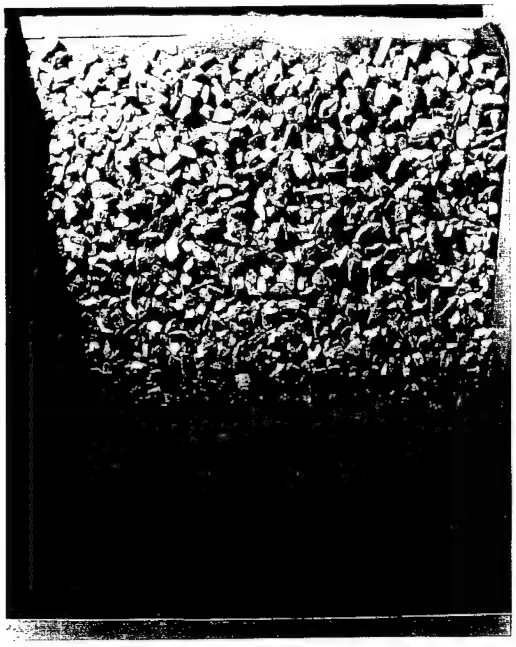

Top of Ramp

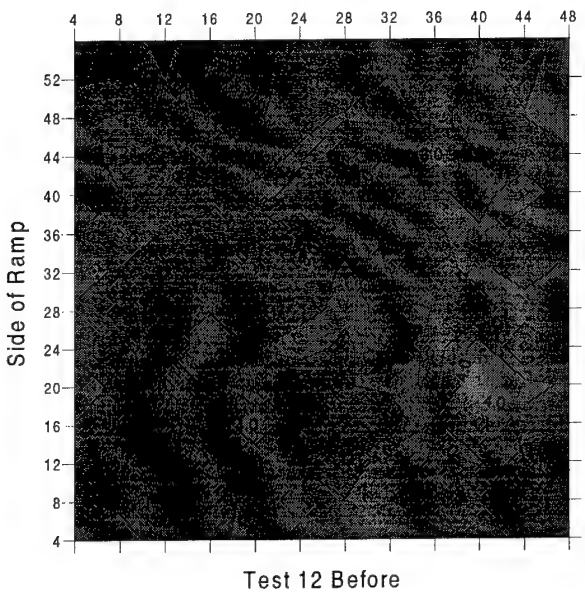

Test 12 Before

Top of Ramp

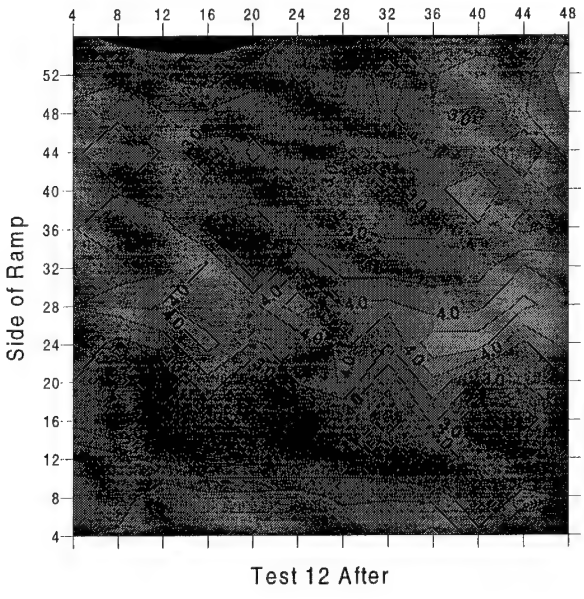

Test 12 After

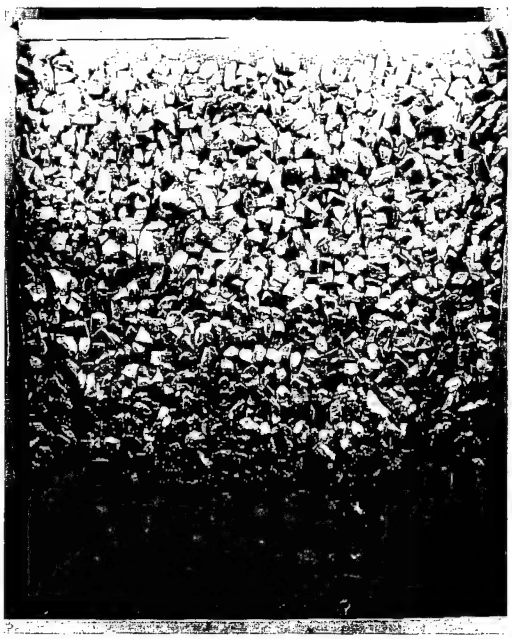

Top of Ramp

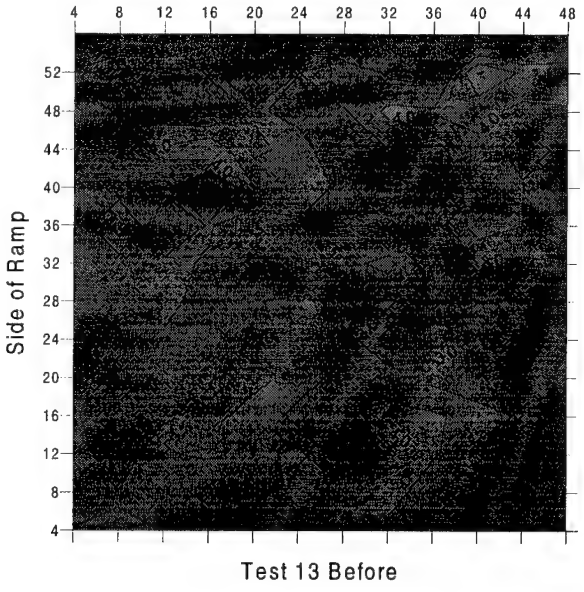

Test 13 Before

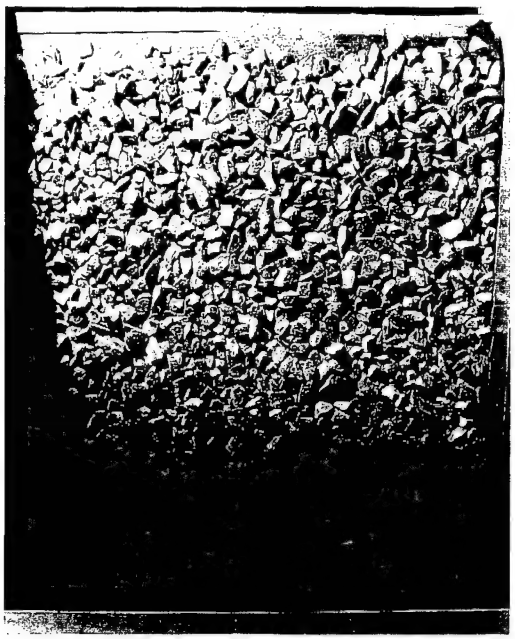

Top of Ramp

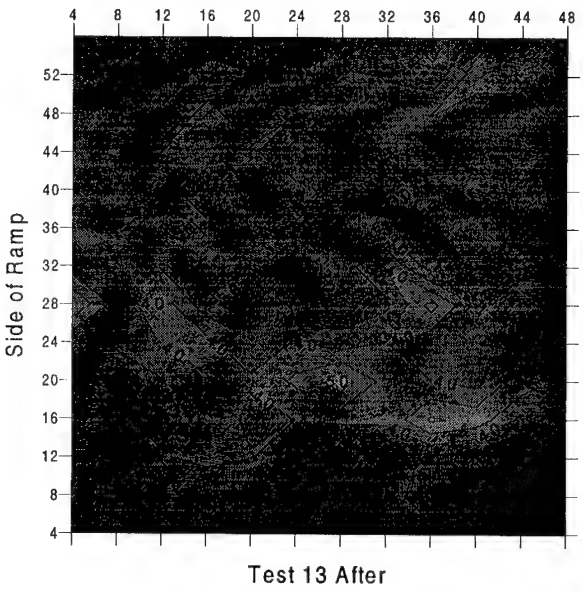

Test 13 After

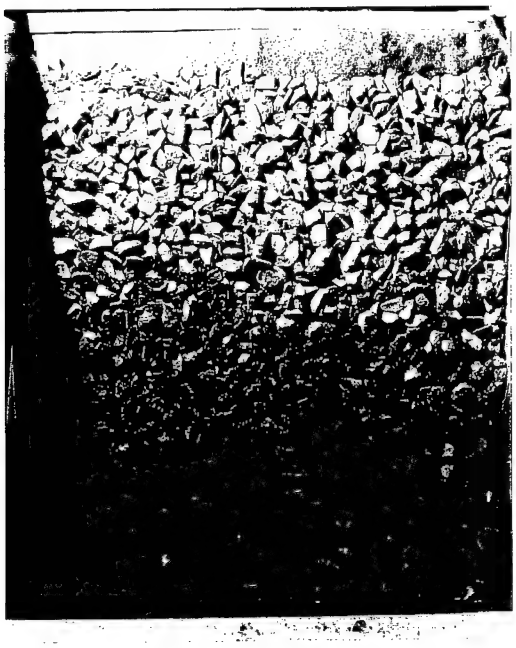

Top of Ramp

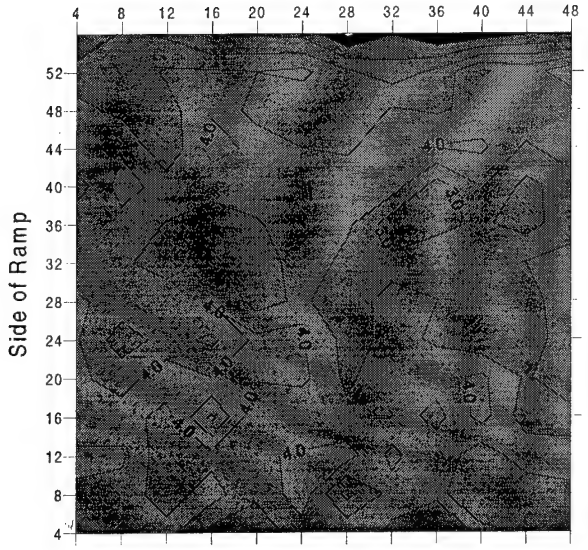

Test 14 Before

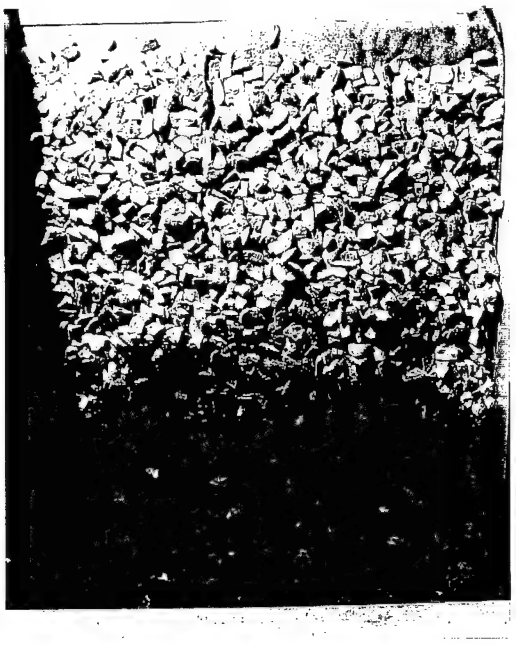

Top of Ramp

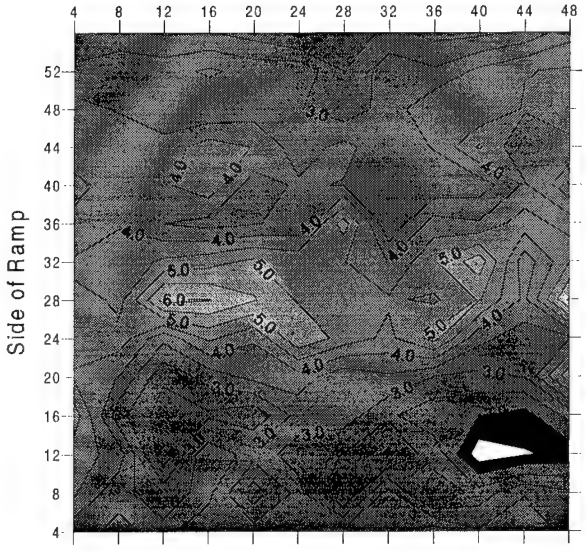

Test 14 After

Top of Ramp

Top of Ramp

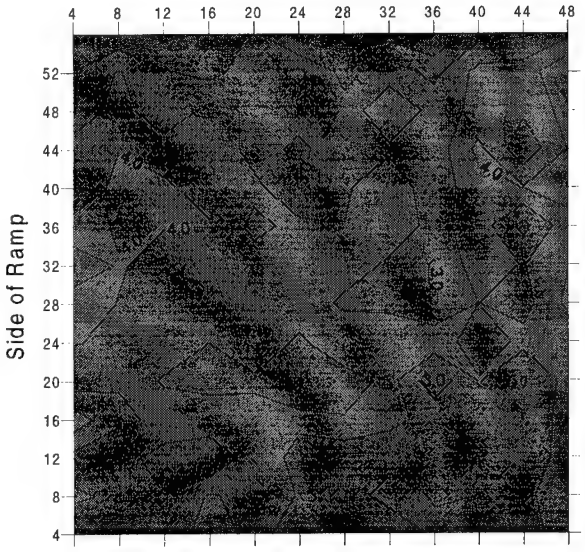

Test 15 Before

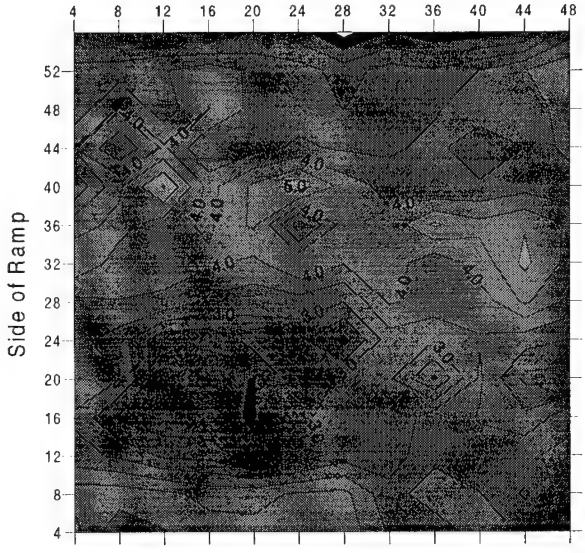

Test 15 After

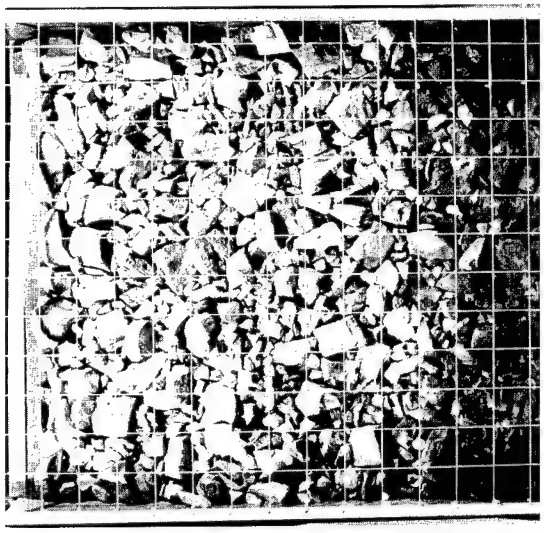

Test 16 before.

Test 16 after.

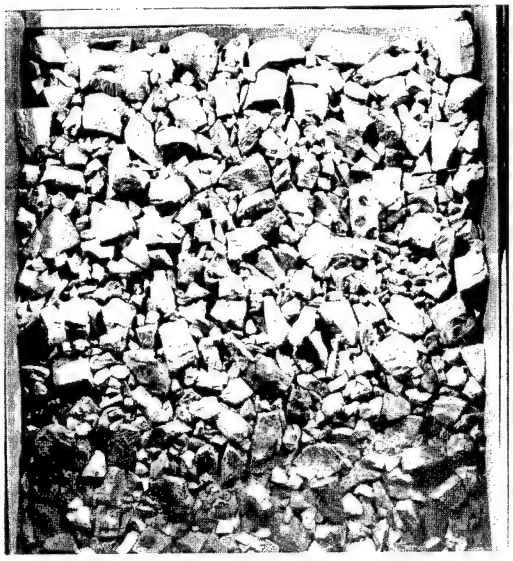

Test 17 before.

Test 17 after.

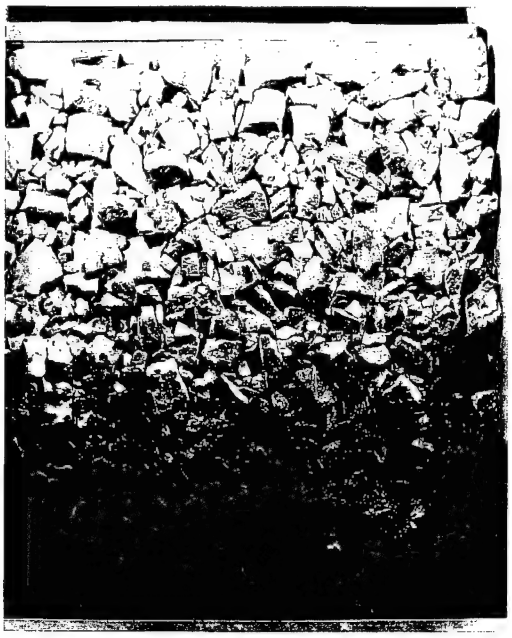

Top of Ramp

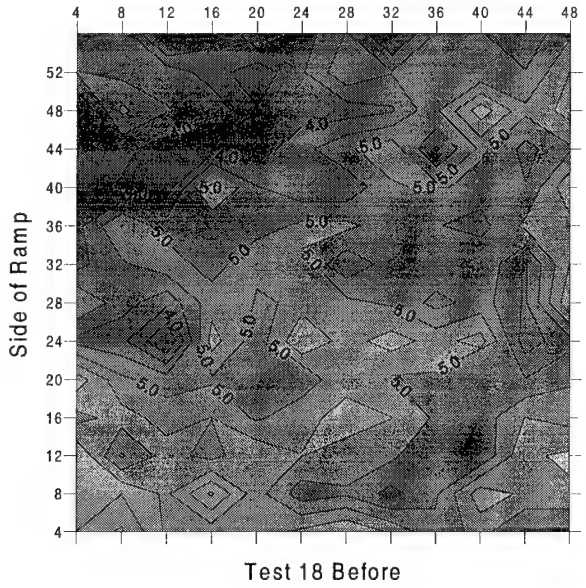

Test 18 Before

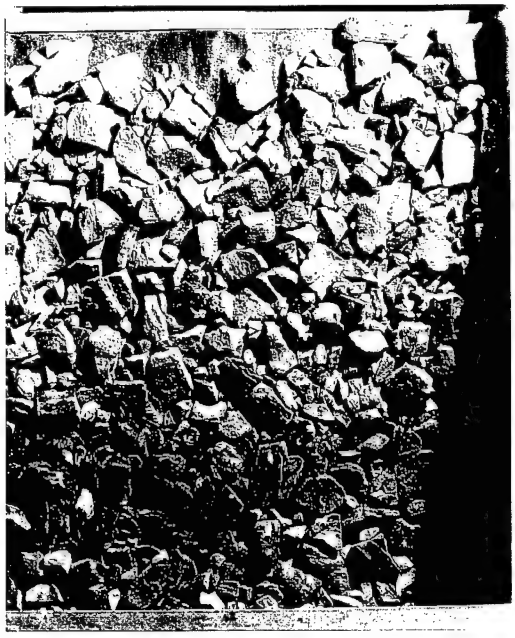

Top of Ramp

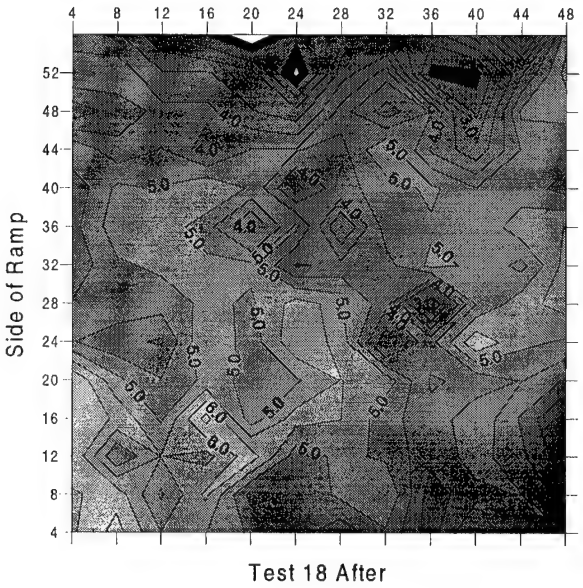

Test 18 After

Top of Ramp

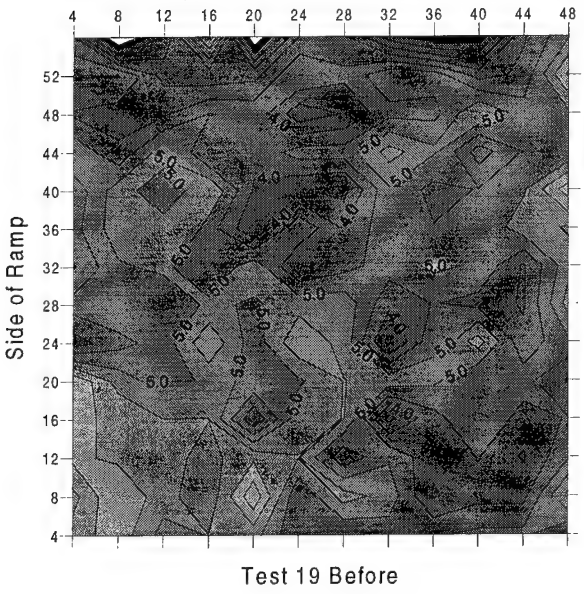

Test 19 Before

Top of Ramp

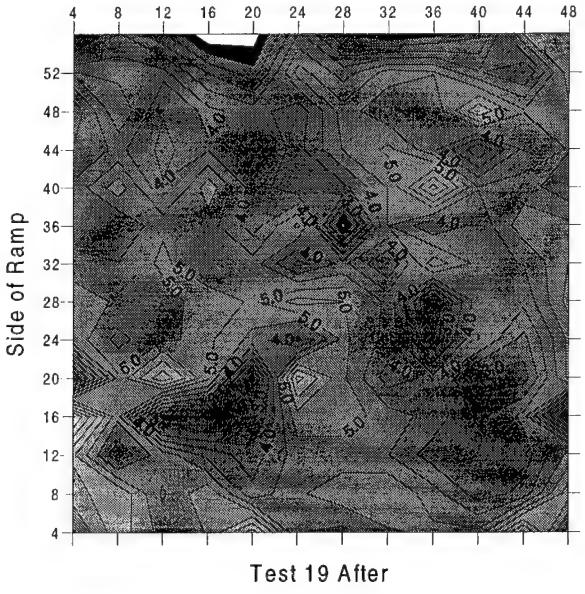

Test 19 After

Top of Ramp

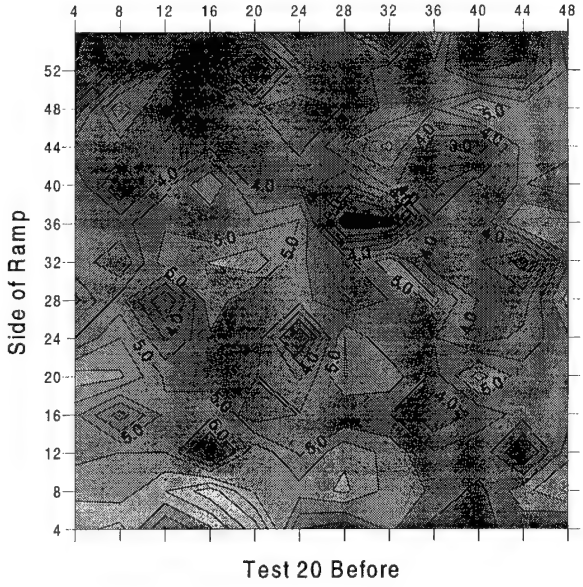

Top of Ramp

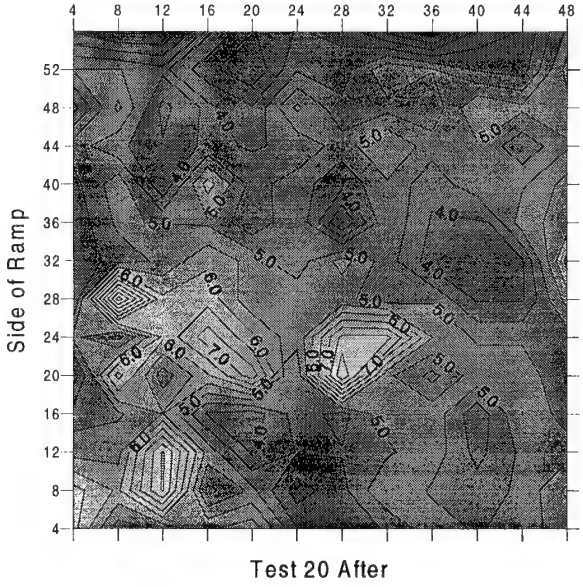

Top of Ramp

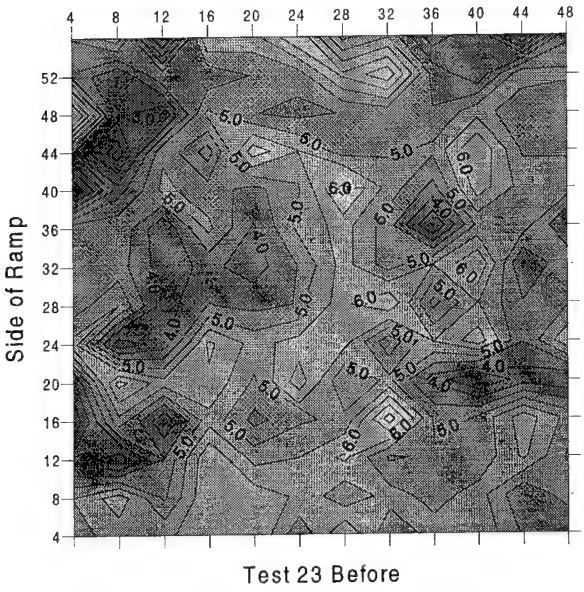

Test 23 Before

Top of Ramp

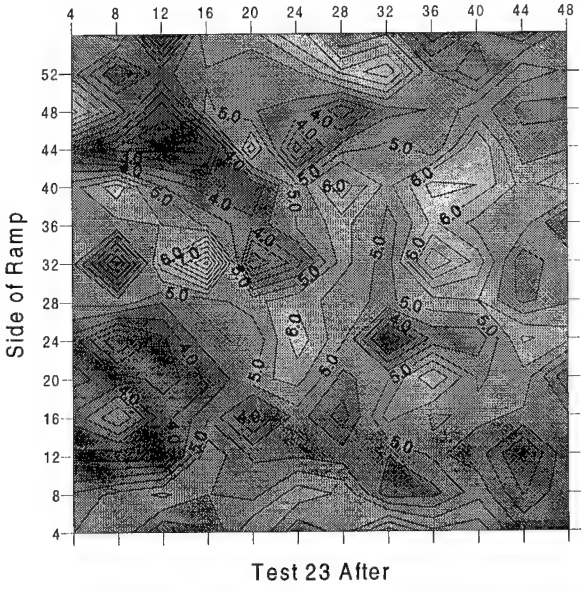

Test 23 After

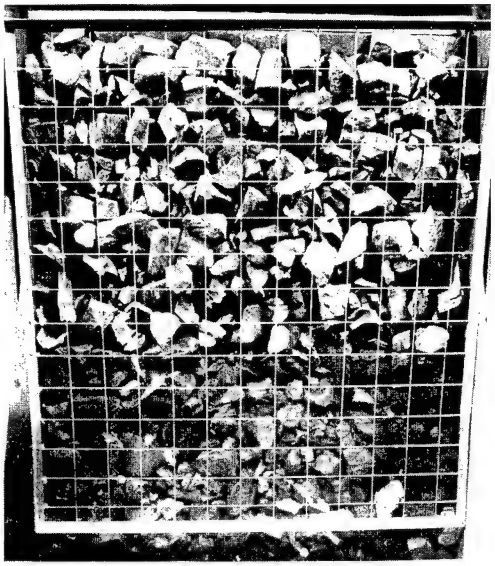

Test 22 before.

Test 22 after.

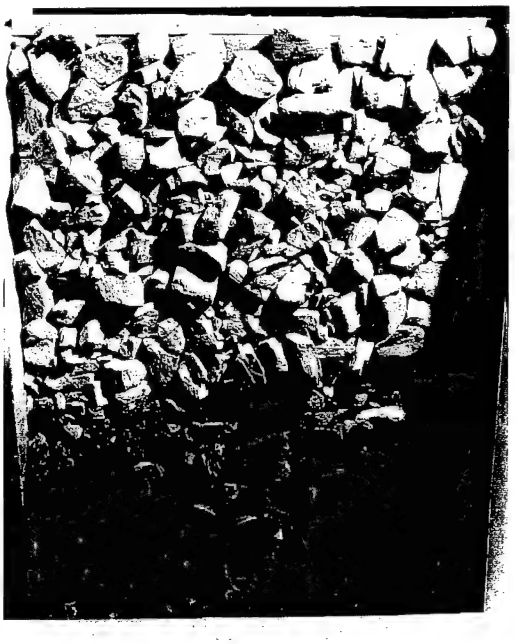

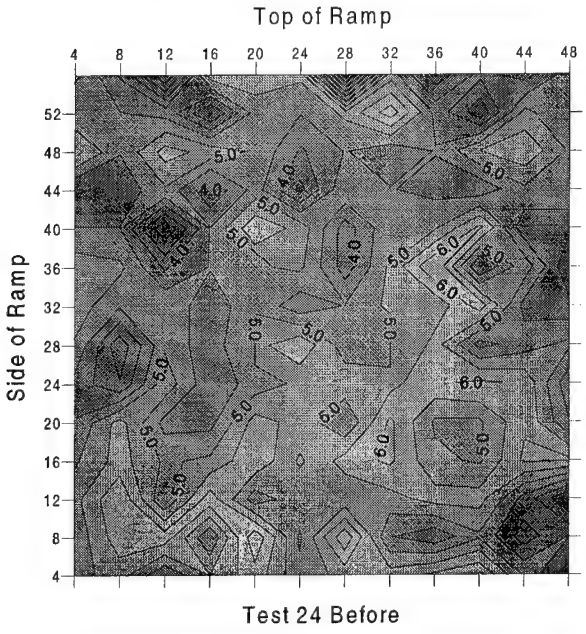
Top of Ramp
Side of Ramp
4 8 12 16 20 24 28 32 36 40 44 48
52 48 44 40 36 32 28 24 20 16 12 8 4
Test 24 Before

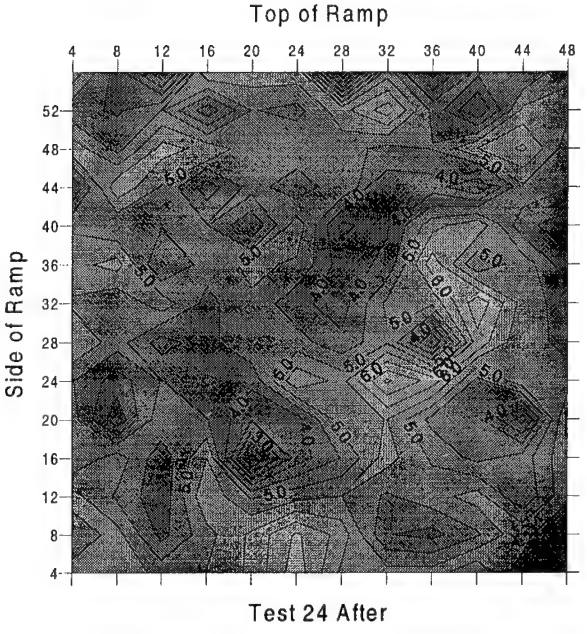
Top of Ramp
Side of Ramp
4 8 12 16 20 24 28 32 36 40 44 48
52 48 44 40 36 32 28 24 20 16 12 8 4
Test 24 After

Top of Ramp

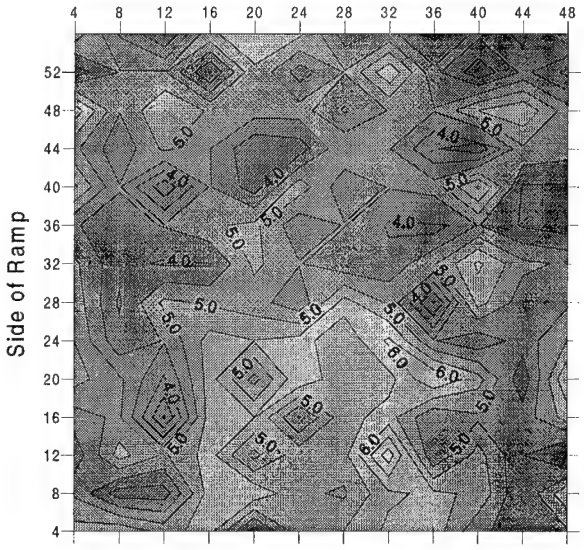

Test 25 Before

Top of Ramp

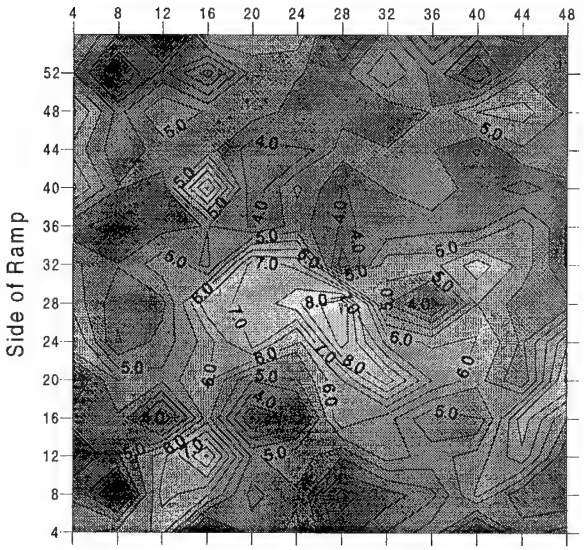

Test 25 After

Test 26 before.

Test 26 after.

Test 27 (frozen)

Test 28 before.

Test 28 after.

Test 29 before.

Test 29 after.

Test 30 before.

Test 30 after.

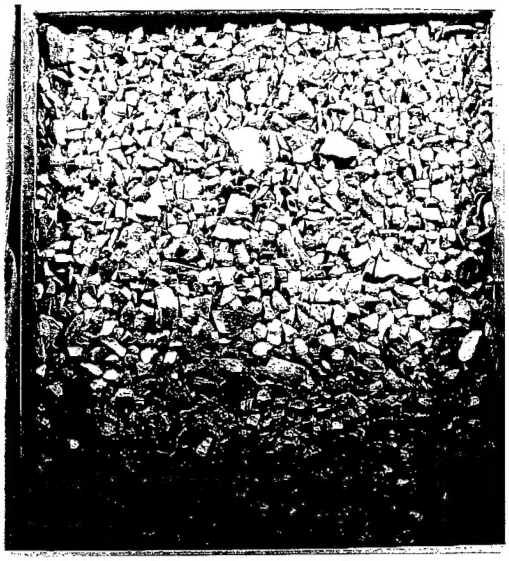

Test 31 before.

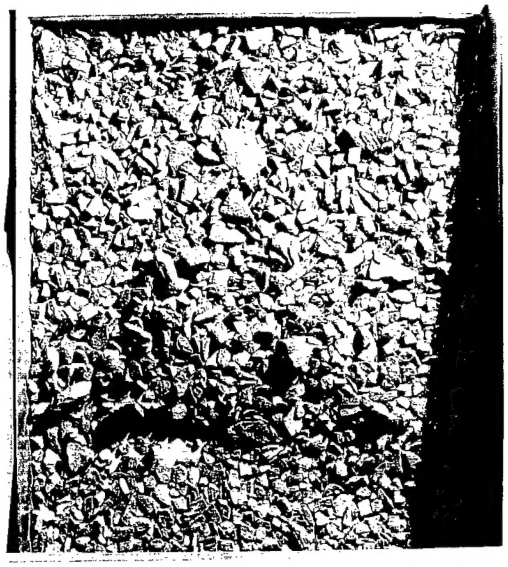

Test 31 after.

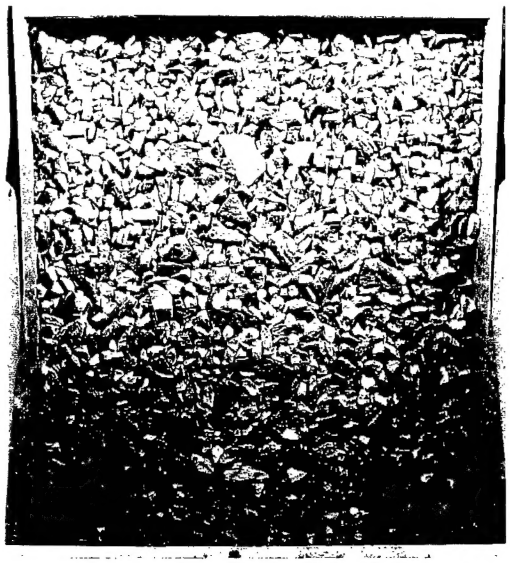

Test 32 before.

Test 32 after.

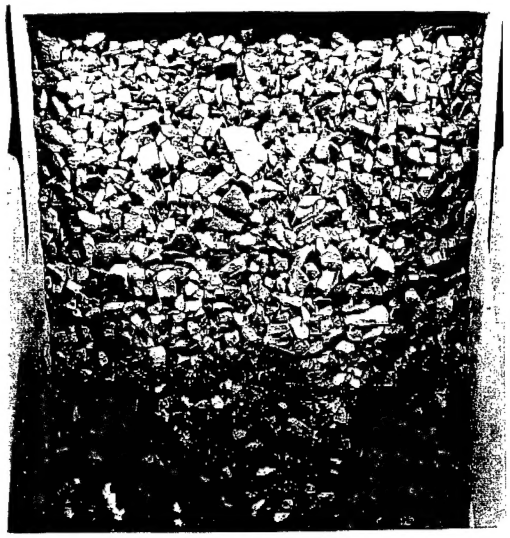

Test 33 before.

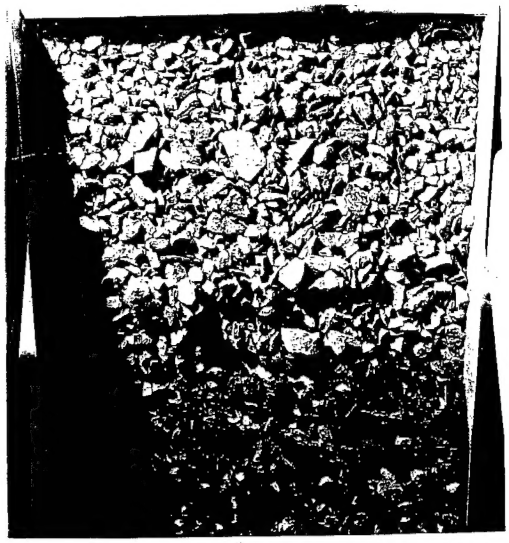

Test 33 after.

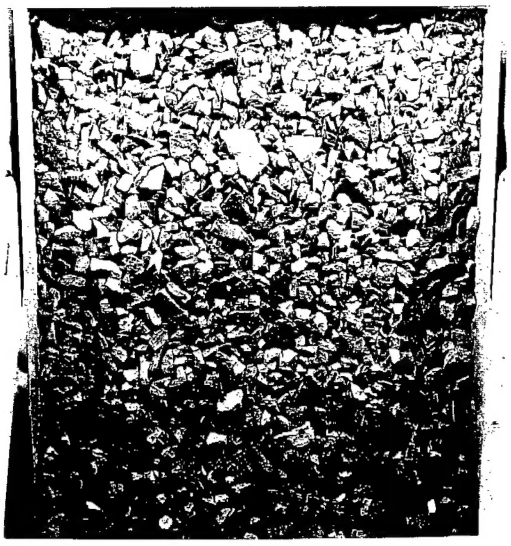

Test 34 before.

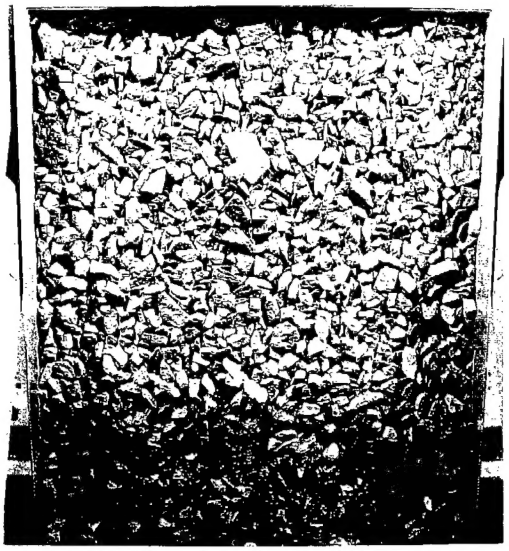

Test 34 after.

Test 35 before.

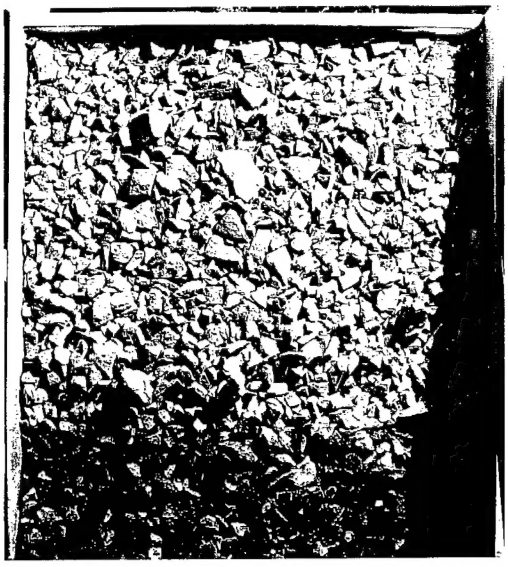

Test 35 after.

REPORT DOCUMENTATION PAGE

Form Approved
OMB No. 0704-0188

1. AGENCY USE ONLY (Leave blank)	2. REPORT DATE	3. REPORT TYPE AND DATES COVERED
	September 1996	

4. TITLE AND SUBTITLE

Ice Action on Riprap:
Small-Scale Tests

5. FUNDING NUMBERS

CWIS 32548

6. AUTHORS

Devinder S. Sodhi, Sharon L. Borland and Jesse M. Stanley

7. PERFORMING ORGANIZATION NAME(S) AND ADDRESS(ES)

U.S. Army Cold Regions Research and Engineering Laboratory
72 Lyme Road
Hanover, New Hampshire 03755-1290

8. PERFORMING ORGANIZATION REPORT NUMBER

CRREL Report 96-12

9. SPONSORING/MONITORING AGENCY NAME(S) AND ADDRESS(ES)

Office of the Chief of Engineers
Washington, DC 20314-1000

10. SPONSORING/MONITORING AGENCY REPORT NUMBER

11. SUPPLEMENTARY NOTES

12a. DISTRIBUTION/AVAILABILITY STATEMENT

Approved for public release; distribution is unlimited.

Available from NTIS, Springfield, Virginia 22161.

12b. DISTRIBUTION CODE

13. ABSTRACT (*Maximum 200 words*)

We conducted 35 small-scale experiments to assess the damage on riprap-covered banks by ice shoving. A review of literature on this subject revealed very little experience or guidance available for the design of riprap in the cold regions, where presence of moving ice can cause substantial damage to a riprapped bank. During the experimental program, we changed the slope of the model riprap bank, the size and the mix of rocks, and the thickness of model ice sheets. Results of these tests are presented in terms of measured horizontal and vertical forces, outcome of interaction as pileup or ride-up events, and damage to the model riprap bank. From the observations made during the tests, the damage to the riprap appears to take place during pileup events, because the incoming ice sheet is forced to go between the riprap and the piled-up ice, bringing with it rocks from the bottom to the surface of an ice pile. To sustain no damage to the riprapped protective layer, maximum rock size (D_{100}) should be twice the ice thickness for shallow slopes (1V:3H) and about three times the ice thickness for steeper slopes (1V:1.5H).

14. SUBJECT TERMS

Bank protection, Cold regions, Ice shoving, Lake ice, Riprap, River ice, Sea ice, Shore protection, Small-scale tests

15. NUMBER OF PAGES
70

16. PRICE CODE

17. SECURITY CLASSIFICATION OF REPORT	18. SECURITY CLASSIFICATION OF THIS PAGE	19. SECURITY CLASSIFICATION OF ABSTRACT	20. LIMITATION OF ABSTRACT
UNCLASSIFIED	UNCLASSIFIED	UNCLASSIFIED	UL